Nanostructured particles assembled from natural building blocks for advanced therapies

Yi Ju,[ab#] Haotian Liao,[cd#] Joseph J. Richardson,[e] Junling Guo,*[cfg] and Frank Caruso*[a]

[a]Department of Chemical Engineering, The University of Melbourne, Parkville, Victoria 3010, Australia. E-mail: fcaruso@unimelb.edu.au

[b]School of Health and Biomedical Sciences, RMIT University, Bundoora, Victoria 3083, Australia

[c]BMI Center for Biomass Materials and Nanointerfaces, College of Biomass Science and Engineering, Sichuan University, Chengdu, Sichuan 610065, China. E-mail: junling.guo@scu.edu.cn

[d]Department of Liver Surgery & Liver Transplantation, State Key Laboratory of Biotherapy and Cancer Center, West China Hospital, Sichuan University and Collaborative Innovation Center of Biotherapy, Sichuan 610065, China

[e]Department of Materials Engineering, University of Tokyo, 7-3-1 Bunkyo-ku, Tokyo 113-8656, Japan

[f]State Key Laboratory of Polymer Materials Engineering, Sichuan University, Chengdu, Sichuan 610065, China. E-mail: junling.guo@scu.edu.cn

[g]Bioproducts Institute, Departments of Chemical and Biological Engineering, Chemistry, and Wood Science, The University of British Columbia, Vancouver, BC, Canada

[#]Y.J. and H.L. contributed equally to this work

Abstract
Advanced treatments based on immune system manipulation, gene transcription and regulation, specific organ and cell targeting, and/or photon energy conversion have emerged as promising therapeutic strategies against a range of challenging diseases. Naturally derived macromolecules (e.g., proteins, lipids, polysaccharides, and polyphenols) have increasingly found use as fundamental building blocks for nanostructured particles as their advantageous properties, including biocompatibility, biodegradability, inherent bioactivity, and diverse chemical properties make them suitable for advanced therapeutic applications. This review provides a timely and comprehensive summary of the use of a broad range of natural building blocks in the rapidly developing field of advanced therapeutics with insights specific to nanostructured particles. We focus on an up-to-date overview of the assembly of nanostructured particles using natural building blocks and summarize their key scientific and preclinical milestones for advanced therapies, including adoptive cell therapy, immunotherapy, gene therapy, active targeted drug delivery, photoacoustic therapy and imaging, photothermal therapy, and combinational therapy. A cross-comparison of the advantages and disadvantages of different natural building blocks are highlighted to elucidate the key design principles for such bio-derived nanoparticles toward improving their performance and adoption. Current challenges and future research directions are also discussed, which will accelerate our understanding of designing, engineering, and applying nanostructured particles for advanced therapies.

1. Introduction

Recently developed therapeutic strategies have resulted in new paradigms for the management and treatment of diseases. For example, breakthroughs including adoptive cell therapy (e.g., engineered circulatory and immune cells),[1,2] immunotherapy (e.g., direct immune modulators, monoclonal antibodies, checkpoint inhibitors, oncolytic viruses, and vaccines),[3,4] gene therapy (e.g., gene silencing, RNA interference, antisense therapy, gene and genome editing),[5,6] and active targeted drug delivery (e.g., antibody–drug conjugates)[7] have sparked fundamental and applied questions surrounding the design of advanced therapies. Despite significant academic progress, only a limited number of advanced therapeutic strategies have resulted in successful clinical translation. Key reasons for this lack of clinical success include recognition and sequestration by the immune system, off-target cytotoxicity, limited durability, heterogeneity, and in the context of cancer, poor tumor penetration and low immunogenicity. To solve these challenges, scientists with interdisciplinary expertise must work collaboratively to extend the boundaries of biomedicine.

Nanostructured particles are colloidal particles with diameters ranging roughly from ten to a few hundred nanometers that have solid, hollow, or core–shell structures. Owing to their small size and readily tunable morphology and surface properties, nanostructured particles have been widely applied in various biomedical applications, including sensing and diagnosis, and medical imaging, and the delivery of drugs, genes, and vaccines.[8,9] Compared with conventional drug formulations, nanoparticle-based drug delivery systems offer distinct advantages such as: (1)

increased drug solubility and stability; (2) drug release in a controlled or localized manner, and; (3) overcoming of biological barriers.[10] These advantages have driven researchers to develop numerous particle platforms for therapeutic applications.[11-13] For example, inorganic nanoparticles have been widely used in the clinic as biomedical imaging agents and as a source of iron for those with iron deficiencies and have been explored in laboratories for use as drug delivery vehicles.[14] However, their clinical use for advanced therapeutics remains limited because of their potential toxicity, rapid blood clearance, non-degradability, and lack of biological motifs.[15] Alternatively, organic nanoparticles consisting of biomolecules or synthetic polymers offer opportunities for fine tuning the biological and chemical nature of the particles.[16] However, the preparation of synthetic polymers can require organic solvents and multiple chemical components, and often involve costly and/or precisely controlled fabrication conditions that can hamper scale-up and clinical translation.

Although numerous synthetic polymeric nanoparticles have been proposed and developed for biomedical applications in the literature,[12,17,18] there is an emerging interest in using bio-derived or bio-inspired compounds such as proteins, polysaccharides, lipid, polyphenols, and cell membrane components (e.g., exosomes) as building blocks for particle assembly. Nature's blueprint for these molecules provides fundamental advantages over their synthetic counterparts, including inherent high biocompatibility, natural bioactivity, high abundance, generally low cost, ease of modification, and biodegradability,[19-22] thereby providing opportunities to engineer materials for advanced therapeutic applications. Moreover, some natural building blocks possess intrinsic chemical or biological properties that favor particle assembly and/or specific biomedical applications. For instance, the metal coordination properties of natural polyphenols, such as tannic acid (TA) and epigallocatechin gallate (EGCG), have been extensively applied in the assembly of pH-responsive drug-loaded nanoparticles[23] with controlled drug release in intracellular compartments. Alternatively, functional polysaccharides and proteins, such as hyaluronic acid (HA) and Herceptin (Trastuzumab), have been shown to preserve their targeting and therapeutic effectiveness upon assembly into nanoparticles.[24,25] Most notably, recent breakthroughs in the development of messenger RNA (mRNA) vaccines for severe acute respiratory syndrome coronavirus-2 (SARS-CoV-2) employ lipid nanoparticle (LNP) formulations,[26] of which the ionizable lipids were originally developed for chemotherapy.[27] In addition, lipid-based cancer cell membranes containing tumor antigens have been successfully used to modify nanoparticle surfaces to mimic antigen-presenting cells for cancer immunotherapy,[28] whereas red blood cell (RBC) membranes containing a self-marker (CD47) have been applied as a stealth building block for particle assembly to inhibit phagocytosis by immune cells and achieve long-term in vivo circulation.[29] The drive to use naturally occurring materials, which often can also be considered "green" or "sustainable", offers great potential for expanding the toolbox of building blocks for functional nanoparticles.

In this review, we focus on the assembly of nanoparticles using natural building blocks and highlight the importance of nanostructured particles, such as self-assembled nanoparticles,

core–shell nanoparticles, and hollow capsules, for overcoming key challenges associated with various advanced therapeutics (Fig. 1). Natural building blocks are defined as materials produced by cells and organisms. The major classes of natural building blocks useful for particle assembly, including proteins, lipids, polysaccharides, small-molecule catecholamines, natural polyphenols, cell membranes, and exosomes, are introduced and discussed in relation to their natural properties, comparable performance, and inclusion into nanoparticle design principles. The properties and applications of different classes of natural building blocks are summarized and compared with a focus on their major applications in emerging advanced therapies. Specifically, the promise of natural building blocks is highlighted in terms of applicable therapies including (1) adoptive cell therapy, (2) immunotherapy, (3) gene therapy, (4) active targeted drug delivery, (5) photoacoustic therapy and imaging, (6) photothermal therapy (PTT), and (7) combinational therapy (e.g., chemo-immunotherapy, photo-chemotherapy, and photo-immunotherapy). Furthermore, we look to nature to compare the advantages and disadvantages of different natural building blocks and highlight the relationships between the properties of the natural building blocks and the engineered nanoparticles in regard to how these can guide application for advanced therapies. Finally, we provide a perspective on the current challenges and trends in the assembly of natural building blocks into particles and offer viable near-term strategies and design principles that can further improve their utility in biomedicine.

2. Engineered nanostructured particles from natural building blocks

2.1 Proteins

Proteins are a large class of natural macromolecules consisting of one or more chains of amino acid residues. Within organisms, proteins exhibit a variety of functions, including catalyzing metabolic reactions, replicating DNA, responding to stimuli, forming cell structures, and mediating molecule transportation. Owing to their amphiphilicity to both drugs and solvents, proteins have been regarded as suitable materials for the preparation of drug delivery systems. Protein-based nanomedicine platforms for drug delivery have been proven to be biodegradable, metabolizable, and amenable to surface modification for the attachment of drugs and targeting ligands. In this section, we introduce the most widely used protein-based nanoparticles in advanced therapies based on three different types of proteins, including albumin, ferritin, and gelatin, and summarize their biochemical features for nanoparticle assembly. Their application in vaccine delivery, active targeted drug delivery, and cancer theranostics is also discussed.

2.1.1 Albumin. Albumin, which is synthesized by liver hepatocytes, is the most abundant plasma protein in human blood.[30,31] Traditionally, albumin serves as a transporter protein with cellular receptor engagement, multiple ligand binding sites and a long circulatory half-life owing to its interaction with the recycling of the neonatal Fc-receptor.[32] Albumin has a high binding affinity not only for endogenous solutes in plasma, including metal ions, fatty acids, amino acids and metabolites[33-36] but also for many exogenous drugs such as paclitaxel, platinum-based drugs, chlorin e6 (Ce6), and celastrol.[37-40] Albumin can sequester inorganic ions through biomineralization in alkaline conditions (Fig. 2a), which can trigger the formation of metal ions

into ion complexes and subsequent nanoclusters coated with albumin.[41] This ability to biomineralize has attracted considerable interest for the use of albumin-biomineralized nanoparticles for PTTs, as they generally require metals to convert light into heat.[42-48]

The self-assembly of albumin and antitumor drugs increases the in vivo stability of the drugs[49-51] and promotes drug targeting to the tumor site, as tumor cells actively metabolize albumin to compensate for their increased need for amino acids and energy.[52-56] For example, the paclitaxel-loaded albumin nanoparticle Abraxane® has been approved by the US Food and Drug Administration (FDA) for the treatment of breast cancer,[57] owing to the fact that the nanoformulation of albumin-bound paclitaxel can overcome some of the toxicities associated with the Cremophor-based formulation of paclitaxel[58] and, through the presence of albumin, displays high affinity for osteonectin, a metastasis-related extracellular matrix glycoprotein overexpressed in various aggressive cancers (Fig. 2b).[59-62] The basic structure of Abraxane® comprises 6–7 paclitaxel molecules noncovalently bound to a single albumin, which leads to paclitaxel–albumin primary aggregates of 4–14 nm in diameter, which subsequently aggregate to form albumin–paclitaxel particles of approximately 130 nm in diameter.[63,64] This albumin-bound therapeutic can target an albumin transporter expressed on vascular endothelial cells, activating transport across the tumor vessel wall and allowing paclitaxel to accumulate in tumors.[65] For example, paclitaxel was used to induce the self-assembly of albumin modified with either cyclic Arg–Gly–Asp peptide or photosensitizer Ce6. These modifications endowed the assemblies with molecular targeting to specifically recognize αvβ3-integrin overexpressed tumor cells and also enabled combined photodynamic and chemotherapy.[66]

As osteonectin is overexpressed in atherosclerotic lesions,[67] self-assembled human serum albumin nanocages can be fabricated for rheumatoid arthritis therapy (Fig. 2c).[68] It has also been demonstrated that nanoparticles made from denatured bovine serum albumin can specifically target activated neutrophils adherent to the blood vessel wall, which leads to nanoparticle-loaded neutrophils crossing the blood vessel wall as the neutrophils can transmigrate in response to inflammation induced by pathogen invasion.[69] These findings also demonstrate the use of an albumin-based nanoparticle platform for in situ hijacking of activated neutrophils to deliver therapeutics across the blood vessel barriers to disease sites (Fig. 2d). Moreover, functionalizing nanoparticles of ovalbumin (OVA) with a densely packed “brush” conformation of poly(ethylene glycol) (PEG) can considerably reduce the nonspecific uptake of the OVA nanoparticles by dendritic cells, leading to successful in vivo translation of prolonged blood circulation for therapeutic nanoparticles.[70]

2.1.2 Ferritin. Ferritin is a ubiquitous iron storage protein produced by almost all living organisms, including animals, higher plants, fungi, and bacteria, and regulates iron homeostasis by sequestering excess iron in its core.[71] Ferritin is composed of heavy (H-chain) and light (L-chain) chain subunits that self-assemble into spherical, cage-like nanoparticles with an outer diameter of 12 nm and a cavity diameter of 8 nm.[72-74] These ferritin nanocages can maintain the

intact structure of ferritin under harsh conditions such as high pH and high temperatures.[75-77] These features, as well as its amenability to chemical and recombinant modification, good biodegradability, high water solubility, particle uniformity, and remarkable capacity for drug loading,[78,79] make ferritin nanoparticles a versatile carrier platform for diverse therapies.[80,81] For example, hybrid influenza nanoparticles can be formed by genetically fusing haemagglutinin to ferritins, which leads to the spontaneous formation of eight trimeric viral spikes on the self-assembled nanoparticle surface that confer broad protective immunity against diverse influenza viruses (Fig. 3a).[82] This structure-based, self-assembling synthetic nanoparticle vaccine platform improves the potency and breadth of influenza virus immunity, providing a foundation for building broader vaccine protection against emerging influenza viruses and other pathogens.

In the human body, ferritin can catalyze the oxidation of iron from ferrous to ferric forms and can house up to 4500 iron atoms in the form of ferrihydrite.[83] These properties have enabled the synthesis of a series of arginine–glycine–aspartic acid (RGD)-modified ferritin nanocages with a high metal-loading efficiency for targeted cancer therapies. Specifically, these nanocages have shown that RGD–ferritin drug delivery is a safe and efficient technology and holds great potential in clinical translation.[84-86] In addition, small CuS nanoparticles (~8 nm) can be encapsulated inside the cavity of ferritin nanocages.[87] These CuS–ferritin nanocages were applied in PTT and, when compared to free copper, were shown to achieve superior cancer therapeutic efficiency with good biocompatibility and higher tumor accumulation.[87]

Cancer stem cells can preferentially recruit ferritin to facilitate propagation and tumorigenicity,[88] which has inspired the application of human ferritin (Hft) nanocages as a suitable biomimetic nanovehicle to deliver various therapeutic agents against cancer stem cells (Fig. 3b).[89,90] The use of an intein-mediated trans-splicing approach yielded an antigen/adjuvant-loaded ferritin nanoparticle that codelivered antigen and adjuvant and induced a more potent protective immunity than other formulations.[91] This approach is complementary to known technologies for nanoparticle functionalization and overcomes instability issues that can occur with cargo loading while enabling the simultaneous incorporation of adjuvants with epitopes to precisely and effectively enhance antigen-specific immune responses.[92-94]

Importantly, ferritin can bind to transferrin receptor 1 (TfR1), which is overexpressed in 98% of primary and metastatic human cancers.[95,96] Additionally, TfR1 is expressed at high levels in endothelial cells at the blood–brain barrier as well as on brain tumor tissues,[97,98] suggesting that ferritin nanoparticles could be natively used as tumor-targeted drug carriers,[99,100] especially for the treatment of brain cancers.[101,102] Moreover, the three-fold axis symmetry of ferritin makes it conducive for fusion with antigens to recapitulate complex trimeric class I glycoproteins, increasing the immune response for weakly immunogenic targets.[103] Currently, ferritin nanoparticles are being evaluated as a vaccine platform for influenza, Epstein–Barr virus, and coronavirus disease 2019 (COVID-19) (Fig. 3c).[103-105]

2.1.3 Gelatin. Gelatin is a water-soluble polypeptide obtained from the acid, alkaline, or enzymatic hydrolysis of collagen, the main protein component of the skin, bones, and connective tissues of animals, including fish and insects.[106] The high biocompatibility and biodegradability of gelatin makes it widely suitable for use in food, pharmaceutical, and medical applications.[107-111] Despite limited reports on using gelatin nanoparticles for therapeutic applications, gelatin nanoparticles have been used for cancer therapy. Specifically, it has been shown that the gelatin nanoparticles can rupture to promote their deep penetration into tumor tissues when interacting with matrix metallopeptidase-2 (MMP-2) overexpressed by tumor cells (Fig. 4a,b), allowing for the targeted delivery of anticancer agents to tumor sites.[112,113] Additionally, a core–shell gelatin@calcium phosphate nanoparticle has previously been engineered to enable the separate encapsulation of drug molecules with different characteristics in the core and shell to avoid interactions between the different drug molecules (Fig. 4c), as a strategy to overcome multidrug resistance.[114,115]

2.2 Lipids

Lipids are a large and diverse group of organic compounds that are fatty acids or fatty acid derivatives and are characterized by their high solubility in nonpolar solvents and generally negligible solubility in water. As a main constituent of cell membranes, lipids have various functions including protection, compartmentalization, energy storage, and signaling. Owing to features such as high loading efficiency, high biocompatibility, and ease of preparation, multifunctional lipid-based nanoparticles offer great promise for the delivery of biopharmaceuticals. In this section, we introduce recent advances in lipid-based nanoparticles (Fig. 5) for advanced therapeutic applications including gene therapy, mRNA vaccine delivery, and cancer immunotherapy.

2.2.1 Liposomes. Liposomes are vesicles consisting of at least one lipid bilayer and can vary in size from <100 nm to 2.5 mm in diameters. The formation of liposomes is often a spontaneous process that occurs due to interactions between water molecules and the hydrophilic head groups of the lipids, where the hydrophobic tails group together. As lipids are amphipathic in nature, liposomes can encapsulate both hydrophobic and hydrophilic molecules. Thus, liposomes have been widely used as delivery systems for numerous drugs.[116,117] The high similarity between the lipid bilayer of liposomes and cell membranes can facilitate cellular uptake, while the inclusion of cationic 1,2-dioleoyl-3-trimethylammonium-propane chloride salt lipids can impart additional fusogenic properties to cell membranes that enhance the delivery of the encapsulated cargo (Fig. 6a,b).[118-120] Furthermore, the addition of molecules such as PEG and transferrin to the surface of liposomes can prolong the blood circulation time of the resulting liposomes through minimizing recognition and clearance by the reticuloendothelial system (Fig. 6c).[121]

The lipid bilayer can be destabilized during photodynamic therapy by the singlet oxygen generated by photosensitizers, which can trigger the release of the encapsulated cargo at the target site.[118,122,123] As demonstrated, liposome–gold nanoparticle hybrid systems can be

degraded by enzymatic reaction into smaller particles, achieving both hepatobiliary and renal clearance of the lipid-coated gold nanoparticles for PTTs.[124] To regulate the pancreatic stellate cells (PSCs) in pancreatic tumors,[125] an MMP-2-responsive peptide hybrid liposome was constructed via co-assembly. These peptide–liposome nanoparticles could be degraded by MMP-2, which is secreted by both PSCs and tumor cells, through a site-specific peptide cleavage manner, leading to the release of an antifibrosis drug that enhanced the perfusion of the encapsulated therapeutics.

2.2.2 Lipid nanoparticles. LNPs are defined as nanosized lipid systems composed of a discontinuous mixture of the different lipid components at different ratios that generally have lipid compartments in their core. Rather than having a hollow core as liposomes do, LNPs can have a nanostructured core, a homogeneous core and shell, multilamellar vesicular structures, or other self-assembled morphologies, depending on their formulation and cargo.[126-128] LNPs have been widely used as carriers of nucleic acids because the ionizable lipids that are used in many LNP formulations can electrostatically complex with the negatively charged phosphate backbone of nucleic acids. These formulations facilitate cellular uptake and endosomal escape of the nucleic acids.[129,130] Other types of lipids used for LNP formations (Fig. 7a) include: (1) phospholipids, which help in the structuring of the LNP bilayer and inhibit clearance by endosomal compartments;[131,132] (2) PEGylated lipids (PEG-conjugated lipids), which can increase the circulation time of LNPs in the body and protect LNPs from endocytosis by immune cells;[133-137] and (3) cholesterol, which enhances LNP stability and promotes fusion between LNPs and cell membranes.[132,133,135,137]

The design of LNPs for mRNA delivery and physiological barriers/possible administration routes for LNP–mRNA systems has previously been discussed.[27] Recent breakthroughs in mRNA–LNP vaccines have provided both protection and enhanced delivery, which has allowed mRNA–LNP vaccines to be approved for in vivo use against infectious diseases.[138] Numerous studies have reported the delivery of small-interfering RNA (siRNA) and mRNA in distinct LNPs.[139] However, by adjusting the ratio of RNA to lipid, new LNP formulations can be developed that simultaneously improve the delivery of both siRNA and mRNA (Fig. 7b). Additionally, the combined use of ionizable lipids and negatively charged proteins can drive the electrostatic self-assembly of LNP–protein nanocomplexes, enabling LNPs to deliver genome-editing proteins for gene therapy.[140] The use of LNPs as a carrier for Cas9/single-guide RNA delivery has proven to enable Cas9 to enter the cell nucleus for effective genome editing in response to the reductive intracellular environment.[131,132,140-143] Moreover, it was reported that a core-shell LNP structure with gold nanoclusters as the core could be used for Cas9/single-guide RNA-based gene therapy through the photothermal release of cargo (Fig. 7c,d).[144,145] By modifying the gold nanocluster core with human immunodeficiency virus (HIV)-1-transactivator of transcription peptides, the Cas9/single-guide RNA could reach the cell nuclei, which allowed for the effective knock-out of target genes.[145]

LNPs constructed from glycolipids, natural components of cell membranes that can be synthesized from fatty acids and sugars, have also been widely studied as drug delivery systems because of their amphiphilic nature, negligible toxicity, and biodegradability.[146] Meanwhile, the carbohydrate headgroups of glycolipids can interact with saccharide receptors with high specificity, promoting the bioadhesion of glycolipids with cell membranes.[147] These properties make glycolipids promising components for targeted drug delivery. For example, glycolipid-based LNPs can deliver mRNA that encodes costimulatory receptors to enhance T cell-mediated cancer immunotherapy, thereby proving the value of glycolipids as a useful delivery material for the modulation of T-cell function.[148] Similarly, glycolipid nanoparticles could be modified with a targeting peptide to allow for glioblastoma-targeted gene therapies, and demonstrated high efficiency in enhanced cellular uptake and pathologically functional recovery of the blood–brain barrier.[149,150]

2.2.3 Solid lipid nanoparticles. Solid lipid nanoparticles (SLNs) are nanospheres made from solid lipids (those with higher melting temperatures over >39°C) and obtained using high shear homogenization and ultrasound dispersion techniques. The benefits of using solid lipids rather than liquid lipids are the increased control over the release kinetics of the encapsulated compounds and the improved stability of the incorporated chemically sensitive lipophilic ingredients.[151] The lipid matrix of SLNs is made from physiological lipids, which can reduce the harmfulness caused by acute or chronic toxicity.[152] The application of SLNs in gene therapy for the treatment of glioblastoma was previously demonstrated;[153] for example, integrin-binding RGD (iRGD)-conjugated SLNs carrying siRNA against epidermal growth factor receptor (EGFR) and programmed cell death 1 ligand 1 (PD-L1) were prepared and their uptake by tumor cells could be primed by a short burst of radiation therapy, leading to activation of an immune response and inhibition of tumor growth (Fig. 8a). Cationic SLNs (cSLNs) have also attracted attention for the efficient delivery of compounds with low water solubility and various genetic materials (Fig. 8b).[154-157] For example, cSLNs were demonstrated to effectively bind to nucleic acids, protect them from DNAase I degradation, and deliver them into living cells.[158] However, a high surface charge and low PEG density on cSLNs could induce systemic platelet (PLT) activation and aggregation through intrinsic coagulation pathways, causing a high risk of thrombus.[159] Thus, pretreatment of recipients with anticoagulants should be considered to enhance the therapeutic efficacy of cSLNs.[159]

2.3 Polysaccharides

Polysaccharides are polymeric carbohydrate molecules that are formed through a series of condensation reactions among monosaccharides. As natural polymers, polysaccharides have proven to be highly stable, nontoxic, hydrophilic, and biodegradable. Moreover, the hydrophilic groups of polysaccharides, such as hydroxyl, carboxyl, and amino moieties, can interact with biological tissues noncovalently, resulting in high bio-adhesion. Thus, the half-life of nanoparticle carriers assembled from polysaccharides can be prolonged, leading to an increase in the bioavailability of the loaded drugs. These merits have inspired the application of

polysaccharides and their derivatives as nanocarriers for both the in vitro and in vivo delivery of bioactive agents for imaging, gene therapy, and vaccination. In this section, we introduce the most widely used polysaccharide-based nanoparticles, including chitosan (CS), HA, and dextran (DEX), and summarize their biochemical features for nanoparticle construction and biomedical applications in advanced therapeutics. Glycogen is another example of a biological polysaccharide nanoparticle that can be obtained through extraction processes from animal tissues or sweet corn.[160] The use of glycogen nanoparticles for biomedical application has been elaborated in a recent review.[161]

2.3.1 Chitosan. CS is a natural polycationic polymer derived from the deacetylation of chitin, a biocompatible polysaccharide abundant in crustacean shells. Compared to chitin, CS is relatively more reactive and can be transformed into various forms (e.g., powder, paste, film, and fiber).[162] The amino and hydroxyl groups along the CS chains enable the formation of stable covalent bonds between CS and various molecules of interest (Fig. 9a).[163-165] Moreover, the positive charge and mucoadhesive properties of CS make it ideal for drug delivery (Fig. 9b).[166] For example, a drug delivery system based on a tumor-hypoxia-activated photo-trigger (TAP) was synthesized by covalent conjugation of the amine groups of glycol chitosan and the carboxyl groups of TAP. This hypoxia-activated photo-trigger enabled the photo-release of anticancer drugs, in which the positive charge of the CS nanoparticles ensured efficient endocytosis by mammalian cells.[167] Solvent-free microfluidics can be used to tune the physicochemical properties of CS nanoparticles, such as size and surface potential, to maximize cellular uptake, which in turn has been shown to considerably increase the effectiveness of the loaded drugs (Fig. 9c).[168]

It was reported that nanoparticles synthesized from two ureido-conjugated chitosan derivatives exhibited favorable pH-sensitive characteristics, which could delay the release of amoxicillin in gastric acids and enable effective delivery to the target, *Helicobacter pylori*, at its survival region in the gut.[169] Loaded with whole tumor cell lysates, a cancer vaccine based on CS nanoparticles functionalized with mannose for dendritic cell (DC) targeting could be taken up by endogenous DCs within the draining lymph node following subcutaneous administration, which resulted in an increase in serum interferon-γ and interleukin-4 levels.[170] Moreover, folate-modified CS nanoparticles containing interferon-induced protein-10 gene were reported to reduce the proportion of myeloid-derived suppressor cells and regulatory T cells and increase the percentage of $CXCR3^+CD8^+$ T cells, which improved the antitumor response of $CD8^+CD28^+$ cytotoxic T lymphocytes.[171,172] In addition, the deacetylated amine groups along the CS chain are protonated at neutral pH and can interact with negatively charged siRNA, which increases the stability of siRNA in the blood stream. Therefore, CS-based nanoparticles have been widely used as carriers of siRNA (Fig. 9d) to inhibit tumor progression[173,174] and overcome drug resistance.[175,176]

2.3.2 Hyaluronic acid. HA is a primary component of the extracellular matrix and plays a structural role in connective tissues owing to its hydrodynamic properties and interactions with

other extracellular matrix components.[177] The medical use of HA as a drug carrier is advantageous because of its high solubility, long half-life, and ideal drug distribution in tumors.[178-180] Moreover, HA has a strong affinity to CD44 (Fig. 10a), which is overexpressed by many tumor cells.[181,182] Compared to linear HA, HA-based nanoparticle copolymers have demonstrated improved resistance to hyaluronidase degradation while maintaining their ability to interact with CD44 (Fig. 10b).[183] This makes HA suitable for active tumor targeting delivery.[184,185] For example, HA–polyethyleneimine nanoparticles encapsulating microRNA-125b can be used to target peritoneal macrophages, which internalize the HA nanoparticles and then migrate to macrophage-ablated lung tissues.[186] This phenomenon can promote the repolarization of tumor-associated macrophages toward the M1 phenotype. Moreover, HA nanoparticles based on HA/2,3,5-triiodobenzoic acid can enhance the cellular uptake of doxorubicin (DOX) via interaction with CD44, which subsequently improves the antitumor efficacy of DOX.[187] As the overexpression of CD44 is the representative hallmark of atherosclerosis in its pathogenic process, HA nanoparticles also have potential for the diagnosis and therapy of atherosclerosis.[188] For example, it has been shown that an oxygen-generating nanocomplex encapsulating a manganese dioxide nanoparticle in an indocyanine green-modified HA nanoparticle can overcome oxygen consumption during photodynamic therapy, leading to significant tumor growth inhibition.[189] For image-guided PTT,[190] multifunctional nanocomposites of CuS loaded into Cy5.5-conjugated HA nanoparticles have been applied for tumor detection as the Cy5.5 fluorescent signal is quenched by CuS inside the particle but after degradation by hyaluronidase present in the tumor, a strong fluorescence signal appears in the tumor. Similarly,[191] adamantane-modified Ce6 photosensitizer can be loaded into HA by supramolecular interactions between β-cyclodextrin and adamantane, enabling the isolated storage of different components and facile tuning of the loading ratio between cargos (Fig. 10c).

2.3.3 Dextran. DEX is the generic name that is applied to a large class of α-D-glucans, in which the predominance of α-1,6-linkages is a common feature.[192,193] Owing to its properties such as colloidal stability, hydrophilicity, and inertness in biological system, DEX has been used for the assembly of polymeric drug delivery carriers.[194] For example, iron–DEX nanoparticles coupled with major histocompatibility complex-immunoglobulin dimers and costimulatory anti-CD28 could enhance T cell activation in a magnetic field.[195] This generated a large number of activated antigen-specific T cells and inhibited the growth of melanoma cells, thereby demonstrating a clinically relevant application for adoptive cancer immunotherapy (Fig. 11a).[195] In another study, amphiphilic polysaccharide nanoparticles of 5β-cholanic acid conjugated to a dextran sulfate (DS) backbone were synthesized for the targeted delivery of methotrexate to inflamed joints in rheumatoid arthritis (RA).[196] These DS-based nanoparticles were selectively taken up by activated macrophages via scavenger receptor class A-mediated endocytosis and effectively accumulated in inflamed joints, implying their targetability to RA tissue (Fig. 11b).[196] Spermine-modified acetylated dextran (AcDEX) nanoparticles coloaded with the non-genotoxic molecule Nutlin-3a and the cytokine granulocyte–macrophage colony-stimulating factor could release Nutlin-3a in a pH-dependent fashion, inducing endosomal escape and demonstrating

intrinsic immune adjuvancy on monocyte derived DCs, which then upregulated the expression of CD83 and CD86 costimulatory markers on the cell surface.[197] This nanoparticle system showed promising in vitro results leading to cancer cell death and consequent stimulation of antigen presenting cells with the priming of T cells. Moreover,[198] a spermine-modified AcDEX-based functional nanoparticle allowed for the pH-triggered drug delivery of CHIR99021 and SB431542 to increase the efficiency of direct reprogramming of fibroblasts into cardiomyocytes after ischemic insult. These observations highlight the potential of DEX-based nanoparticles for potential tissue regeneration therapies owing to their improved drug delivery and the efficient reduction in tissue damage caused by ischemia.

It has been shown that DEX-based nanoparticles conjugated with amino vitamin B12 derivatives for the oral delivery of insulin can lead to a significant reduction in blood glucose while protecting insulin from GI enzymatic cleavage.[199,200] In light of the upregulation of reactive oxygen species (ROS) in the ischemic neuron, a bioengineered ROS-responsive nanocarrier composed of a DEX polymer core modified with ROS-responsive boronic esters was developed for the stroke-specific delivery of a neuroprotective agent (NR2B9C) against ischemic brain damage.[201] These targeted "core–shell" nanoparticles allowed for the controlled release of NR2B9C triggered by high intracellular ROS in ischemic neurons and could drastically prolong the systemic circulation of NR2B9C, which enhanced the active targeting of the particles to the ischemic area (Fig. 11c). In contrast, the coating strategy using AcDEX could increase the dispersity and biocompatibility of nanoparticles, facilitating the nucleation process to further grow the particles.[202-204] The introduction of AcDEX in porous silicon nanoparticles (Fig. 11d) prevented cargo release by blocking the pores of the porous silicon nanoparticles, where the decomposition of AcDEX under acidic environments allowed for intracellular drug release.[202,204]

2.4 Small-molecule catecholamines

Catecholamines, such as dopamine, epinephrine, and norepinephrine, are natural organic compounds that function as neurotransmitters in the body (Fig. 12a) and are widely used as vasopressors in the clinic.[205] Catecholamines can also be found in the adhesive proteins of marine mussels, and inspired by this, dopamine has been used to coat a wide range of inorganic and organic substrates via self-polymerization into polydopamine (PDA) in basic environments.[206] Other catecholamines, such as norepinephrine,[207,208] 3,4-dihydroxy-L-ppinhenylanaline (L-DOPA),[209] and 5-pyrogallol 2-aminoethane,[210] have a chemical structure similar to that of dopamine and are known to undergo oxidative polymerization to form poly(catecholamine) films. The obtained poly(catecholamine) share the biocompatibility and surface-independent coating properties of PDA,[211] therefore affording a versatile platform for film deposition and particle engineering. In this section, we introduce catecholamine-based nanoparticles, mainly focusing on PDA nanoparticles owing to their wide applications for advanced applications including delivery and diagnostics.

2.4.1 Properties of poly(catecholamine). Mytilus edulis foot protein 5 (Mefp-5) secreted from

the byssal plaque of mussels is an adhesive protein that largely consists of DOPA and lysine amino acids.[212] Inspired by the coexistence of catechol groups (from DOPA) and amine groups (from lysine) in Mefp-5, dopamine has been explored as a small-molecule catecholamine containing both a catechol and an amine group that can undergo oxidation in alkaline pH conditions and self-polymerize into PDA.[206] Of particular importance, PDA can be coated on virtually any natural or synthetic substrate, including metals, oxides, polymers, ceramics, bacteria, and cells, and can serve as a platform for secondary reactions to conjugate drugs, antibodies, or biomolecules via covalent or noncovalent interactions. Studies suggest that the intermolecular assembly of PDA is driven by both covalent and noncovalent pathways, although the exact mechanism(s) remain(s) unclear.[213,214] During PDA formation, dopamine is sequentially oxidized in solution to form covalently bonded oligomers, which are then physically assembled via noncovalent interactions, including hydrogen bonding, π–π stacking, van der Waals forces, and cation–π interactions.[215,216] In addition to their strong adhesive properties, PDA displays biocompatibility,[217,218] excellent near-infrared (NIR) absorbance,[219] efficient radical scavenging activity,[220] and strong metal-chelating capacity.[221,222] The surface of PDA can be readily functionalized with amines or thiol-terminated therapeutics or biomacromolecules in aqueous solutions via Michael addition or Schiff base reactions.[223,224] For example, PDA has been functionalized with zwitterionic peptides to generate low-fouling surfaces.[223] Furthermore, the synthesis of PDA is simple and inexpensive as it can be obtained using a simple immersion protocol in the presence of ambient air. Consequently, PDA has attracted wide interest in materials science and biomedicine.[225,226] For example, PDA-based nanoparticles have been employed as drug delivery carriers, photothermal agents, and photoacoustic contrast agents for theranostics applications.[227-235]

Norepinephrine is another example of a natural catecholamine that can be used as a building block for nanomaterial construction although it mainly functions as a neurohormone and neurotransmitter in the body for regulating blood pressure, heart rate, and responsiveness to stress and fear.[236,237] Specifically, norepinephrine can undergo oxidative polymerization to form polynorepinephrine (PNE) in basic environments.[207] Similar to dopamine, the oxidative polymerization of norepinephrine is attributed to its chemical structure, which contains a catechol and a primary amine. Importantly, PNE coatings have been found to share the material-independent coating properties of PDA (Fig. 12b) and have been successfully coated on a large range of materials, including metal oxides, ceramics, semiconductors, and synthetic polymers.[208] Furthermore, the presence of the alkyl hydroxyl group in norepinephrine allows the PNE coatings to serve as a platform for the ring-opening polymerization of biodegradable polymers. Compared to PDA coatings, PNE coatings exhibit a smoother surface at the nanometer scale (Fig. 12c-f) owing to the formation of an intermediate, 3,4-dihydroxybenzaldehyde, during the polymerization process.[208] PNE nanoparticles have been recently developed and proposed as drug delivery carriers owing to their high biocompatibility and high drug loading capacity.[238]

2.4.2 Self-assembled PDA nanoparticles. Besides being able to form coatings, dopamine can

self-assemble into PDA nanoparticles in basic conditions or after treatment with oxidative agents. The size of PDA nanoparticles can be tuned from several nanometers to hundreds of nanometers in aqueous alkaline solutions by the titration of different ratios of dopamine to sodium hydroxide or ammonium hydroxide.[219,220] The particle size is also influenced by the reaction temperature,[220] pH,[228] buffer,[239] and additives (such as oxidants and alcohols).[240,241] During the synthesis of PDA nanoparticles, functional substances, such as anticancer drugs,[228,242] targeting moieties,[243,244] plasmid DNA,[245] and photosensitizers,[246,247] can be simultaneously incorporated via covalent coupling, noncovalent interactions, or physical entrapment. For example, the loading of hydrophobic photosensitizer Ce6 into PDA nanoparticles was reported to occur through π–π interactions between PDA and Ce6.[246] Ce6 was entrapped within the polymer matrix of PDA and exhibited a sustained release for 5 days in biological media. The obtained nanoparticles demonstrated combined photodynamic and PTT against bladder cancer cells. Anticancer drugs, such as camptothecin and DOX, were efficiently loaded onto the surface of PDA nanoparticles through hydrophobic interactions and π–π stacking.[228,244] Furthermore, the resultant drug-loaded PDA particles can be subsequently functionalized with targeting ligands. For example, triphenylphosphonium was conjugated on the surface of DOX-loaded PDA nanoparticles as a targeting moiety for mitochondria. The obtained particles could deliver DOX to the mitochondria of breast cancer cells to overcome drug resistance in long-term anticancer chemotherapy.[244] Owing to the chelating ability of PDA, PDA nanoparticles can also be loaded with metals, such as manganese (Mn), copper (Cu), iron (Fe), technetium (Tc), and the resultant metal-loaded particles have been applied for in vivo bioimaging, including magnetic resonance imaging,[233,248] photoacoustic imaging (PAI),[249] single-photon emission computed tomography,[232] and positron emission tomography (PET).[250]

Pure PDA nanoparticles display strong NIR absorption and a high photothermal conversion efficiency (40% at 808 nm), which is sufficient for tumor PTT.[219] For example, it was reported that exposure to an 808 nm laser at 2 W cm^{-2} for 5 min could efficiently suppress tumor growth in vivo following the intratumoral injection of colloidal PDA nanoparticles with an average size of 160 nm (Fig. 13a–c).[219] Moreover, the photothermal conversion ability of PDA nanoparticles could be used to ablate deep brain tissue in vivo via NIR irradiation (Fig. 13 d–f).[251] An ablation volume of 6.5 mm^3 was achieved without significantly damaging the adjacent cortical surface after the intrahippocampal administration of PDA nanoparticles, followed by 10 min of transcranial NIR irradiation at 808 nm. In another recent study,[252] PDA nanoparticles were applied as a photothermal conversion platform to stimulate neuronal activity. The PDA nanoparticles could activate neuron-like cells through increasing the intracellular temperature upon NIR irradiation (Fig. 13 g,h). The intracellular temperature increment mediated by NIR irradiation of the PDA nanoparticles led to an intracellular Ca^{2+} influx in differentiated neuron-like cells.

Furthermore, PDA has antioxidant abilities owing to the abundant phenolic groups that can function as radical scavengers. PDA nanoparticles have shown promise in treating inflammation,

periodontal disease, and Parkinson's disease.[253-255] For example, PDA nanoparticles with a diameter around 80 nm efficiently eliminated ROS induced by H_2O_2 or lipopolysaccharide in vitro, and subsequent in vivo studies using a murine acute peritonitis model confirmed the anti-inflammatory properties of PDA nanoparticles.[255] Moreover, 160 nm PDA nanoparticles served as robust antioxidants for ROS removal in murine periodontitis models for oxidative stress-induced periodontal disease.[256] PDA nanoparticles were also applied as antioxidative enzymes for photodynamic therapy, where RBC cell membranes were coated onto hemoglobin/PDA nanoparticles.[257] The presence of PDA allowed for the encapsulation of a photosensitizer (methylene blue) by post-adsorption and prevented hemoglobins from oxidative damage during circulation in vivo. Upon NIR irradiation, the pseudo RBCs accumulated in tumors and supplied oxygen in situ to achieve a strong photodynamic therapy efficacy with a high tolerance to intratumoral extreme hypoxia. Similarly, lipid-coated PDA nanoparticles were applied as antioxidant and neuroprotective agents to protect neuron-like cells from ROS-induced damage.[252]

PDA nanoparticles can also serve as antigen delivery carriers for cancer immune therapy. The antigen, OVA, or other proteins that contain primary amines or thiol groups can readily be conjugated to PDA nanoparticles through Michael addition or Schiff base reactions.[258] For example, OVA-coated PDA nanoparticles enhanced the uptake of OVA by bone-marrow-derived DCs, prolonged the antigen retention time in lymph nodes, and suppressed tumor growth by activating cytotoxic T cells in vivo. Furthermore, tumor cell lysates could be covalently conjugated to the surface of PDA nanoparticles, which effectively promoted tumor antigen uptake and DC maturation.[259] Interestingly, pure PDA nanoparticle were found to promote DC maturation and delay tumor growth by stimulating T cells and improving the immunosuppressive microenvironment within the tumor. In addition, adjuvant-loaded PDA nanoparticles have been developed for photothermal immunotherapy, taking advantage of the high photothermal efficacy of PDA. For example, an immune adjuvant imiquimod (toll-like receptor 7 agonist) was encapsulated into PDA nanoparticles during the self-polymerization of PDA.[260] The surfaces of the PDA nanoparticles were further functionalized with anti-PD-L1 antibodies and the presence of anti-PD-L1 enabled the specific targeting of PDA nanoparticles to PD-L1-overexpressed tumor cells and blockage of the immune checkpoint PD-L1 in tumor cells. Upon NIR irradiation, the PDA nanoparticles inactivated the tumor cell and promoted the DC uptake of tumor cells, forming an in situ-assembled cancer vaccine that could induce the maturation of DCs and promote the differentiation of naïve T cells into cytotoxic T cells (Fig. 14a–c), thereby killing tumor cells and providing long-term protection from tumor recurrence in mice. Similarly, imiquimod could be loaded into mesoporous PDA nanoparticles with high efficiency via hydrophobic interactions and π–π interactions.[261] The surfaces of the PDA nanoparticles were then functionalized with polyvinyl pyrrolidone to enhance lymphatic drainage (Fig. 14d), and the obtained nanoparticles could serve as efficient adjuvants to promote DC maturation and CD8+ T cell response. A combination of three therapies including PTT, immunotherapy, and chemotherapy were recently demonstrated by adsorbing imiquimod (serving as an immune

adjuvant) and DOX (serving as a chemotherapy drug) onto PDA nanoparticles (serving as a photothermal conversion agent) via π–π stacking and electrostatic interactions.[262] The synergetic toxicity of DOX and hyperthermia destroyed the local tumors, and together with the loaded immune adjuvant, the particle system could induce a systemic immune response to protect against tumor recurrence.

2.4.3 PDA-coated nanoparticles. PDA coatings have been reported to improve the colloidal stability, physiological stability, and in vivo biocompatibility of nanoparticles,[218,263] and serve as a functional layer for drug loading for advanced therapies.[218,263,264] Various small-molecule drugs such as cisplatin,[265] hesperetin,[266] docetaxel,[267] and desipramine[268] can be loaded into PDA-coated nanoparticles through metal chelation, π–π stacking, hydrophobic interactions, or electrostatic interactions. For example, the catechol groups in PDA-coated micelles were employed to immobilize the anticancer drug bortezomib (BTZ) through the formation of boronic acid–catechol bonds.[269] BTZ was released from the PDA shells in a pH-responsive manner because the boronic acid–catechol bond could be cleaved in acidic conditions. Furthermore, the PDA shell on the micelles enabled drug release in response to NIR irradiation and PTT for cancer treatment. In another example, a thin PDA coating on gold nanorods could suppress the cytotoxicity of a surfactant template and allow for high cisplatin loading, targeting ligand (RGD peptide) conjugation, and chelator-free iodine-125 labeling (Fig. 15a–d).[265] Specifically, cisplatin was loaded onto PDA through the metal chelation of catechol groups, which enabled pH-dependent drug release, where the photothermal effects thoroughly ablated tumors and inhibited relapse via a combined chemo-photothermal synergistic antitumor effect. Recently, PDA has been used to modify the surface of exosomes by forming PDA coatings in mild ambient conditions.[270] The PDA coating could also serve as a platform for secondary reactions to conjugate functional molecules (e.g., PEG and fluorophores) to the PDA-coated exosomes.

PDA can be used to coat colloidal drug crystals to improve their colloidal stability and long-term storage, and enable the controlled release of cargo. For example, a NIR-responsive drug delivery system was developed simply by coating PDA on DOX nanoparticles.[271] The PDA coating extended the blood circulation time of the DOX nanoparticles and inhibited the leakage of DOX during circulation. Furthermore, NH_4HCO_3 could be introduced into the PDA-coated DOX nanoparticles during the self-polymerization of dopamine. During NIR laser irradiation, CO_2 and NH_3 gas were produced from the encapsulated NH_4HCO_3 due to the hyperthermia induced by the PDA shell, which triggered the disassembly of PDA and released DOX in the tumor environment (Fig. 15e–g), thereby enabling advanced chemo-PTT. Similarly, a thin layer of PDA could be coated on insulin particles, facilitating pH-responsive insulin release.[272] Sustained insulin release was maintained over 40 h at pH 7.4, whereas less than 30% was released at pH 5.4. Moreover, the PDA shells were stable in various pH buffers over 60 days. Recently, a PDA-coated siRNA nanogel was developed for gene-mediated PTT.[273] The PDA shell protected siRNA from enzymatic degradation and endowed the nucleic acid nanogel with photothermal responsiveness. Under NIR irradiation, the heat generated by the PDA shell triggered the endo/lysosome escape

of siRNA and promoted efficient gene silencing against heat-shock-protein 70, which is overexpressed in tumor cells.

Recent studies have shown that a PDA coating can facilitate the mucopenetration of nanoparticles for potential mucosal delivery of therapeutics. For example, PDA-coated carboxylated polystyrene nanoparticles diffused 6-fold slower in mucus than in water, whereas polystyrene nanoparticles without a PDA coating diffused 1000-fold slower.[274] The enhanced mucopenetration of PDA was due to the hydrophilicity and negative surface charge of PDA, which allowed the nanoparticles to minimize the interactions with negatively charged and hydrophobic mucin particles.[275]

2.4.4 Hollow PDA capsules. Hollow PDA capsules can be prepared through the deposition of thin PDA coatings on sacrificial template particles, followed by the selective removal of the template particles. For example, different organic and inorganic particles, including silica,[276,277] calcium carbonate,[278] manganese carbonate,[272] metal–organic frameworks,[279] polystyrene,[280,281] and emulsion droplets,[282,283] have been used as sacrificial templates to prepare PDA capsules with different sizes and morphologies. The shell thickness can be readily controlled by tuning the dopamine concentration, reaction time, or number of coating cycles.[276,280] The obtained PDA capsules exhibit high stability at different pH (2–11) and negligible cytotoxicity to mammalian cells.[276,280] Functional cargo, including hydrophobic drugs (e.g., thiocoraline), magnetic nanoparticles, and quantum dots, have been preloaded in emulsion nanodroplets, followed by PDA coating and core removal, where the chemicals and materials remain in the encapsulated PDA capsules after template removal (Fig. 16a).[282] For example, a pH-responsive drug release system was engineered by conjugating DOX on the surface of PDA capsules through a pH-labile linker (Fig. 16b).[224] Over 85% of the loaded DOX was released over 12 h at endosomal/lysosomal pH, whereas less than 20% DOX was released at neutral pH (Fig. 16c). Moreover, the DOX-loaded capsules demonstrated cytotoxicity to HeLa cells compared to free DOX (Fig. 16d,e). Ionic liquids (ILs) have also been encapsulated into PDA capsules and used to generate hyperthermia using tumor microwave thermal therapy.[284,285] For example, PDA nanocapsules with an average size of 140 or 500 nm were prepared using silica templates and subsequently filled with ILs via an ultrasonic method under vacuum. The obtained IL-loaded PDA nanocapsules successfully generated hyperthermia and could eradicate cancer cells in vitro and in vivo under microwave irradiation, Meanwhile, DOX was loaded onto the PDA nanocapsules through π–π stacking and electrostatic interactions to achieve a combined chemotherapy and microwave thermal therapy.[285] Alternatively, PDA nanocapsules with a diameter of 200 nm could be formed using dimethyldiethoxysilane-based emulsion templates, followed by template removal using ethanol.[286] The obtained PDA nanocapsules served as a highly efficient theranostics platform for PAI and PTT due to the strong NIR absorbance of PDA (Fig. 16f–h). Interestingly, PDA nanocapsules exhibited higher PAI ability with more than two-fold higher intensity than solid PDA nanoparticles, which was likely due to the hollow structure of the nanocapsules producing harmonic imaging at certain ultrasound powers.

2.4.5 PDA-enabled single-cell nanoencapsulation. Single-cell nanoencapsulation, where single cells are encapsulated within a thin coating, can endow living cells with exogenous properties that they do not naturally possess. For example, PDA films were coated on the surface of *Saccharomyces cerevisiae* (yeast cells) (Fig. 17a–g),[287] where the average PDA coating thickness was around 30 nm and could be increased by multiple coating steps. The PDA coating on yeast could inhibit cell division, protect cells from a harmful enzyme (lyticase), and serve as a platform for secondary surface functionalization. In another example, PDA coatings containing Fe_3O_4 were deposited onto *Rhodotorula glutinis*, enabling the coated cells to serve as a whole-cell biocatalyst for the production of chiral alcohols.[288] The PDA shell significantly improved the catalytic activity of the encapsulated cells, displaying 5 times higher productivity than native cells, likely due to the electron transfer ability of the PDA shell. The reusability of the cells was also largely improved (8 times higher than native cells) due to the cytoprotective and magnetic properties provided by the incorporated Fe_3O_4. Furthermore, RBCs were encapsulated in a PDA shell to cover the antigenic epitopes, which protect the cells from coagulation reactions.[289] The PDA shell had negligible effects on the structure, viability, or physical properties (such as osmotic fragility and deformability) of the RBCs. Importantly, PDA-coated RBCs had similar in vivo survival profiles to native RBCs, demonstrating the potential for applications in blood transfusion practices.

In addition, owing to the tissue adhesive properties of PDA, PDA-coated microparticles can be deposited on pancreatic islets, forming a cell–particle hybrid, with negligible impact on the viability and functionality of the pancreatic islets.[290] A potent calcineurin inhibitor (FK506) was loaded into the PDA-coated particles and sustainably released from the cell–particle hybrids, which suppressed the host immune reaction and prolonged the survival of the xenogenic islet graft in vivo. The PDA-based hybrid cell–particle system modulated the local immune responses and had minimal influence on immune functions relating to systematic circulation and other tissues, highlighting its promise as a platform for clinical pancreatic islet transplantation.

2.5 Plant-based natural polyphenols

Polyphenols are naturally occurring compounds that are widely found in plants and display intrinsic biological properties, including biocompatibility, anti-oxidation, free radical scavenging, UV absorption, metal ion coordination, and other biological activities.[291] The catechol and gallol moieties in many polyphenols can interact with diverse surfaces through metal–phenolic coordination, hydrogen bonding, covalent bonding, and hydrophobic and electrostatic interactions.[23] This makes polyphenols a versatile and suitable building block for the design of nanomaterials for therapeutic applications.[292] Furthermore, a range of bioactive moieties, including targeting ligands, drugs, prodrugs, imaging contrast agents, and tracking molecules, can be encapsulated within or functionalized onto polyphenol-based nanoparticles,[293,294] thereby enabling diverse biomedical applications and emerging properties for advanced therapies. In this section, we summarize the properties of polyphenol building blocks and introduce different types

of polyphenol-based nanoparticles followed by a discussion of their application in advanced therapies, including checkpoint blockade immunotherapy, adoptive cell therapy, chemodynamic therapy, photodynamic therapy, and PTT.

2.5.1 Properties of natural polyphenols. From the chemical point of view, "polyphenol" refers to chemical compounds that possess multiple aromatic rings with at least one hydroxyl group bonded to the aromatic ring.[295] Generally, polyphenols are produced through plant metabolism and are widely distributed in different plants, fruits, and vegetables.[296] For example, green tea, grapes, coffee beans, olives, onions, and malt are rich in EGCG, TA, caftaric acid, caffeic acid, hydroxytyrosol, quercetin, and procyanidin C2, respectively.[296-298] Most polyphenols can be obtained by chemical extraction and purification from their plant sources, while some polyphenols can be accessed by chemical synthesis,[299,300] or biosynthesis using yeast or mammalian cells.[301,302] In addition to their large abundance in nature, polyphenols display diverse chemophysical and biological properties, including UV absorbance,[303] anti-oxidant,[304,305] antibacterial,[306,307] anti-fibrillogenic,[308] and anticarcinogenic properties.[309] As a result, polyphenols have been traditionally and historically used in the food industry, leather manufacturing, cosmetics, and the pharmaceutical industry.[310,311]

Recently, polyphenol-based materials including nanofilms, particles, and hydrogels have attracted growing interest due to the development of these materials based on the functional properties of universal surface adherence and metal-chelating capability arising from the presence of catechol and gallol groups.[312,313] These chemical moieties (catechol and gallol groups) allow polyphenols to interact with a broad range of biomolecules, including proteins, carbohydrates, lipids, and nucleic acids, through hydrogen bonding, covalent bonding, hydrophobic interactions, π interactions, electrostatic interactions, and metal coordination.[23,314] Therefore, nanoengineered polyphenol particles have attracted growing interest and have emerged as promising candidates for biomedicine owing to their biocompatibility, "green" preparation process, and tunable physiochemical properties.[291,315]

2.5.2 Metal–phenolic network-based nanoparticles. Metal–phenolic network (MPN) assembly is a facile and versatile platform for thin-film and particle engineering using coordination complexes of natural polyphenols and metal ions (Fig. 18a–c).[313] There has been tremendous interest in MPN-based nanoparticles owing to their considerable merits including: (i) ease and speed of preparation (generally <30 s); (ii) tunable physicochemical properties, including size (from 120 nm to 10 μm), stiffness (from 56 to 871 mN m^{-1}), structure (solid, hollow, porous), shape (planar, spherical, ellipsoidal), and surface chemistry (secondary surface functionalization); (iii) high biocompatibility and biodegradability; (iv) wide choice of phenolic ligand and metal ion precursors for specific applications (medical imaging, drug delivery, tumor targeting); and (v) possibility for large-scale synthesis.[19,316-319]

Specifically, self-assembled MPN nanoparticles can be prepared simply by mixing metal ions

with natural polyphenols in aqueous solutions.[320] A variety of lanthanides and transition metal ions can form complexes with natural polyphenols to generate a library of functional MPN particles for medical imaging, including magnetic resonance imaging (MRI),[321,322] PET,[323] and luminescence imaging.[316,324] Moreover, the self-assembly of natural polyphenols can be used to incorporate small-molecule anticancer drugs into the MPN particle system, leading to a hybrid particle system for cancer theranostics. For example, BTZ, a boronate proteasome inhibitor for cancer therapy, was complexed with four different natural polyphenols, including TA, EGCG, catechin, and procyanidin, through boronate–catechol complexation (Fig. 19a). Ferric iron was used to stabilize the hybrid BTZ–polyphenol nanoparticle system and enabled MRI (Fig. 19d,e). The formation of catechol–boronate dynamic covalent bonds enabled the pH-controlled release of BTZ in the tumor microenvironment (Fig. 19b,c).[325] Similar strategies have been used to incorporate cisplatin prodrug with EGCG on the basis of the coordination between Fe(III) and polyphenols. The obtained hybrid particles could be doped with gadolinium ions for MRI to track the in vivo delivery of the nanoparticles. Combined chemotherapy and chemodynamic therapy was realized through the controlled release of cisplatin and Fe(III) ions after cellular internalization, leading to the production of toxic ROS species catalyzed by an iron-based Fenton reaction.[326] In another study, p53 plasmid was encapsulated in a 120 nm-sized Fe(III)–TA-based nanoparticle, which was designed to eradicate cancer cells through a ferroptosis/apoptosis hybrid pathway.[327] The ferric ions were released from the MPNs upon cellular internalization, which triggered the Fenton reaction to produce ROS and liquid peroxide. Meanwhile, p53-expressed proteins inhibited elimination of the liquid peroxide, leading to oxidative stress induced by ferroptosis.

The green tea polyphenol (EGCG) and samarium ions (Sm(III)) can be used to engineer self-assembled nanoparticles with a hydrodynamic size of 61 nm (Fig. 19f–i), which demonstrate enhanced inhibition to metastatic melanoma without negative side effects to healthy cells.[328] Specifically, the Sm^{III}–EGCG nanoparticles showed stronger therapeutic effects compared to the individual components and generated tumor cell apoptosis through mitochondrial pathways. A similar self-assembled particle system integrated with (−)-epicatechin (EC) and Sm(III) has been introduced for adenosine triphosphate depletion and ROS-enhanced combination chemotherapy against colon cancer.[329] The incorporation of EC and Sm(III) also enabled a synergistic therapeutic effect through a mitochondrial dysfunction process. A transformable nanoparticle was recently developed through the assembly of TA, DOX (a small-molecule anticancer drug), and indocyanine (a photothermal agent).[330] The nanoparticle could transform from hydrophilic at physiological pH to hydrophobic in acidic tumor microenvironments and intracellular compartments. This enabled the nanoparticles to have a prolonged blood circulation, enhanced cellular internalization, and rapid lysosome escape. Furthermore, particles incorporated with indocyanine showed a PTT-mediated deep tumor penetration effect upon laser treatment.

In the form of nanofilms, MPNs can be coated on a variety of organic and inorganic substrates owing to the universal adherence properties of phenolic groups. For instance, Fe^{III}–TA MPN

systems have been coated on hydrophobic drug crystals (small-molecule anticancer drug paclitaxel).[331,332] The coating significantly enhanced colloidal stability (over 6 months) of the drug nanoparticles, which exhibited higher antitumor activity compared to the commercial formulation of Taxol. Moreover, Fe^{III}–TA-based MPNs can be used to improve the stability and control the release of coated sorafenib nanocrystals, a clinically used protein drug that incudes ferroptosis.[333] As demonstrated, the Fe^{III}–TA MPN coatings could release sorafenib at acidic lysosomal pH due to the pH-dependent MPN coating. The presence of TA converted the released and ferroptosis-generated Fe^{3+} into Fe^{2+}, which promoted the intracellular production of lipid hydroperoxides for enhanced ferroptosis therapy. Furthermore, a photodynamic agent, methylene blue, was encapsulated with the sorafenib nanocrystals through molecular interactions with the MPNs for imaging-guided photodynamic therapy. Upon tumor accumulation, the concomitant release of sorafenib and methylene blue induced a multimodal combination of imaging-guided photodynamic therapy and ferroptosis therapy.

Recently, MPNs have also been reported as a versatile coating to instigate the endosomal escape of nanoparticles owing to the "proton-sponge" effect arising from the buffering capacity of MPNs (Fig. 20a), which can provide an alternative strategy for the cytosolic delivery of therapeutics.[334] Furthermore, MPN coatings have been found to inhibit amyloid formation, which is associated with Alzheimer's disease. Specifically, investigation into the inhibition of amyloid fibrils using MPN-coated gold nanoparticles containing different metal ions (Fe^{III}, Al^{III}, Cu^{II}, Ni^{II}, Zn^{II}, or Co^{II})[335] demonstrated that Co^{II}–TA-coated gold nanoparticles exhibited the highest inhibition (90%) among the MPN-coated gold nanoparticles examined, whereas the remaining MPN-coated gold nanoparticles showed a similar level of activity to the pristine TA-coated gold nanoparticles (30%). In a related study, the use of a Co^{II}–TA-based MPN coating was demonstrated to facilitate the orientation-specific immobilization of antibodies on nanoparticles, leading to more than 2-fold greater cell targeting (Fig. 20b–d).[336] Molecular dynamics simulations suggested that the Co^{II}-based MPNs had a higher concentration of solvent-exposed Co^{II} compared with the other metal ion-based MPN systems, which facilitated coordination with the histidine-rich portion of the antibody Fc region, thereby effectively conjugating the Fc region of the antibody to the nanoparticles.

MPNs have also been coated on plasmonic nanoparticles to achieve combination therapy. For example, a nanotheranostics particle system was engineered by coating metal (Gd^{3+})–polyphenol (TA) networks on a DOX-loaded mesoporous silica-coated gold nanorod.[337] The presence of Gd^{3+} and the gold nanorod enabled MRI, computed tomography, and photothermal imaging for imaging-guided therapy, while the polyphenol worked synergistically with DOX to prevent invasion and metastasis for combined therapy. Similarly, MPNs assembled from TA and metal ions (Fe^{III}, V^{III}, or Ru^{III}) exhibited a high photothermal efficiency (40%).[338] This photothermal effect was independent of the particle substrate (polymeric or inorganic nanospheres) or the thickness of the MPN coatings. Moreover, the potency of Fe^{III}–TA-coated poly(lactic-*co*-glycolic acid) (PLGA) nanovesicles for photo-responsive usage has been studied for in vivo photothermal

tumor ablation, photothermal imaging, and PAI.

MPN hollow capsules with highly defined physiochemical properties (e.g., size, shape, shell thickness, stiffness, and surface chemistry) can be prepared by depositing MPNs on sacrificial templates (Fig. 21a),[339] which provides additional degrees of versatility for drug delivery. For example, the loading of functional proteins, polysaccharides, and small-molecule drugs into MPN capsules was achieved through template-directed assembly where the cargo was pre-adsorbed onto the templates, followed by MPN coating and template removal.[318,340] Furthermore, MPN capsules have been endowed with medical imaging properties (e.g., MRI, PET, and ultrasound imaging) as well as tunable disassembly profiles by incorporating different metal ions (Fig. 21b–f),[316,341] which enables the controlled release of encapsulated drugs in intracellular compartments. For example, anticancer drug DOX was incorporated into Al^{III}–TA capsules through the assembly of MPNs on DOX-loaded calcium carbonate ($CaCO_3$) templates, followed by $CaCO_3$ dissolution.[340] The capsules exhibited a high drug loading capacity (1.3 pg per capsule) due to the high surface area of the porous $CaCO_3$. The pH-dependent disassembly of the Al^{III}–TA capsules allowed for the controlled release of DOX in acidic intracellular compartments (e.g., endosomes or lysosomes) and led to enhanced drug effectiveness (Fig. 21g,h). Furthermore, MPN capsules were recently applied to pulmonary delivery where Fe^{III}–TA capsules were aerosolized by a commercially available nebulizer.[318] The capsules remained intact without significant loss of the encapsulated cargo. Tuning the aerodynamic diameter of the capsules by increasing the capsule shell thickness facilitated precise control of capsule deposition in a human lung model. Notably, in vivo studies demonstrated that the MPN capsules were highly biocompatible and biodegradable, as assessed following intratracheal administration in mice.

Inspired by natural building blocks, synthetic analogues can be engineered for specific applications. The functionality of MPNs can be further extended based on the design and engineering of synthetic phenolic-derived building blocks. For example, catechol-functionalized HA and PEG were used to assemble MPN particles that demonstrated enhanced stealth and targeting abilities in vitro.[342-344] A protein corona derived from human serum was found to significantly improve the targeting of HA-based MPN capsules to tumor cells in vitro by reducing nonspecific capsule–cell interactions.[345] More recently, the preparation of PEG-based MPN nanocapsules of three different sizes (50, 100, 150 nm) through supramolecular template-assisted assembly was demonstrated where a 14 nm gold nanoparticle was encapsulated into the nanocapsules to quantitatively track the bio–nano interactions of the nanocapsules in vitro, ex vivo and in vivo by mass cytometry.[346] The 50 nm MPN nanocapsules displayed a longer in vivo blood circulation time (half-life 4–5 h) than their 150 nm counterparts, which was consistent with the ex vivo results that showed that decreasing the size of the MPN nanocapsules led to reduced association with immune cells in human blood. In another example, a plant-inspired hydrogel was developed based on Ag-lignin nanoparticles.[347] The Ag-lignin nanoparticles were assembled with a dynamic catechol redox system to continuously generate

catechol groups in the hydrogel networks, endowing the hydrogel with long-lasting adhesiveness.[347]

2.5.3 Polyphenol–protein nanoparticles. Polyphenols have traditionally been used in the leather tanning industry owing to their strong interactions with proteins.[348] With advances in materials science and nanotechnology, a variety of protein–polyphenol nanoparticles have been engineered for advanced therapies. For example, a micellar nanocomplex was self-assembled by the complexation of EGCG with Herceptin (Trastuzumab, an anticancer antibody) in aqueous solutions (Fig. 22a–c).[25] Hydrophobic interactions were found to drive the complexation of EGCG with Herceptin, as the nanocomplexes were effectively disassembled by Tween 20, Triton X-100, and sodium dodecyl sulphate due to hydrophobic competition. As a result of the synergism of ECGC and Herceptin, the obtained nanocomplexes demonstrated higher inhibitory effects in vitro and better tumor growth reduction in vivo than free Herceptin.

Recently, TA-modified proteins have been introduced as a promising system for heart-targeted therapies (Fig. 22d–f).[349] By simply mixing proteins with TA at an optimized stoichiometric ratio, TA-functionalized (TANNylated) proteins were assembled via hydrogen bonding. Similar to PEGylated proteins, TANNylated proteins show prolonged blood circulation in vivo compared with non-TANNylated counterparts. Interestingly, TANNylated proteins accumulated in the heart, where they penetrated the endothelium to bind to myocardium extracellular matrix owing to their high affinity to elastin and collagen rather than glycocalyx in the blood vessels. Therapeutic proteins, peptides, and viruses can be TANNylated using this strategy, which enables specific targeting to the heart.

More recently, a library of protein–polyphenol capsules using TA and more than 10 proteins with different molecular weight, isoelectric point, and aliphatic index were introduced.[350] Depending on the peptide backbone and the majority of the exposed protein surface, protein–polyphenol interactions were driven either by hydrogen bonding, hydrophobic interactions, ionic interactions, or a combination of the three (Fig. 22g,h). Importantly, the bioactive functions of the proteins were preserved after being assembled into capsules, which allowed for catalysis and cancer cell targeting to be performed by the capsules. In a follow-up study, a supramolecular protein–TA nanoparticle platform was developed through template-mediated assembly using mesoporous silica.[351] Three therapeutic proteins including cytochrome C, immunoglobulin G, and β-galactosidase were assembled with TA on sacrificial mesoporous silica, followed by template removal using hydrofluoric acid. These protein–TA nanoparticles were stable in serum for more than 1 week but rapidly disassembled and consequently released functional proteins in the cytosol upon cellular uptake, likely due to the competitive binding of intracellular glutathione. The bioactivity of proteins was maintained after intracellular delivery as evidenced by catalysis hydrolysis induced by β-galactosidase and cell apoptosis included by cytochrome C (Fig. 22i). Furthermore, the nanoparticles were capable of endosomal escape (Fig. 22j) because the particle surface charge switched from negative to positive in the intracellular acidic environment due to

the isoelectric point of the proteins.

Besides taking advantage of protein–polyphenol interactions, enzymes have been used to mediate the assembly of MPNs. For example, the kinetics of MPN film formation could be readily tuned by the glucose oxidase-catalyzed reaction of D-glucose, which produces hydrogen peroxide to accelerate the oxidation of Fe^{2+} to Fe^{3+} in MPN films composed of Fe^{III}–TA complexes.[352] The optimized kinetics of generating Fe^{3+}–TA species facilitated film formation, producing MPN films with 9 times higher thickness compared to the air oxidation-based method. In another example, tyrosinase was used to expand the toolbox for MPN assembly by converting monophenol groups of molecules to catechol groups.[353] Based on this strategy, a wide range of monophenol-containing molecules (including small molecules, peptides, and proteins) that do not natively contain catechol groups could be assembled on planar and particle surfaces through enzyme-mediated assembly, while still preserving the inherent function of the building block molecule.[353] Recently, a self-assembled ternary complex constructed from TA, enzyme (β-galactosidase), and phenylboronic acid-conjugated polymers were reported.[354] The obtained ternary complex could deliver β-galactosidase to the target tumor in a mouse model, protect the enzyme from degradation by proteinase, and release them upon cellular internalization.

2.5.4 Polyphenol-enabled cell engineering. Cell engineering is conventionally based on complex processes involving gene editing for specific cell properties. The universal adhesion properties of polyphenols have enabled polyphenols and functional biomolecules, including proteins, DNA, and mRNA, to be assembled on cell surfaces, which can endow living cells with exogenous chemical and biological properties. For example, Fe^{III}–TA-based MPNs were used to coat the surface of yeast cells, forming a cell-in-shell structure (Fig. 23a–c).[355] This artificial shell with an average thickness of ~10 nm was generated within 10 s and served as a protective layer against harmful environments such as UV-C irradiation, lytic enzymes, and silver nanoparticles. Interestingly, cell division was suppressed by the Fe^{III}–TA shell and could be fully recovered upon disassembly of the MPN shell under mild conditions.[356] Moreover, Fe^{III}–TA MPNs could be used to incorporate magnetic nanoparticles and DNA into the MPN shells for cells.[357] Different living cells, including yeast, bacteria, and mammalian cells were compatible with MPN coating, which protected the cells from external aggressors including reactive oxygen damage and UV light irradiation. RBCs have also been coated with polyphenols, which act as immunoprotective shells to shield the immune-provoking epitopes on the surfaces of RBCs.[358,359] For example, Fe^{III}–TA-based MPN shells (20 nm) effectively attenuated the antibody-mediated agglutination of RBCs without disturbing oxygen diffusion or hemoglobin function (Fig. 23d–f).[359] This strategy could potentially help to tackle blood-type mismatch problems, contributing to the development of universal blood for blood transfusion.

Recently, polyphenol-enabled single-cell encapsulation was developed for immunotherapy and cell-based therapy. Specifically, a personalized tumor microparticle vaccine was engineered by coating Al^{III}–EGCG MPNs onto individual living tumor cells, followed by inactivation of the

cells by hypotonic treatment.[360] The microparticle vaccine contained tumor cell lysate with around 98% of the proteins from the cell encapsulated, which is a high antigen loading capacity. The MPN coordination complexes enabled the pH-dependent protein release upon cellular uptake. Moreover, the MPN shells protected antigens from degradation in vivo, enhanced the uptake efficiency of antigens by DCs, and extended the retention time of antigens in the lymph nodes. DCs were activated by the microparticles, followed by the enhanced expression of co-stimulation markers and Th1-related cytokines. The universality of this strategy was further demonstrated using five types of mouse tumor cells and one type of human tumor cells. Moreover, additional cellular functions could be achieved by incorporating bioactive molecules on cellular surfaces through metal–phenolic coordination-mediated assembly.[361] Polyphenol-functionalized nanocomplexes were first assembled by mixing TA with different biomolecules including proteins, DNA, mRNA, polysaccharides, and viral carriers. Simple mixing the nanocomplexes with living cells led to a biohybrid system with nanocomplexes assembled on the cell surfaces, referred as "Cellnex". This strategy was applied to a wide range of cell types including erythrocytes, T cells, monocytes, macrophages, DCs, and natural killer (NK) cells for potential cell-based therapies (Fig. 23g,h). For example, OVA-integrated erythrocyte systems (OVA/Erythrocyte$_{nex}$) were found to enhance protein delivery to lungs following intravenous delivery in vivo with 11-fold higher accumulation than their free protein counterpart (Fig. 23i), which could be potentially used for targeted pulmonary drug delivery. Moreover, an immune checkpoint inhibitor (PD-L1 antibody) was integrated with macrophages via MPNs and the obtained anti PD-Li/macrophage system demonstrated enhanced delivery of the antibody to tumors (Fig. 23j), which in turn led to the improved efficacy of immune checkpoint blockade therapy in vivo.[361] A similar strategy was developed to prepare a nanoparticle-based exoskeleton from abiotic materials to protect living mammalian cells from harmful environments and endow them with new properties.[362] A range of nanoparticles including metal–organic frameworks, mesoporous silica particles, and iron oxide nanoparticles were coated on individual cells through TA-mediated interparticle binding. The as-prepared hybrid cells demonstrated resistance to endogenous and exogenous stressors, including osmotic stress, ROS, pH and UV exposure, as well as properties foreign to native cells, such as multifluorescence, magnetism, and conductivity.

2.6 Cell membranes

Cells are complex systems consisting of interconnected subcellular machineries encapsulated by cell membranes that separate the cells from external environments. The basic structure of a cell membrane consists of phospholipids, embedded with proteins that serve various functions. During the last decade, extensive attention has been directed toward the surface modification of nanoparticles using cell membranes. This has allowed researchers to design nanoparticles exhibiting cell-like behavior for various biomedical applications. For example, cell membranes coated on nanoparticles can generate biointerfacing properties, such as enabling homologous targeting depending on the source cells. In addition, cell membranes on nanoparticles can inherit antigenic diversity from the source cell, enabling the particles to evade clearance by the immune

system, which in turn prolongs the circulation of the particles.[363] This section summarizes the main types of cell membranes that are currently being applied for the surface functionalization of nanoparticles.

2.6.1 Red blood cell membrane-coated nanoparticles. As the most abundant cells in blood, RBCs function as oxygen carriers.[364] Given that the self-recognition of homologous RBCs is achieved by a variety of molecules residing on the RBC membrane,[365] RBC membranes can be used to prolong the blood circulation of RBC-coated nanoparticles by avoiding clearance by the immune system (Fig. 24a).[366-370] RBC membrane shells have also been shown to adsorb various pore-forming toxins (PFTs) (Fig. 24b).[371] Accordingly, RBC membrane-coated nanoparticles can exhibit effective virulence neutralization of PFTs via spontaneous particle entrapment (Fig. 24c), thereby contributing toward the immunogenicity and efficacy of toxoid vaccines.[372] When serving as antigen carriers in immunotherapies, RBC membranes can prevent antigens from clearance by blood, deliver the antigens to the targeted site (depending on the ligands on the RBC membranes), and present them to immune cells after phagocytosis by antigen-presenting cells.[373-376] To further improve the fabrication process of RBC membrane-capped nanoparticles,[376] a microfluidic electroporation process was used. This method provided a more-complete cell membrane coating with enhanced treatment effects compared to conventional extrusion,[376] suggesting that the combination of microfluidic electroporation and RBC membrane-coated nanoparticles could be used in future cancer therapies.

2.6.2 Platelet membrane-coated nanoparticles. PLTs are small, colorless cell fragments that form clots and stop or prevent bleeding once blood vessels are broken. They are implicated in hemostasis and arterial thrombosis, as well as other physiological and pathophysiological processes such as immune evasion,[377,378] sub-endothelium adhesion,[379,380] and pathogen interactions.[379,381] In addition to displaying selective adhesion to the vasculature and enhanced binding to PLT-adhering pathogens, PLT membrane-coated nanoparticles have demonstrated decreased cellular uptake by macrophage-like cells and the disappearance of particle-induced complement activation in autologous human plasma (Fig. 25a).[382] In patients diagnosed with cancer, PLTs can interact with tumor cells and play an important role in tumor metastasis.[383] This phenomenon has attracted interest in using PLT membrane-cloaked nanoparticles for targeted cancer therapies (Fig. 25b).[384] Moreover, a biological coating method fusing membrane from both RBCs and PLTs has led to the generation of particles with properties from both source cells (Fig. 25c).[385] This strategy opens the door for hybrid cell membrane-cloaked nanoparticles combining the strength of various cell types in advanced therapies.

2.6.3 Leukocyte membrane-coated nanoparticles. Leukocytes (also known as white blood cells) are the largest blood cells with diameters ranging from 7 μm (small lymphocytes) to 20 μm (monocytes). Unlike RBCs, they are nucleated and independently motile. They can defend the body against infection and disease through several mechanisms: (1) ingesting foreign materials and cellular debris; (2) destroying infectious agents and cancer cells; and (3) producing

antibodies. It has been asserted that leukocytes have the potential to be employed as carriers for targeted treatment. For example, the innate inflammation-directed chemotactic ability of macrophages can drive leukocyte membrane-coated nanoparticles to accumulate in chronic inflammatory tumor tissues, offering promise for targeted chemotherapy.[386] Because macrophages can actively bind to metastatic cancer cells via interactions between the α4 integrins of the macrophage and the vascular cell adhesion molecule-1 of cancer cells,[387-392] it was shown than macrophage membrane decoration increased cellular uptake of coated emtansine liposomes in metastatic breast cancer cells and exerted inhibitory effects on cell viability (Fig. 26a).[393] While eliciting tumor-specific immune responses by targeting cancer cells, coatings obtained from membranes of NK cells can induce pro-inflammatory M1-macrophage polarization to generate cell-membrane immunotherapy and provide a cell-membrane immune inducer for stimulating the immune system during tumor immunotherapy (Fig. 26b).[394] The natural adhesion of $CD4^+$ T cell membranes and gp120 proteins on HIV can lead to the inhibition of gp120-induced killing of bystander T cells (Fig. 26c), leading to T-cell-mimicking nanoparticles effective against HIV infection.[395] Neutrophil membrane-coated nanoparticles can neutralize pro-inflammatory cytokines, suppress synovial inflammation, target deep into the cartilage matrix, and provide strong chondroprotection against joint damage, demonstrating their potential as an anti-inflammatory platform for RA management (Fig. 26d).[396] Altogether, these results imply that the dual functions (targeting ability and immune regulation) of leukocyte membrane coatings can be a potent strategy for targeted immunotherapies.

2.6.4 Cancer cell membrane-coated nanoparticles. In the modern age of precision medicine, the application of cancer cell membrane (CCM)-cloaked nanoparticles has been widely pursued for the targeted treatment of solid tumors based on the strong adhesion between homotypic tumor cells.[397] This intercellular homologous binding ability based on membrane proteins can be used to modify the surface of nanoparticles to provide them with antigens from the source of tumor cells, which can be recognized by the immune system to elicit immunogenicity against the tumor, also referred to as "cancer vaccination" (Fig. 27a).[398-401] For instance, a CCM-coated PLGA nanoparticle loaded with toll-like receptor 7 agonist showed enhanced uptake by antigen-presenting cells, which were then stimulated to maturation status to trigger an antitumor immune response (Fig. 27b).[398] Owing to the high inter-heterogeneity of cancers among different individuals, the isolation of CCMs from the specific tumor mass can contribute to a more efficient fusion between nanoparticles and the targeted tumor (Fig. 27c),[14,402-407] which allows for a more personalized therapy for individuals. Moreover, the immune-evading properties inherited from the source cancer cells can stabilize and prolong the circulation of CCM-coated nanoparticles, thus promoting their ability to reach the target site (Fig. 27d).[14,402]

2.7 Exosome-based nanoparticles

Exosomes are nanostructured extracellular vesicles (40–120 nm in diameter) secreted by most cell types.[408,409] Exosomes contain a large number of proteins, coding/non-coding RNAs, and lipids that reflect their original cell sources and transfer different cellular information to

neighboring cells or even to distant tissues (Fig. 28).[410-416] Exosomes themselves have demonstrated therapeutic potential depending on the their inner contents.[417-422] As an ideal nanostructured carrier, exosomes are characterized by several features, including high stability under physiological conditions, nonimmunogenicity, nontoxicity, and high biocompatibility.[423-425] Additionally, their size allows them to escape from the mononuclear phagocyte system and they can diffuse into tumors passively via the enhanced permeability and retention effect.[426] Moreover, the phospholipid bilayer of exosomes can directly fuse with plasma membranes to enhance cellular uptake.[427] Exosomes contain a series of cell-specific transmembrane proteins, such as α- and β-chains of integrins, immunoglobulin-family members, and cell surface peptidases. These membrane proteins provide exosomes with the ability to target cells and facilitate intercellular communication.[428]

2.7.1 Exosomes derived from mesenchymal stem cells. Exosomes derived from mesenchymal stem cells (MSCs) can function as an extension of the biological role of MSCs as tissue stromal support cells, which provides a rationale for the therapeutic efficacy of MSC exosomes for tissue regeneration in a wide spectrum of diseases (Fig. 29a,b).[429-432] Consistent with the function of their parent cells, MSC exosomes can help maintain tissue homeostasis for optimal tissue function and target housekeeping biological processes that operate ubiquitously in all tissues. This is critical in maintaining tissue homeostasis, enabling cells to recover critical cellular functions, and initiate repair and regeneration processes.[433]

2.7.2 Exosomes derived from cancer cells. Cancer cells can be targeted by their own exosomes, which can influence cancer progression and the microenvironment within the tumor.[434,435] This phenomenon has inspired the use of cancer-derived exomes as potential carriers for the targeted delivery of antitumor agents.[436-439] For example, exosome-sheathed DOX-loaded porous silicon nanoparticles were generated by exocytosis DOX from tumor cells.[439] These particles exhibited enhanced tumor accumulation, extravasation from blood vessels, and penetration into deep tumor parenchyma following intravenous administration (Fig. 30a).[439] To overcome the resistance of therapy caused by tumor hypoxia, exosomes isolated from hypoxic tumor cells have been used for cancer therapy, as they are preferentially taken up by hypoxic tumor cells (Fig. 30b).[436]

2.7.3 Exosomes from other sources. To achieve the controllable and reversible loading and delivery of therapeutic proteins,[440] an optogenetically engineered exosome was created by integrating a reversible protein–protein interaction module controlled by blue light with the endogenous process of exosome biogenesis. This engineered exosome could successfully deliver soluble proteins into the cytosol via controlled, reversible protein–protein interactions (Fig. 31a). By anchoring superparamagnetic nanoparticles onto reticulocyte (RTC)-derived exosomes (Fig. 31b), the magnetization of RTC exosomes could be increased in a controllable manner while retaining their superparamagnetic characteristics.[426] Such a strategy could separate exosomes from blood efficiently and provide RTC exosome nanoparticles with robust targeting.[441] For example, the macrophage-derived exosome nanoparticles (Fig. 31c) not only targeted

macrophages recruited in tumor tissues but also functioned as an “invisible cloak” for the incorporated cargo, diminishing clearance by the mononuclear phagocyte system, as well as reducing the toxicity and immunogenicity induced by the loaded cargo.[442,443] In addition, exosomes derived from macrophages or embryonic stem cells (Fig. 31d) have been used in the treatment of diseases of the central nervous system, such as Parkinson’s disease[441,444] and glioma,[445,446] as these types of exosomes have been shown to be able to cross the blood–brain barrier and selectively be taken up by brain microglial cells, the resident macrophages of the brain.[447]

3. Cross-comparisons and functional roles

It is a significant challenge to establish a framework for predicting the performance and functionality of engineered nanostructured particles composed of natural building blocks. Predictive success lies in knowing and understanding the underlying mechanisms of a variety of biological processes and how the properties of bio-derived compounds can be manipulated to exploit these processes. Progress in this space will benefit not only from robust and systematic studies of advanced therapies but also from understandings into natural building blocks and how their unique properties can be integrated into functional roles in therapeutic particle systems. This section summarizes the key fundamental requirements for these emerging advanced therapies and cross-checks these requirements against the functional properties of the various natural building blocks (e.g., molecular structure, physicochemical properties, and biological interactions) (Fig. 32).

(1) Cell-based therapies (also termed cellular therapy, cell transplantation, or cytotherapy), which involves the transplantation of living cells into patients for direct therapeutic activity, have experienced remarkable success in the clinic.[361,448] One of the key processes of this therapy is the re-engineering of cells to maximize their efficacy in aiding the native cellular systems to perform their inherent biological function, including delivering bioactive compounds in an organ-specific manner,[449] targeting checkpoint pathways,[361] modulating metabolic pathways,[450] and generating cytokine-producing T cells.[4] Particle engineering provides an alternative and facile way to improve therapeutic potency by integrating nanoparticles on the surface of living cells.[451,452] Natural polyphenols have been used to form self-assembled nanoparticles with bioactive compounds (e.g., therapeutic drugs, DNA/RNA, and antibodies) and the phenolic groups (catechol/galloyl groups) of the bioactive nanocomplexes can form interfacial interactions with the cell surface.[361,453] The stimuli-responsive property of such metal-coordination networks enables the triggered release of bioactive compounds at targeted sites, which can be honed in on by the chemotaxis of cellular systems.

(2) Immunotherapy focuses on the modulation of the immune system, generally though four different mechanisms: checkpoint inhibition, oncolytic virus therapy, T-cell therapy, and cancer vaccination.[3] The use of particle-based systems during immunotherapy focuses on the precise delivery of immuno-responsive compounds. Therefore, nanosystems based on proteins, lipids,

polyphenols, and exosomes have been engineered to improve the targeting and infiltration of immunomodulatory payloads into tissues and cells.[454,455] Moreover, polysaccharides or engineered fusogenic proteins can provide additional targeting abilities to the nanoparticles.[456] The immune response can be further enhanced by the presentation of antigens generated by adjuvant therapy.[455,457] For instance, PDA-based nanoparticles can function as PTT agents coupled with the co-delivery of immunomodulatory payloads.[458]

(3) Particle-based gene therapy primarily focuses on the targeted delivery of nucleic acids into cells for the purpose of altering the course of a medical condition or disease through the modulation of gene regulation and expression processes. A variety of natural building blocks have been explored to form nanocarriers to conjugate or encapsulate DNA/RNA.[459] Enhanced tumor accumulation can be achieved through the incorporation of antibodies or polysaccharides on the engineered nanoparticles or inclusion of the desired protein sequence into the host cells of exosomes.[460] In addition, the use of biomimetic nanoplatforms involving the integration of cell membranes on solid nanoparticles or DNA nanoparticles has been shown to be an emerging strategy for genetic cargo delivery. Increasing the intracellular delivery of nucleic acids and enhancing their gene expression in cellular translation systems are crucial for future efforts.[461]

(4) Active targeted therapy mainly uses nanoparticles engineered with bioactive ligands or unique molecular structures that interact with specific cell lines or tissue. Proteins,[462] polysaccharides,[463] and the fusogenic proteins of exosomes can readily provide this active targeting ability.[464] In addition, nanostructuring therapeutic cargo is a requirement to achieve prolonged circulation time and tissue penetration.[465] Therefore, nanosystems constructed from lipids, catecholamines, polyphenols, cell membrane-coated nanoparticles, and exosomes have been demonstrated to be efficacious in targeted therapy.

(5) The conversion of light energy into either heat (i.e., PTT) or sound energy (i.e., PAI) through energy-converting materials or molecules has been shown as an effective method for the treatment and diagnosis of cancer.[466] Bio-derived compounds, including proteins, lipids, PDA (a common catecholamine molecule), and polyphenols, have been used to engineer nanocarriers owing to their ability to construct self-assembled nanostructures with the loading or self-forming of light energy transduction domains (e.g., specific molecular structures or inorganic materials). Moreover, the conjugation of antibodies and polysaccharides on a nanocarrier surface can result in the active targeted delivery of photo-conversion agents to the pathological site.[467] Notably, the self-polymerization and metal coordination of catecholamines and polyphenols can provide inherent sites for light adsorption and conversion without the use of inorganic or organic nano-photothermal transduction agents.[468-472] Finally, cargo loading via the intermolecular interactions of bio-derived compounds (for example, polyphenols) can enable the combination of PTT/PAI with other therapies in cancer treatment.[273]

(6) Combination therapy is considered successful when it can produce better therapeutic

responses simultaneously than the individual treatments by themselves. Though a growing number of clinical trials (more than 10,000) and even more preclinical-research articles focus on combination therapies, it is unclear what strategies are best for selecting candidates for combination therapies and deciding how particle-based nanosystems can facilitate the success of such combination therapies.[473] The following discussion focuses on the second question in which natural building blocks can contribute to both the nanostructuring process and the combination therapies. Most natural building blocks (for example, polyphenols) are recognized as safe and biocompatible materials for biomedical applications and thus they can be used for the construction of nanostructured particles.[474] In addition, the use of natural building blocks can bring additional complexity to the biological response as most bio-derived compounds are biologically active.[475] Recent studies have shown that nanostructured particle systems engineered from proteins, dopamine (and other small molecule catecholamines), polyphenols, and exosomes can act as multifunctional platforms for the loading of mono-therapeutic cargo (e.g., chemotherapy, immunotherapy) and for the integration of different therapies, including chemo-immunotherapy,[476] photo-chemotherapy,[477] radio-immunotherapy,[478] and photo-immunotherapy.[479]

4. Design principles

Design principles for engineering natural building blocks into particles, along with viable near-term investigation strategies, to further improve their utility in biomedicine are discussed below (Fig. 33).

(1) Engineering particles with a hierarchical range of sizes can provide critical accessibility to the targeted sites and enhance their interplay with multiscale biological systems. Specifically, nanoscale materials can improve the targeting (mainly due to the prolonged circulation) and infiltration of therapeutic payloads into tissues and cells. Moreover, the assembly of nanostructured particles into microscale materials can facilitate cell-mediated transport and serve as a type of artificial antigen-presenting cell. In addition,, assembling macroscale materials out of nanostructured particles can result in artificial microenvironments to promote cell infiltration and reprogramming.[480] For example, the assembly of chemokine-encapsulating nanoparticles onto erythrocytes enabled lung targeting, leading to the infiltration of effector immune cells into the lungs for cancer immunotherapy.[481]

(2) Nanoparticles that intrinsically activate or suppress the immune system can be a viable step toward establishing a set of design principles for future immunotherapies. For instance, the immunological enhancement properties of some natural building blocks (e.g., chicoric acid) can provide synergetic effects for immunotherapy when incorporated into particles.[482] Manganese porphyrin can facilitate chloride transport and induce immunogenic cell death.[483] Incorporating self-assembled porphyrin nanoparticles can regulate ion transportation in cells. Therefore, the assessment of biological activities of the natural building blocks themselves needs to be considered during particle design.

(3) An understanding of the biological processes involved in the different emerging therapies can provide valuable information on the structural and functional requirements for particle design. For example, the intravascular trek of nanoparticles within the blood circulation system has been divided into stages of administration, margination, adhesion to vascular walls, and internalization. The surface condition of the nanoparticles is directly related to their retention time during circulation.[484] Neutral nanoparticles, as well as those with a slight negative charge, show significantly prolonged circulating half-lives than positively charged nanoparticles. To improve the accumulation, zwitterionic surfaces were designed for nanoparticles.[485] In terms of internalization, the details of different pathways can assist the design of nanoparticles for effective cellular uptake. Clathrin-coated pit-mediated endocytosis uses endocytic vesicles with a diameter of ~100 nm, while phagocytosis has vesicles of ~200 nm.[484] The existing literature and the inherent properties of the natural building blocks can be combined into a checklist of requirements for emerging therapies to combat challenging diseases. Overall, the establishment of comprehensive material design principles is needed to streamline the translation of these materials for clinical applications, while insight into the promising materials being developed and what their individual interactions are on different biological levels are also necessary.

(4) The design of nanoparticles should consider the formation of biomolecular coronas in relevant biological environments. Our studies have shown that human subjects will vary widely in their responses to nanomedicines, which is largely modulated by person-specific biomolecular coronas.[486] There is variation in the composition of biological fluids both within a subject and between subjects. Understanding the impact of this variation upon biomolecular corona formation on nanomaterials will guide the design of nanoparticles for specific therapies. For example, recent studies have revealed that the accumulation of nanoparticles in the liver are due to the enrichment of apolipoprotein E in the biomolecular coronas, which can interact with the low-density lipoprotein receptor on hepatocytes. This suggests the potential to achieve specific organ/tissue targeting by manipulating the composition of the corona through tuning the molecular structure or combination of building blocks.[487,488]

(5) The large-scale, reproducible synthesis of nanoparticles is another requirement to consider for successful clinical translation. The scaling process may alter the physical properties of nanoparticles, especially the size. Nanoparticles with different sizes show different accumulation in vivo (e.g., the uptake by antigen-presenting cells occurs with nanoparticles with sizes of ~300 nm,[489] whereas nanoparticles of ~20 nm in size are ideal for optimal lymph node targeting nanovaccine[490]). Furthermore, the design of nanoparticles should be compatible with upscaling toolboxes (e.g., automated microfluidic systems).[319] A series of detailed, stepwise protocols with accompanying video footage should facilitate the broad use and applications of nanoparticles and allow for proper translation and industry uptake.

5. Conclusion and perspective

The improvement of healthcare outcomes is one of the most important goals for the field of materials science but has an associated list of challenges across different biological levels and bio–nano interactions. Nature provides not only intriguing bio-inspired strategies for materials science but also a versatile toolbox of building blocks for the design and engineering of new materials. The development of nanostructured particles through the employment of bio-derived compounds as fundamental building blocks has accelerated the progress of therapies to combat a range of diseases. A series of advanced therapies have been emerging as new paradigms for the management and treatment of diseases, leading to breakthroughs in preclinical and early-stage clinical studies. One of the most successful examples is the development of lipid systems (e.g., liposomes). They have been studied for decades and are even presented as one of the first FDA-approved nano-drugs with enhanced therapeutic efficacy for cancer treatment (Doxil-PEGylated liposome loaded with DOX). More recently, lipid systems have also provided a safe, robust, and highly effective platform for the delivery of mRNA as vaccines to combat the COVID-19 pandemic. Some highlights of each natural building block in this review are reiterated below.

(1) Proteins exhibit a variety of naturally occurring biological functions such as catalyzing metabolic reactions, replicating DNA, responding to stimuli, and mediating molecule transportation. Additionally, proteins show amphiphilicity to both drugs and solvents. These two main aspects make proteins suitable materials for applications in vaccine delivery, active targeted drug delivery, and cancer theranostics.

(2) As the main constituent of plant and animal cells, lipids serve as structural components of cell membranes. Owing to features such as high loading efficiency, high biocompatibility, and ease of preparation, the design of multifunctional lipid-based nanoparticles offers great promise for the intracellular delivery of macromolecular biopharmaceuticals for gene therapy, mRNA vaccine delivery (e.g., SARS-CoV-2 vaccines for the control of COVID-19 disease), and cancer immunotherapy.[491]

(3) Polysaccharides are natural polymers and have been proven to be highly stable, nontoxic, hydrophilic, and biodegradable. Particularly, the hydrophilic groups of polysaccharides can interact with biological tissues in a noncovalent manner to enable high bio-adhesion. Engineered nanoparticles based on polysaccharides and their derivatives have been used as nanocarriers for the delivery of a range of bioactive agents for bioimaging and gene therapy, as well as adjuvants for vaccines.

(4) Mussel-inspired dopamine and other small molecule catecholamines have the ability to self-polymerize in alkaline conditions, leading to the nanoengineering of a range of materials, including nanostructured thin films, capsules, and nanoparticles, for applications in drug and gene delivery. Additionally, these materials strongly absorb light, which enables catecholamine-based nanoparticles to function as photothermal, photodynamic, and

photoacoustic contrast agents for advanced theranostics applications.

(5) Plant polyphenols are a class of biological building blocks that have undergone rapid development for advanced therapies. The diverse chemical properties of polyphenols (e.g., metal–phenolic coordination, hydrogen bonding, covalent bonding, and hydrophobic, and electrostatic interactions) make them a versatile class of building blocks for the construction of nanoparticles. A range of bioactive cargos, including anticancer drugs, imaging contrast agents, proteins, and nucleic acids, can be encapsulated into polyphenol-based nanoparticles for chemodynamic therapy, PTT, and gene therapy. Furthermore, the inherent properties of natural polyphenols (for example, antioxidant, antibacterial, antiviral properties) impart an additional range of biological functions along with the therapeutic processes. More recently, the interfacial interaction of polyphenols has facilitated the assembly of therapeutic cargos (e.g., proteins, DNA/RNA, drug molecules) on the surfaces of cells. These polyphenol-constructed cellular biohybrids have been used in immune checkpoint therapy and adoptive cell therapy.

(6) Exosomes are characterized by their nonimmunogenicity, nontoxicity, and high biocompatibility. Their size also allows them to escape from the mononuclear phagocyte system and diffuse into tumors passively via the enhanced permeability and retention effect. Moreover, exosomes can be engineered to incorporate a series of cell-specific transmembrane proteins that can target cells and facilitate intercellular communication. These merits have inspired researchers to develop exosomes materials for gene therapy, theranostics multifunctional delivery, protein-based therapy, and immunotherapy.

Although there has been significant progress of using natural building blocks for advanced therapies, several challenges still lie ahead that require the innovative re-design of the nanostructured particle systems. For example, the use of natural building blocks conjugated with synthetic moieties can lead to properties originally absent from natural systems, allowing for the emergence of collective properties beyond the individual components. Moreover, owing to recent developments in synthetic biology, the advanced design of natural biohybrid building blocks can be achieved. For example, synthetic biology allows the rational genetic engineering of a hybrid protein that combines the functional domains of mussel foot proteins (Mfps) containing DOPA and curli fiber subunit protein (CsgA). This hybrid protein could achieve biofilm formation and underwater adhesion, thereby representing a robust, versatile, and modular material platform for a variety of applications. The discovery and investigation of new bioactive molecules can also expand the toolbox of building blocks for the design and engineering of nanostructured particles. However, further experimental studies are necessary to determine whether some of the desirable properties of bio-derived compounds can be translated into biological functions, along with how these materials can be used to address the current challenges in advanced therapies. Notably, substantial effort is required to deepen the understanding of the bio–nano interactions, especially with consideration of the participation of the immune system and how it can cooperate with the inherent biological processes to treat diseases (e.g., material-assisted immunotherapy) and lower

unpredictable immunogenic responses to materials in complex biological system. Some suggestions, which involve an interdisciplinary approach, are given below to the development of nanostructured particles from natural building blocks for emerging advanced therapeutic applications (Fig. 34).

(1) The orthogonal design of natural-derived building blocks: Synthetic strategies can endow natural building blocks, and the resultant nanostructured particles, with properties outside the scope of nature such as light or magnetic responsiveness, low fouling properties, specific molecular rigidity, redox responsiveness, and host–guest or click chemistry functionalities. Orthogonal chemistry can integrate the success of synthetic chemistry and polymer science with bio-derived compounds, thereby providing a versatile platform for the future rational engineering of nanostructured particles. Some of the current challenges in emerging advanced therapies may be addressed through the design and use of these next-generation bio-hybrid natural building blocks.

(2) The biosynthetic engineering of advanced natural building blocks: The rational design of natural building blocks from synthetic biology can also be another versatile avenue to improve the functional properties of natural building blocks. Repurposing natural pathways can be a powerful approach for the future design of functional natural building blocks. For instance, the rational design of phenolic building blocks through the shikimic acid pathway could design new phenolic building blocks with ideal molecular structures and functional groups for the engineering of therapeutic nanoparticles.[492]

(3) Exploring the natural building block toolbox: The further exploration of newly discovered natural products can also provide a new avenue for the development of novel therapeutic particles. For instance, artemisinin and its semi-synthetic derivatives are a group of drugs used against malaria.[493] The formation of nanostructured particles and the integration of targeting domains can significantly improve the therapeutic outcomes (e.g., overcoming drug resistance). However, these natural molecules typically lack functional groups to form self-assembled nanoparticles. Therefore, more advanced particle synthesis strategies are necessary to allow naturally bioactive molecules to form therapeutic nanoparticles.

(4) Big data evaluation of immune responses: Modulation of the immune system has been a growing interest in a variety of promising therapeutics including adoptive cell therapy. Similarly, antibody-based therapies are based on direct cell-mediated cytotoxicity or act as checkpoint inhibitors to restore T cell activity. By using natural building blocks, the bioactivities of engineered particles could potentially regulate or integrate into the pathways of the immune system and enhance therapeutic outcomes. Therefore, the study of the immuno-regulatory principles of natural building blocks is another key segment in the future design and development of therapeutic particles. Currently, natural building blocks show unpredictable properties for biological outcomes, and therefore predicting and/or controlling the immune

response of these natural building blocks is essential for the engineering of advanced therapeutic nanoparticles.

Conflicts of interest

The authors declare no conflict of interest.

Acknowledgements

This research was supported by the Australian Research Council Discovery Project (DP210103114). F.C. acknowledges the award of a National Health and Medical Research Council Senior Principal Research Fellowship (GNT1135806). Y.J. acknowledges the award of a Vice-Chancellor's Postdoctoral Fellowship from RMIT University. J.J.R acknowledged the Japan Society for the Promotion of Science (JSPS) for his fellowship (Grant No. 20F20373). J.G. acknowledges the award of National Talents Program, National Natural Science Foundation of China (22178233), Talents Program of Sichuan Province, Double First Class University Plan of Sichuan University, and State Key Laboratory of Polymer Materials Engineering (grant no. sklpme 2020-03-01). The authors acknowledge Dr Yunxiang He for helpful discussion and assistance with scheme preparation.

Figures

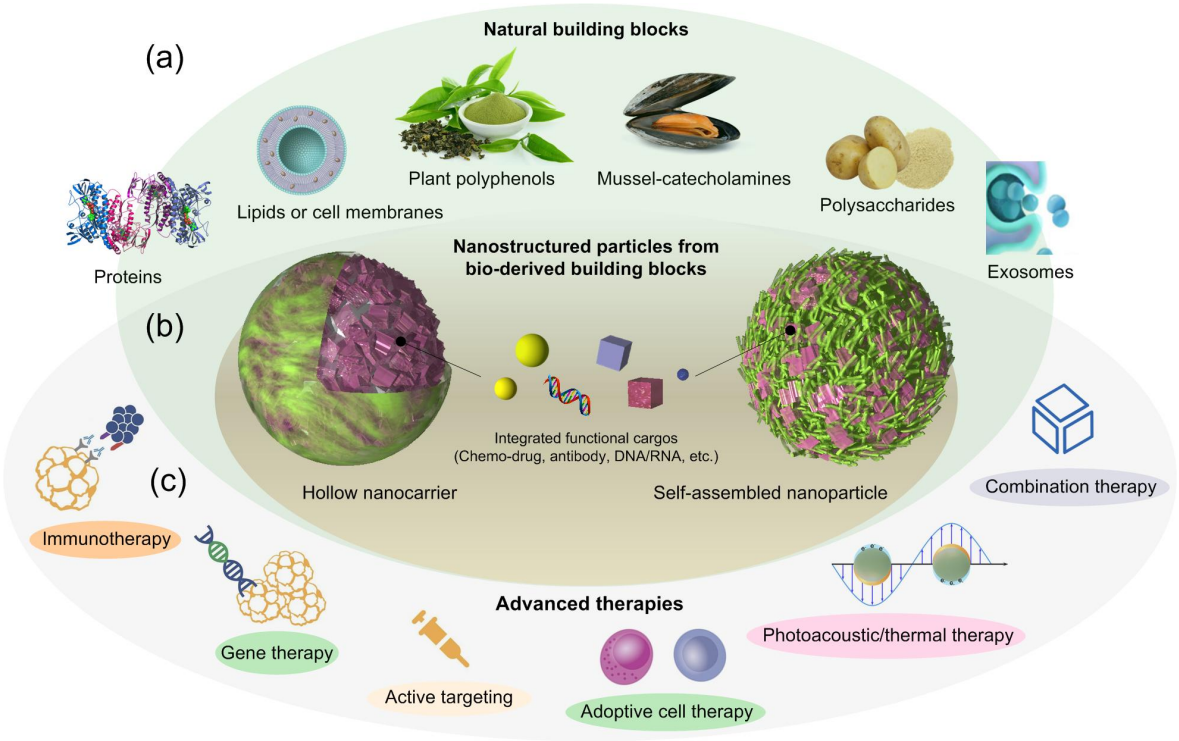

Fig. 1 Development of nanostructured particles using bio-derived natural building blocks for advanced therapies. (a) Representative natural building blocks, including protein, lipids, cell membranes, plant polyphenols, catecholamines, polysaccharides, and exosomes. (b) Assembly of nanostructured particles integrated with functional cargos. (c) Examples of nanoparticle-enabled advanced therapies, including immunotherapy, gene therapy, active targeting, adoptive cell therapy, photoacoustic/thermal therapy, and combination therapy.

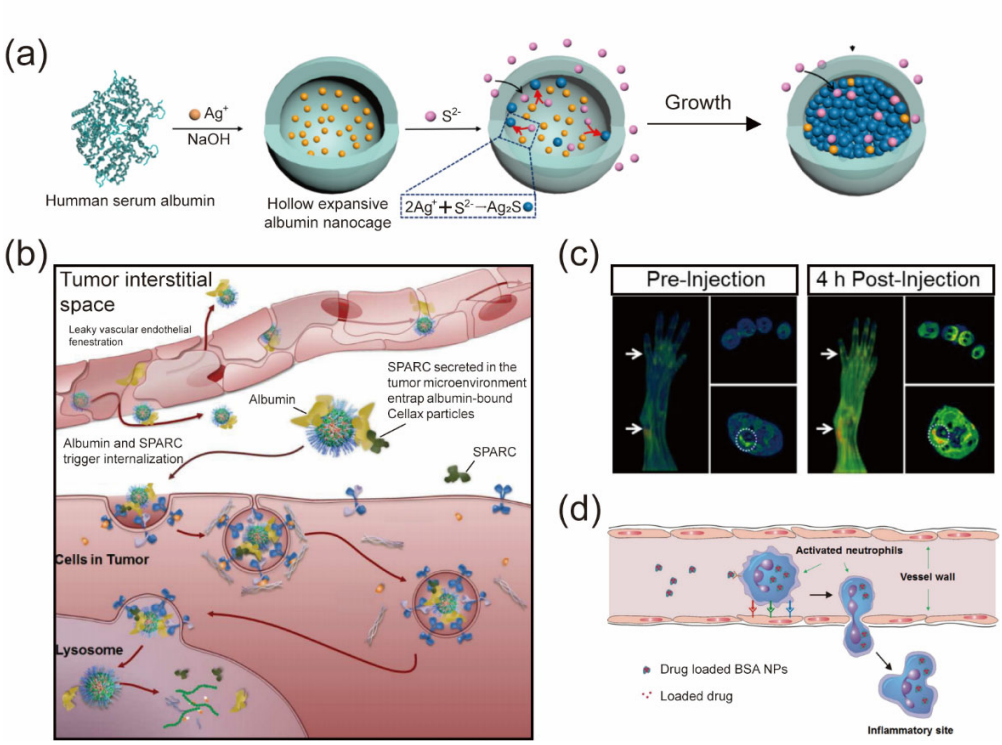

Fig. 2 Application of albumin-based nanoparticles for targeted therapies. (a) Schematic illustration of theranostics Ag_2S nanoparticles synthesized through precise controlled growth in albumin nanocages for NIR-II fluorescence/photoacoustic imaging and photothermal therapy. Adapted from Ref [45] with permission from American Chemical Society. Copyright 2017. (b) Proposed mechanism of delivery for polymer–docetaxel conjugate (Cellax) nanoparticles. The secreted protein, acidic and rich in cysteine (SPARC; osteonectin) produced in the tumor microenvironment binds to the surface albumin on the Cellax nanoparticles and thus traps the particles in the tumor. Reproduced from Ref [62] with permission from Elsevier Ltd. Copyright 2015. (c) In vivo T1-weighted MRI scans of inflamed paws in mice with collagen-induced arthritis before and 4 h after injection of methotrexate@albumin nanoparticles. White arrows and circles indicate changes in the whole view and the cross-section view separately. Reproduced from Ref [68] with permission from American Chemical Society. Copyright 2019. (d) Concept of neutrophil-mediated delivery of therapeutic bovine serum albumin (BSA) nanoparticles (NPs). Reproduced from Ref [69] with permission from American Chemical Society. Copyright 2015.

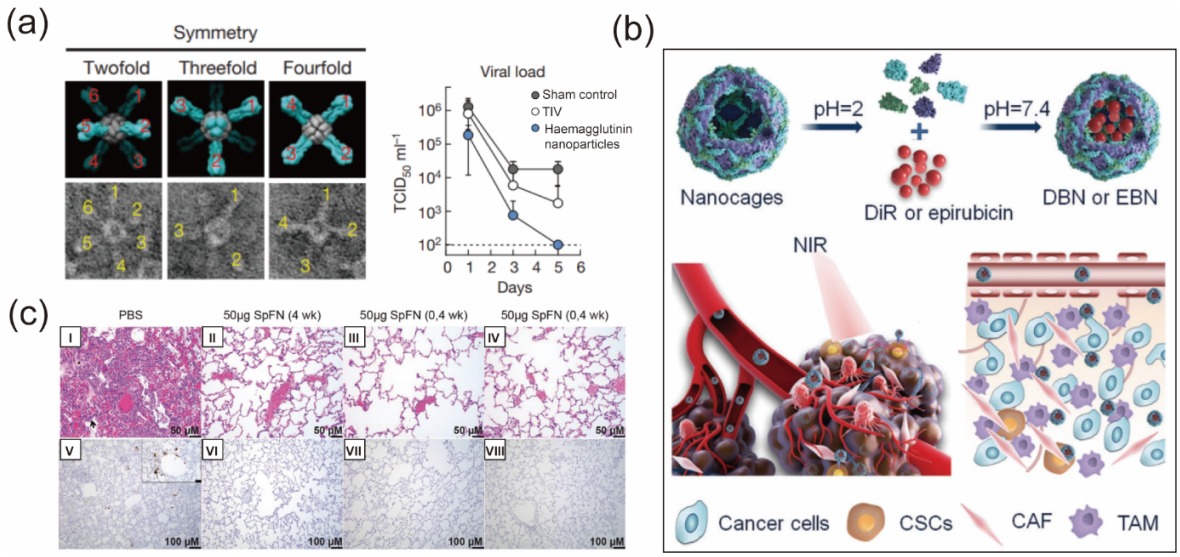

Fig. 3 Application of ferritin-based nanoparticles for vaccination and chemo-photothermal therapy. (a) (Left) Computational models and observed transmission electron microscopy (TEM) images (top and bottom panels) representing octahedral two-, three- and fourfold axes of HFt-haemagglutinin nanoparticles. Visible haemagglutinin spikes are numbered in the images. (Right) Protection of immunized ferrets from 2007 Bris virus challenge. Challenge was performed with $10^{6.5}$ 50% egg infectious dose of 2007 Bris virus through intranasal inoculation. Virus titers in the nasal washes were determined by 50% tissue culture infectious dose ($TICD_{50}$) assay. The mean viral loads of sham control, trivalent inactivated influenza vaccine (TIV) and haemagglutinin nanoparticles (HA-np) with standard deviation at each time point were plotted. Reproduced from Ref [82] with permission from Nature Publishing Group. Copyright 2013. (b) Schematic illustration of deep tumor-penetrated biomimetic HFt nanocages with preferential cancer stem cell (CSC) accessibility for effective antimetastasis therapy. DBN, 1,1-Dioctadecyl-3,3,3,3-tetramethylindotri-carbocyanine iodide-loaded biomimetic nanocage; EBN, epirubicin-loaded biomimetic nanocage; CAF, cancer-associated fibroblast; TAM, tumor-associated macrophage. Reproduced with permission from Ref [89]. Copyright 2018, Tan et al. Published by Wiley-VCH Verlag GmbH & Co KGaA, Weinheim. (c) Histopathology and virus detection in the lungs of spike HFt nanoparticles (SpFN) vaccinated and unvaccinated control rhesus macaques following SARS-CoV-2 respiratory challenge. At 7 days post-challenge, paraffin-embedded lung parenchymal tissue sections were (I–IV) stained with hematoxylin and eosin and (V–VIII) for immunohistochemistry. The symbols (I) show pulmonary macrophages infiltrate. Viral antigen is seen as brown aggregates with an inset at higher magnification (20 μm) showing peribronchiolar virus identified with arrows and arrowheads (VIII). Reproduced with permission from Ref [103]. Copyright 2021, Joyce et al. Published by the American Association for the Advancement of Science.

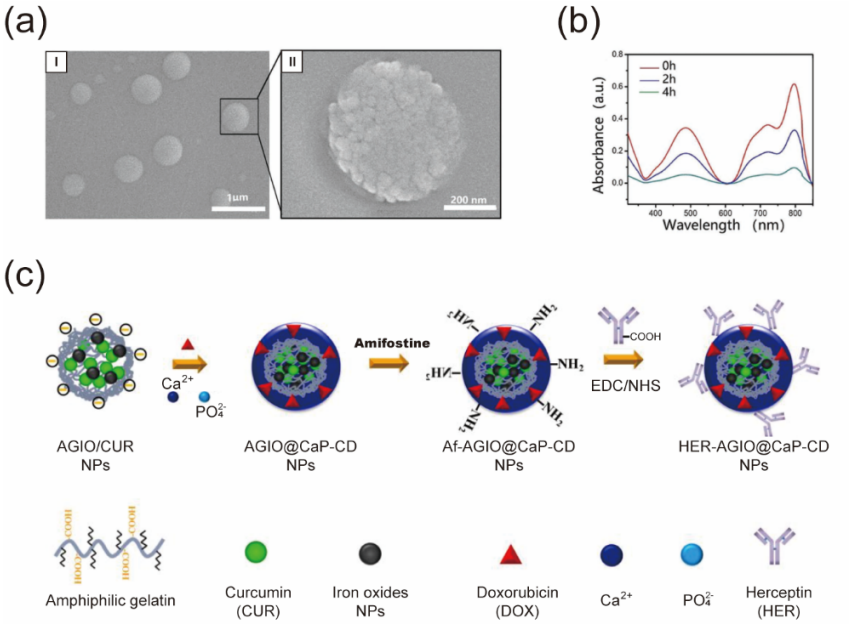

Fig. 4 Application of gelatin-based nanoparticles for photodynamic therapy and intracellular controlled sequential release of multiple drugs. (a) Scanning electron microscopy (SEM) images of resultant atovaquone-indocyanine green (Ato-ICG)-gelatin nanoparticles at low (I) and high (II) magnifications. (b) UV–vis–NIR spectra of Ato-ICG-gelatin nanoparticles before and after the introduction of MMP-2. (a,b) Reproduced from Ref [113] with permission from WILEY-VCH Verlag GmbH & Co. KGaA, Weinheim. Copyright 2019. (c) Schematic illustration showing the synthesis of gelatin@calcium phosphate nanoparticle containing both curcumin and DOX. AGIO, amphiphilic gelatin–iron oxide; Af, amifostine; CD, curcumin and DOX. Reproduced from Ref [114] with permission from Elsevier Ltd. Copyright 2015.

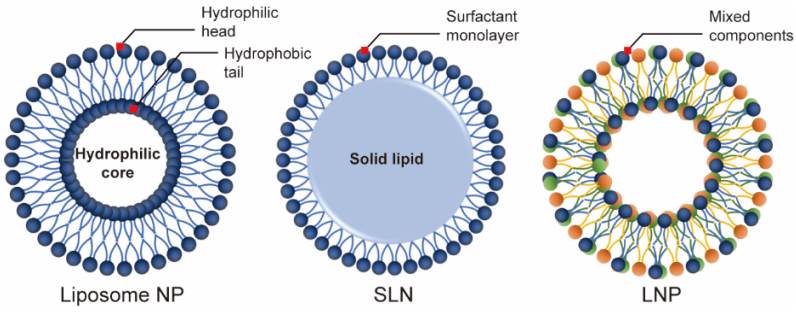

Fig. 5 Comparison of the structures of different lipid-based nanoparticles for advanced therapies.

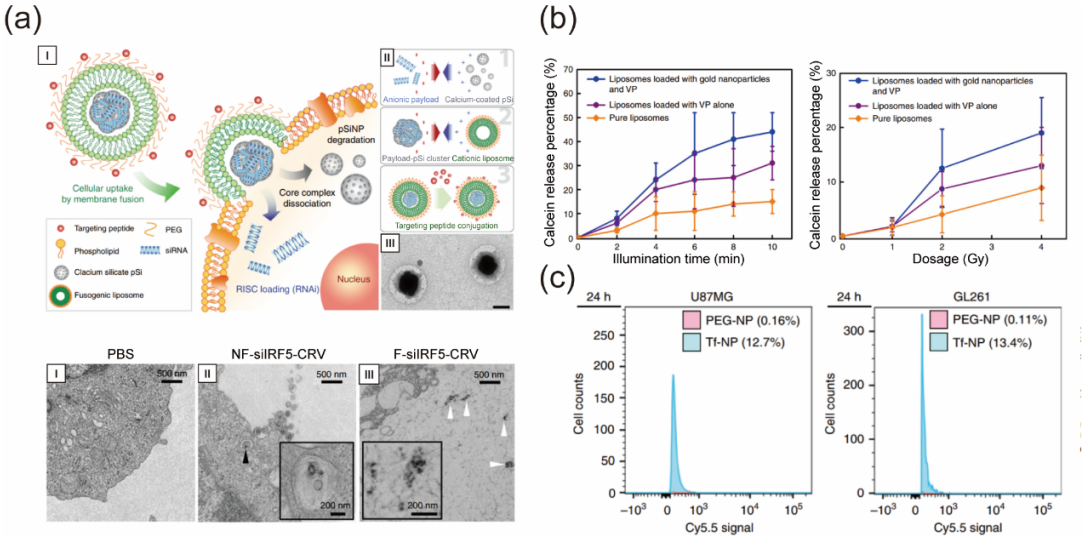

Fig. 6 Application of liposome-based nanoparticles for targeted and photodynamic gene therapies. (a) (Top panel) Fusogenic porous silicon nanoparticle system (F-pSi) based on liposomes. Schematics showing mode of action of F-pSi (I) and nanoparticle synthesis (II), including (1) siRNA loading into the porous silicon nanoparticles and entrapment by precipitation of calcium silicate; (2) coating of the nanoparticle clusters with cationic liposomes; and (3) conjugation of targeting peptides to the liposomal exterior. TEM image of final F-pSi constructs, showing cloudy liposomal coatings around dark and dense porous silicon-based cores (III). Negative staining by 2% phosphotungstic acid. Scale bar indicates 200 nm. (Lower panel) TEM images of Raw 264.7 murine macrophage cells after 10 min incubation with nanoparticles. Cells treated with phosphate-buffered saline (PBS) control confirm the absence of particles (I). Cells treated with nanoparticles containing a nonfusogenic lipid coating (II), siRNA against transcription factor Irf5, and the macrophage-targeting peptide (NF-siIRF5-CRV) display evidence of pinocytotic uptake (as indicated by the arrowheads); inset shows particles localized in vesicles (endosome/lysosome). Cells treated with nanoparticles containing fusogenic lipid coating, siRNA against transcription factor IRF5, and the macrophage-targeting peptide (F-siIRF5-CRV) become localized in the cell cytoplasm (III). Scale bar represents 20 µm. Reproduced with permission from Ref [119]. Copyright 2018, Kim et al. Published by Nature Publishing Group. (b) Calcein release profiles from liposomes under (left) 360 nm irradiation and (right) X-ray radiation. VP, verteporfin. Error bars show standard deviations from four measurements. Reproduced with permission from Ref [118]. Copyright 2018, Deng et al. Published by Nature Publishing Group. (c) Flow cytometry plots and quantification of cellular PEG-liposome or Tf-liposome nanoparticles signal in U87MG and GL261 cells. Reproduced with permission from Ref [121]. Copyright 2018, Lam et al. Published by Nature Publishing Group.

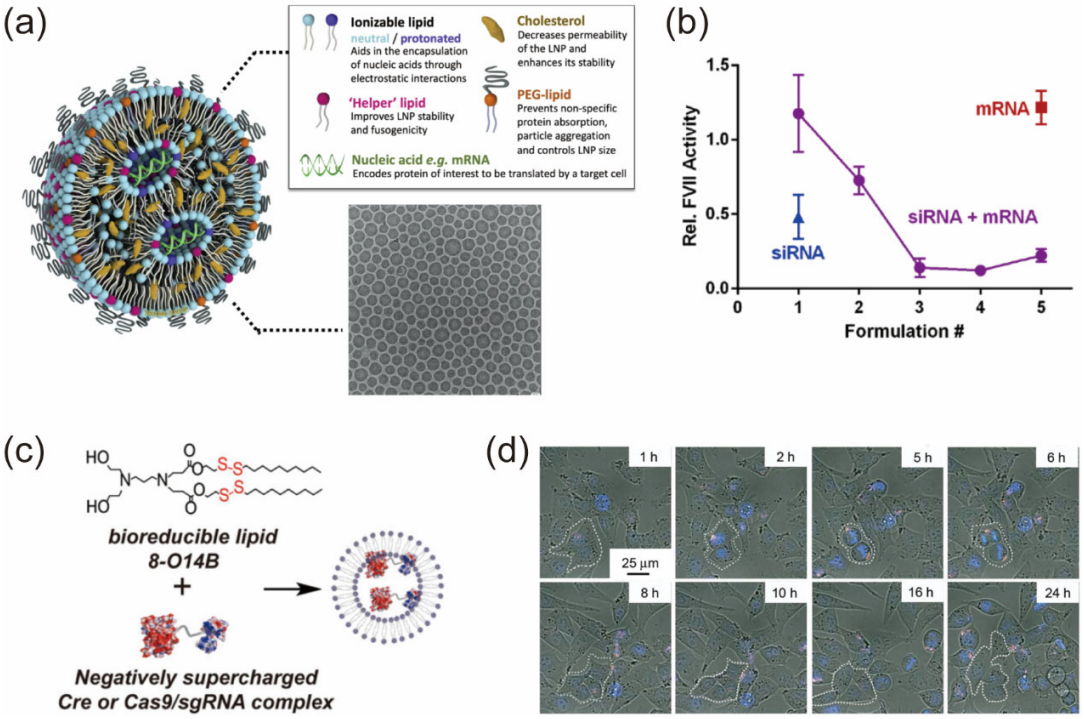

Fig. 7 Application of lipid nanoparticles for mRNA vaccine and gene therapies. (a) Structure of a typical lipid nanoparticle formulation: the cartoon scheme (left) highlights key components of a lipid nanoparticle with payload and how they contribute to its structure and function and a representative cryogenic-TEM image of LNPs with mRNA cargo. Reproduced from Ref [138] with permission from Elsevier Ltd. Copyright 2021. (b) LNPs co-formulated with both RNAs (siRNA + mRNA) induced higher levels of gene silencing than LNPs formulated with siRNA only or mRNA only (control) (n = 3). Reproduced from Ref [139] with permission from American Chemical Society. Copyright 2018. (c) Design of bioreducible lipid-like materials and negatively supercharged protein for effective protein delivery and genome editing. Cre, Cyclization recombination enzyme; sgRNA, single guide RNA. Reproduced from Ref [140] with permission from National Academy of Sciences of the United States of America. Copyright 2016. (d) Real-time tracking of the PEG-lipid/gold nanoclusters/Cas9 protein/sgPlk1 plasmid nanoparticles (LGCP) incubated with A375 cells for 24 h. (The white circles in the images indicate the distribution of Cas9 proteins and sgPlk1 plasmids within the cells at various time points, the cells highlighted by the white circles also display cellular division with the simultaneous separation of the internalized LGCP.) The A375 cells were incubated with LGCP for 0.5 h, stained with Hoechst 33342 for 15 min. Blue: cell nucleus; Green: FITCCas9 protein; Red: Cy3-sgPlk1 plasmid. Reproduced with permission from Ref [145]. Copyright 2017, Wang et al. Published by Wiley-VCH Verlag GmbH & Co KGaA, Weinheim.

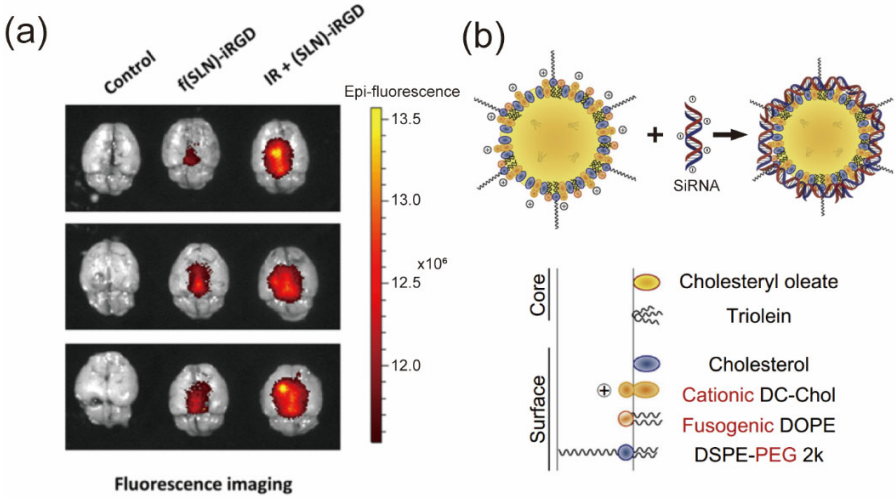

Fig. 8 Application of SLNs for targeted radiation and gene therapies. (a) Mice bearing GL261-Fluc tumors were irradiated (or not as control) and 3 days later received retro-orbital administration of f(SLN)-iRGD:Cy5.5 or PBS control. Twenty-four hours postinjection, brains were removed and imaged ex vivo for Cy5.5. Reproduced from Ref [153] with permission from American Chemical Society. Copyright 2019. (b) Schematic illustration of the formation of cSLN/siRNA complex by electrostatic interactions between positively charged cSLN and negatively charged siRNA. DC-Chol, 3β-[N-(N′,N′-dimethylaminoethane)carbamoyl]cholesterol; DOPE, L-α-dioleoyl phosphatidylethanolamine; DSPE-PEG 2k, 1,2-distearoyl-*sn*-glycero-3-phosphoethanolamine-N-[methoxy polyethylene glycol)-2000]. Adapted from Ref [156] with permission form Elsevier Ltd. Copyright 2013.

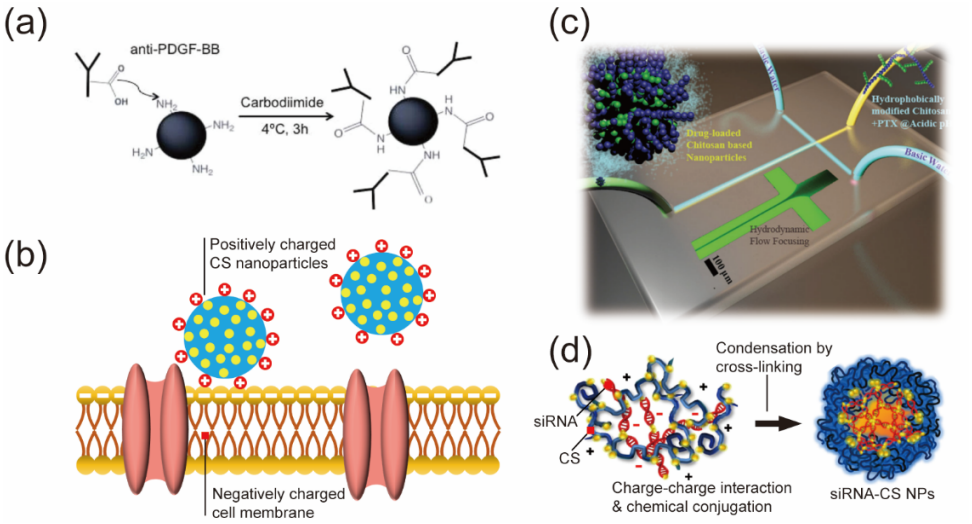

Fig. 9 Application of CS-based nanoparticles for targeted therapies. (a) Schematic representation of antibody immobilization process on the chitosan injectable microparticles. The carboxyl group in the antibody is activated with carbodiimide to form an active ester group that spontaneously reacts with primary amines in the CS particles to form an amide bond. Reproduced from Ref [165] with permission from Wiley-VCH Verlag GmbH & Co KGaA, Weinheim. Copyright 2014. (b) Mechanism of CS nanoparticles used for targeted drug delivery. (c) Schematic representation of a T-shaped microfluidic device, which is used to hydrodynamically focus flow of hydrophobically modified chitosan using a sheath flow of water at basic pH. Inset is a fluorescence image of Rhodamine B hydrodynamically focused with fluorescein sodium streams (scale bar 100 μm). (c) Reproduced from Ref [168] with permission from Wiley-VCH Verlag GmbH & Co KGaA, Weinheim. Copyright 2014. (d) Formation of siRNA-CS nanoparticles. Adapted from Ref [176] with permission from Elsevier Ltd. Copyright 2015.

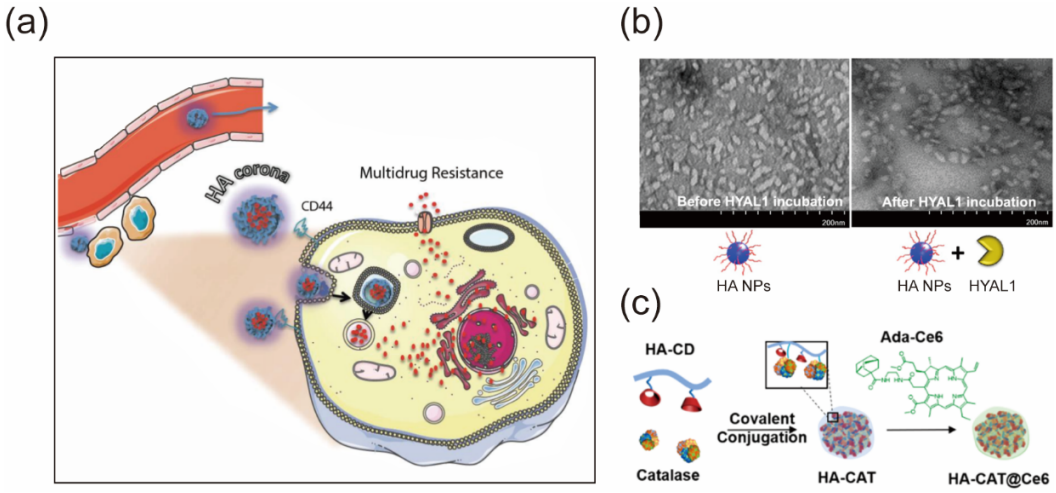

Fig. 10 Application of HA-based nanoparticles for targeted drug delivery. (a) Illustration of the *in vivo* biodistribution of HA-based nanosystems. Reproduced from Ref [177] with permission from Elsevier Ltd. Copyright 2016. (b) Stability of HA nanoparticles (HA NPs) against hyaluronidase 1 (HYAL1) degradation observed by TEM. Reproduced from Ref [183] with permission from Wiley-VCH Verlag GmbH & Co KGaA, Weinheim. Copyright 2020. (c) synthesis of catalase-encapsulated hyaluronic-acid-based (HA-CAT) nanoparticles for Ce6 delivery during photodynamic therapy. CD, β-cyclodextrin; Ada, adamantane; HA-CAT@Ce6, Ce6 encapsulated within HA-CAT nanoparticles. Reproduced from Ref [191] with permission from American Chemical Society. Copyright 2019.

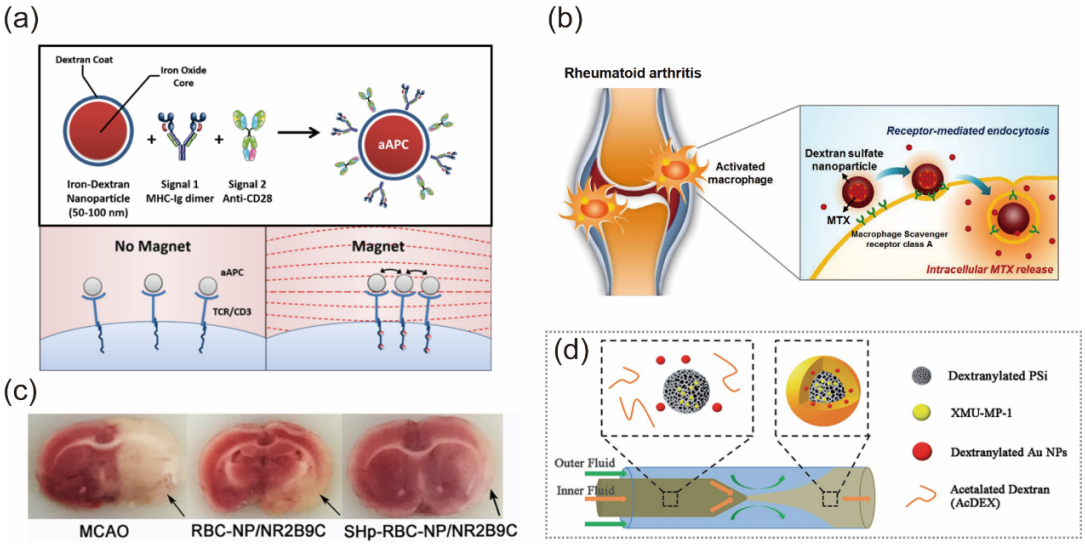

Fig. 11 Application of dextran-based nanoparticles for adoptive cancer immunotherapy and targeted drug delivery. (a) (Top panel) Schematic of nanoscale artificial antigen-presenting cells (nano-aAPC) synthesis by coupling major histocompatibility complex-immunoglobulin (MHC-Ig) dimers and co-stimulatory anti-CD28 to iron–dextran nanoparticles. (Lower panel) A magnetic field was used to drive aggregation of paramagnetic nano-aAPC, resulting in a doubling of T cell receptor (TCR) cluster size and increased T cell expansion in vitro and after adoptive transfer in vivo. Reproduced from Ref [195] with permission from American Chemical Society. Copyright 2014. (b) Schematic illustration of dextran nanoparticles as nanocarriers for targeted RA therapy. MTX, methotrexate. Reproduced from Ref [196] with permission from Elsevier Ltd. Copyright 2017. (c) Representative tissue slices showing that RBC-nanoparticles/NR2B9C and stroke homing peptide (SHp)-RBC-nanoparticles/NR2B9C with a dextran shell can significantly reduce the infarct volume; the arrows indicate the infarct region. MCAO, middle cerebral artery occlusion. Reproduced from Ref [201] with permission from American Chemical Society. Copyright 2018. (d) Schematic illustration of the procedure to prepare a novel nanohybrid based on porous silicon (PSi), gold nanoparticles (Au NPs) and AcDEX by microfluidics. Reproduced from Ref [204] with permission from Wiley-VCH Verlag GmbH & Co KGaA, Weinheim. Copyright 2017.

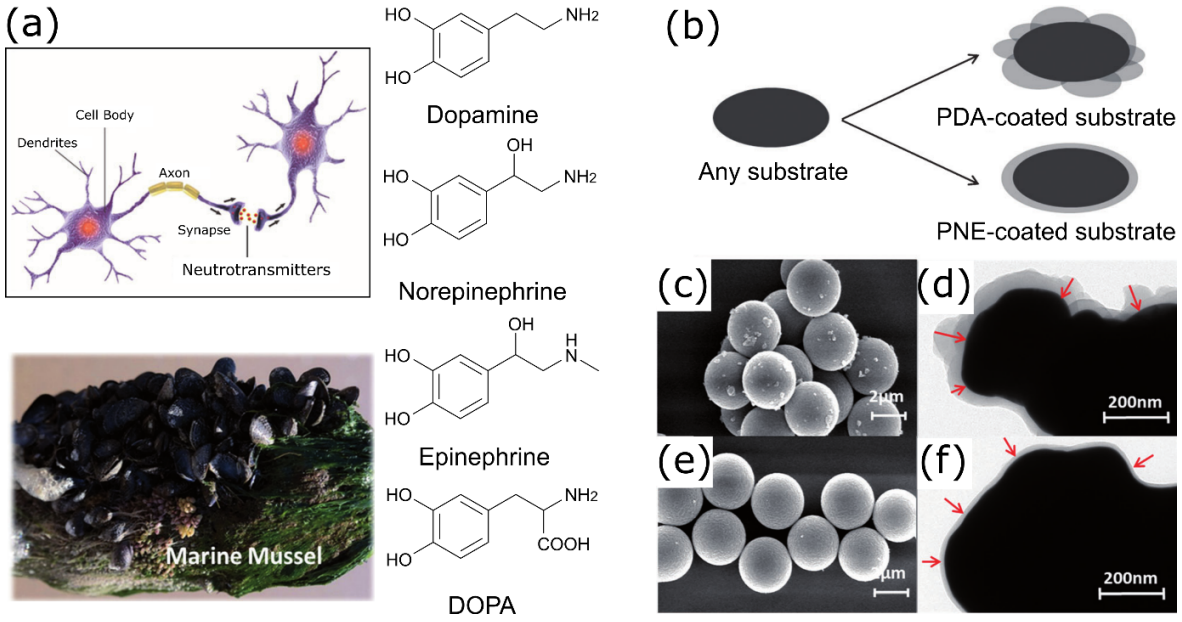

Fig. 12 (a) Catecholamines are found in the brain as neurotransmitters as well as in marine mussels as adhesive foot proteins. (b) Substrate-independent coating of PDA and PNE coating. (c) SEM and (d) TEM images showing a rough and thick PDA coating on polystyrene and sliver particles, respectively. (e) SEM and (d) TEM image showing a smooth and thin PNE coating on polystyrene and sliver particles, respectively. Reproduced from Ref [208] with permission from Wiley-VCH Verlag GmbH & Co KGaA, Weinheim. Copyright 2013.

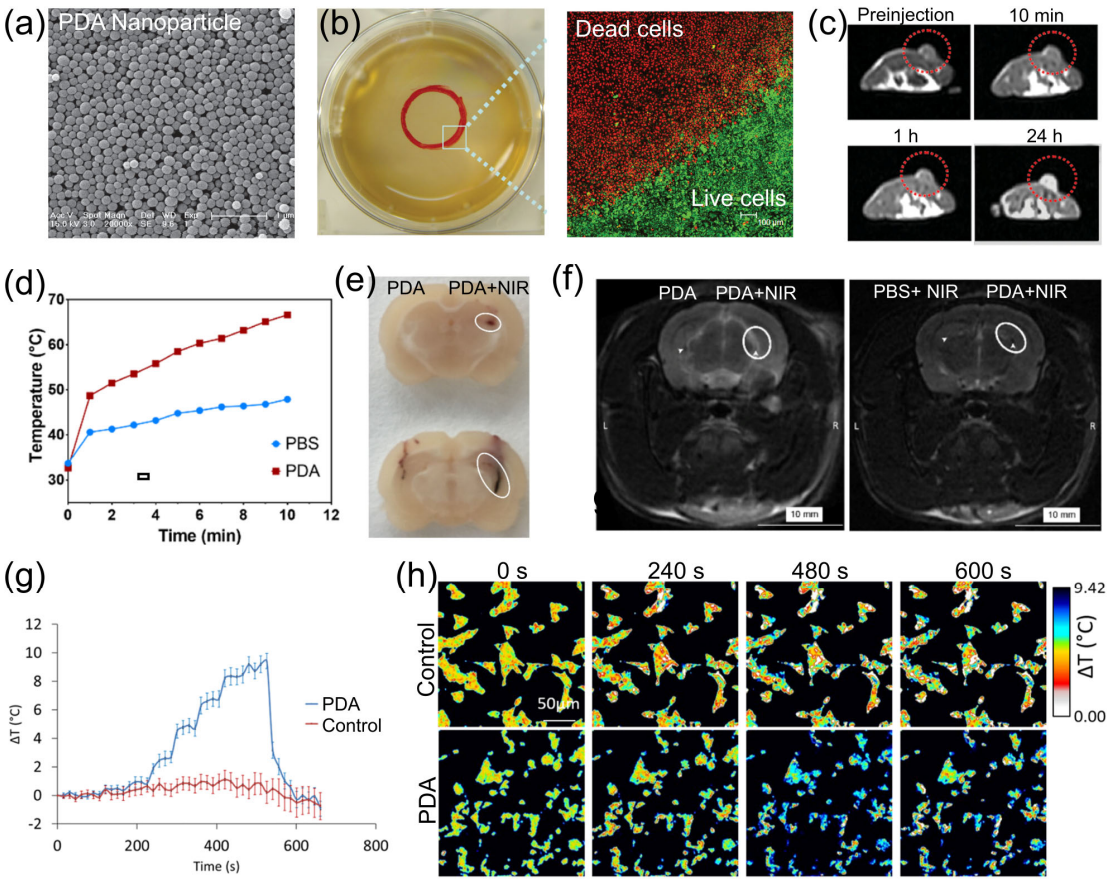

Fig. 13 PDA nanoparticles for photothermal therapy. (a) SEM image of self-assembled PDA nanoparticles. (b) In vitro experiment showing the photothermal effect of PDA nanoparticles. After incubation with PDA nanoparticles and NIR laser treatment (in the red circle), 4T1 cell were killed. (c) In vivo MRI imaging showing Gd-labeled PDA nanoparticles were accumulated in tumor after intravenous injection. (a–c) Reproduced from Ref [219] with permission from Wiley-VCH Verlag GmbH & Co KGaA, Weinheim. Copyright 2013. (d) Changes in the temperature of the brains of rats following injection with PBS or PDA nanoparticles and NIR irradiation. (e,f) photographs and MRI scanning of brain sections of rats treated with PDA or PBS with or without NIR. (d–f) Reproduced from Ref [251] with permission from American Chemical Society. Copyright 2020. (g,h) Temperature increase of neuron-like cells (SH-SY5Y) during NIR irradiation without (Control) or with PDA nanoparticles. (g,h) Reproduced from Ref [252] with permission from American Chemical Society. Copyright 2020.

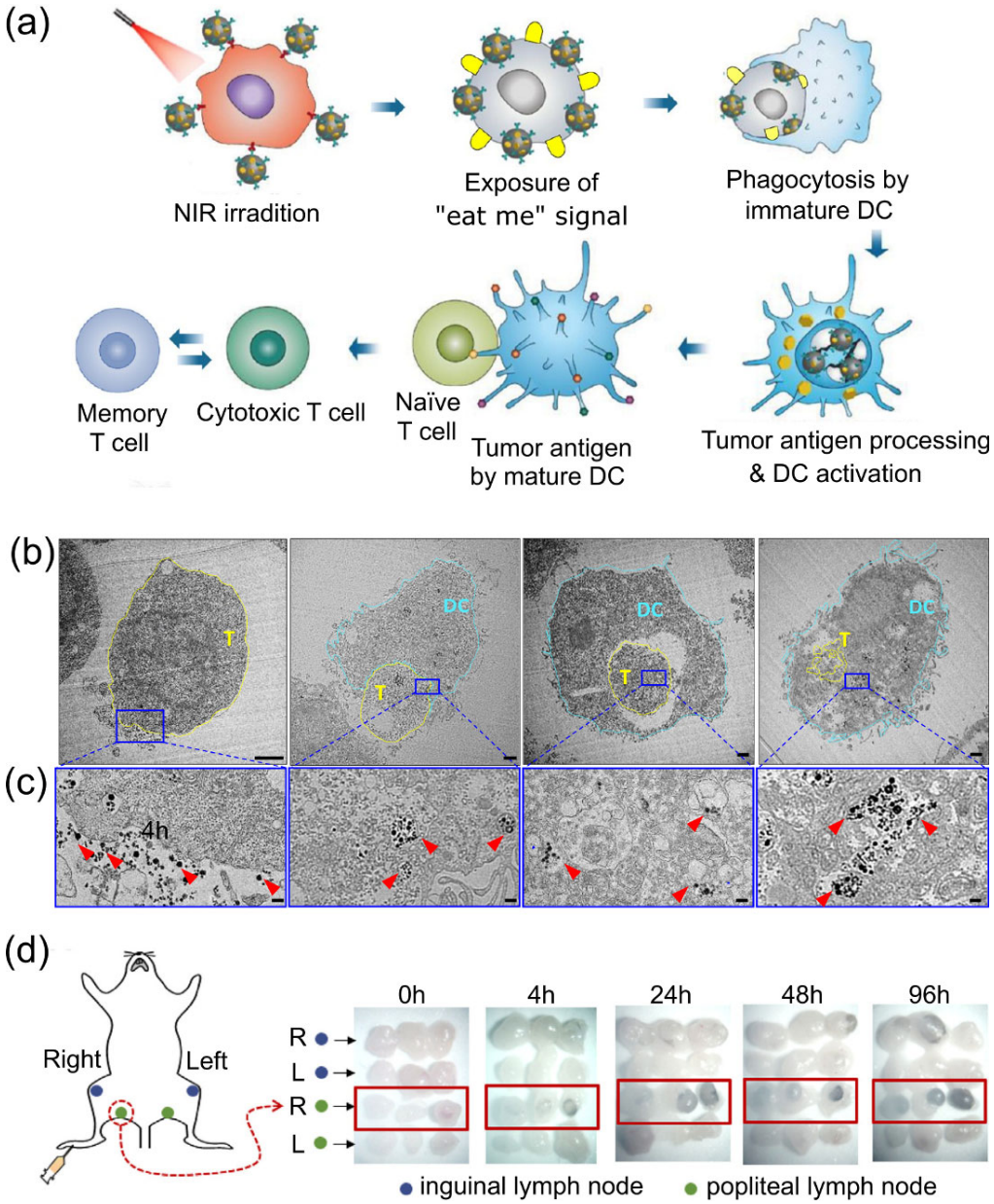

Fig. 14 PDA nanoparticles for immune therapy. (a) Illustration of the mechanism of photothermal immunotherapy using adjuvant-loaded PDA nanoparticles. Anti-PD-L1 antibody-functionalized PDA nanoparticles can target tumor cells. Upon NIR irradiation, the heat generated by the PDA nanoparticles kills tumor cells and promotes the phagocytosis of tumor cells by DCs. Subsequently, the mature DCs facilitate the differentiation of naïve T cells to antitumor cytotoxic T cells. (b) TEM images showing the phagocytosis of tumor cells by DCs. Scale bar: 2 μm. (c) Enlarged images of the corresponding blue-lined box areas in (b). Scale bar: 200 nm. (a–c) Reproduced from Ref [260] with permission from American Chemical Society. Copyright 2019. (d) Lymph node draining of PDA nanoparticles. Scheme of injection site and stereomicroscopy images of lymph nodes isolated at different time points (n = 3) after PDA

nanoparticle injection. (d) Reproduced from Ref [261] with permission form Elsevier Ltd. Copyright 2020.

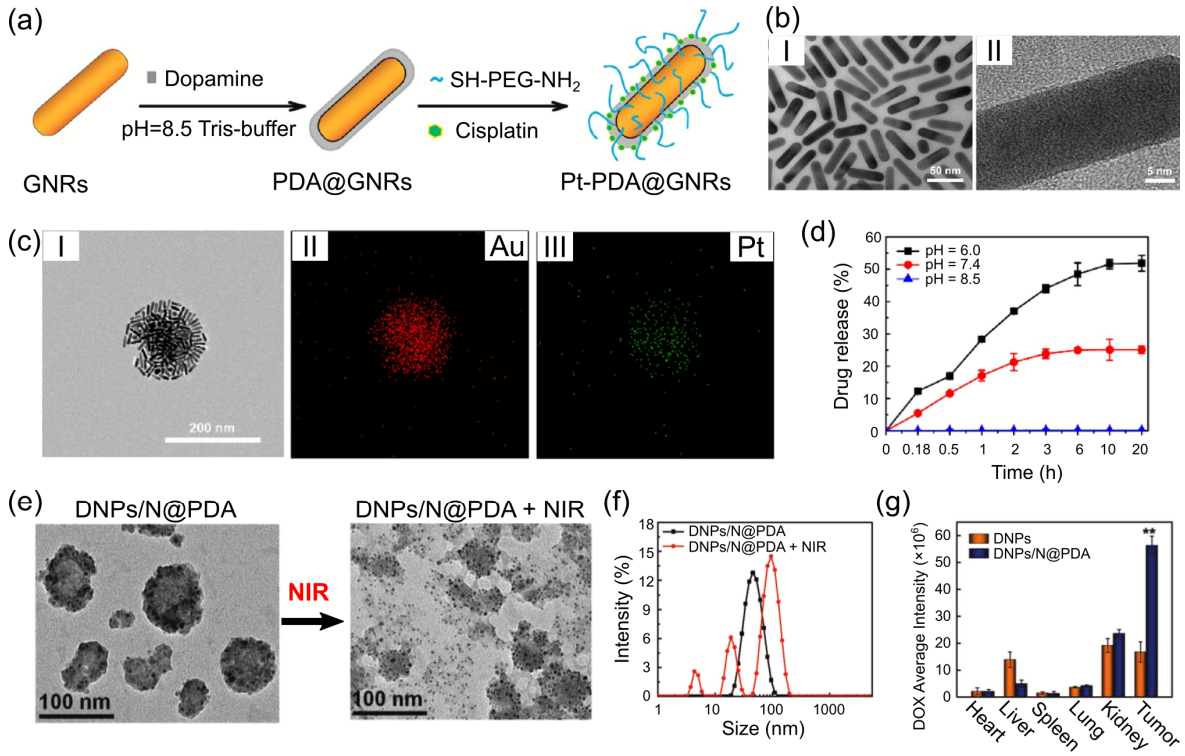

Fig. 15 PDA-coated nanoparticles for controlled drug release. (a) Illustration of PDA coating on gold nanorods (GNRs) that allows the loading of cisplatin and the conjugation of PEG linkers. (b) TEM images of GNRs after PDA coating. (c) Characterization of cisplatin loading on GNRs. TEM image (I), element mappings of Au (II) and Pt (III) of cisplatin-loaded PDA-coated GNRs (Pt-PDA@GNRs). (d) Release profiles of cisplatin from Pt-PDA@GNRs at different pHs. (a–d) Adapted from Ref [265] with permission from American Chemical Society. Copyright 2016. (e) TEM images and (f) hydrodynamic diameter distributions of PDA-coated NH_4HCO_3-encapsulated DOX nanoparticles (DNPs/N@PDA) before and after NIR irradiation. (g) Fluorescence intensity of DOX in tumors and major organs after 24 h intravenous injection of DOX nanoparticles (DNPs) or DNPs/N@PDA in mice. (e–g) Reproduced with permission from Ref [271]. Copyright 2018 Li et al. Published by Wiley-VCH Verlag GmbH & Co KGaA, Weinheim.

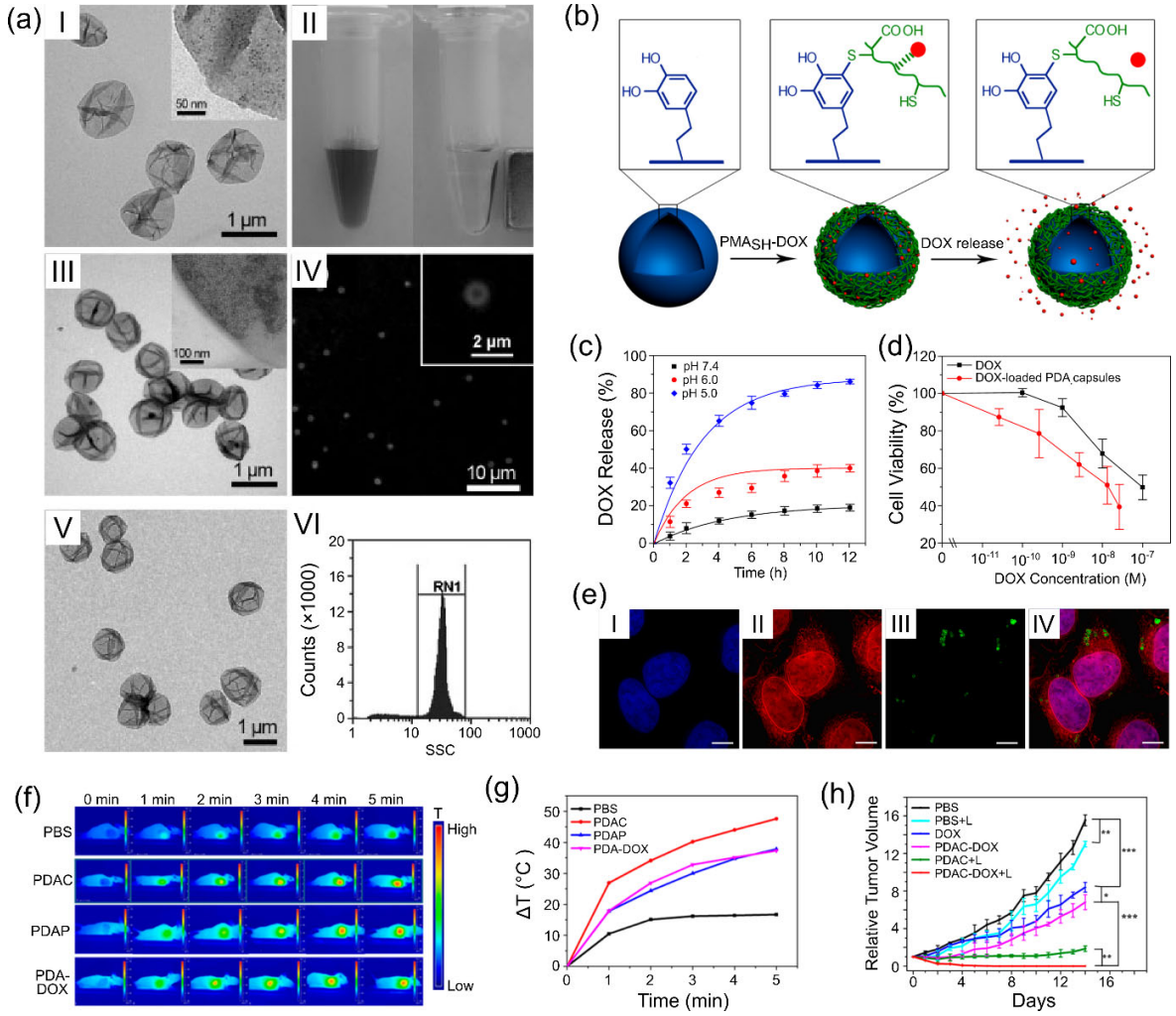

Fig. 16 PDA capsules for controlled drug delivery and cancer chemo-phototherapy. (a) PDA capsules loaded with magnetic Fe_3O_4 nanoparticle (I, II), fluorescent quantum dots (III, IV), hydrophobic drug thiocoraline (V, VI). (a) Reproduced from Ref [282] with permission from Wiley-VCH Verlag GmbH & Co KGaA, Weinheim. Copyright 2010. (b) Illustration of the DOX conjugation on PDA capsules through a pH-labile linker (red dots represent DOX). (c) DOX release profiles from DOX-loaded PDA capsules at pH 5.0, 6.0, and 7.4. (d) Cytotoxicity of DOX-loaded PDA capsules to HeLa cells, relative to free DOX, as a function of drug concentration. (e) Representative deconvolution images of HeLa cells after 24 h incubation with DOX-loaded PDA capsules. Blue, red, and green fluorescence represent stained cell nuclei (I), DOX (II), and AF488-labeled PDA capsules (III), respectively. A merged image of all three fluorescence images is shown in IV. (b–e) Reproduced from Ref [224] with permission from American Chemical Society. Copyright 2012. (f) Infrared thermal images of tumor-bearing mice injected with PBS, PDA capsules (PDAC), PDA solid particles (PDAP), and DOX-loaded PDA capsules (PDA-DOX) at different time points following NIR irradiation. (g) Temperature

changes of tumors measured by an infrared thermal camera in different sample groups under NIR irradiation. (h) Relative tumor volumes in mice after different treatments without or with laser irradiation (indicated as L). (f–h) Reproduced from Ref [286] with permission from American Chemical Society. Copyright 2017.

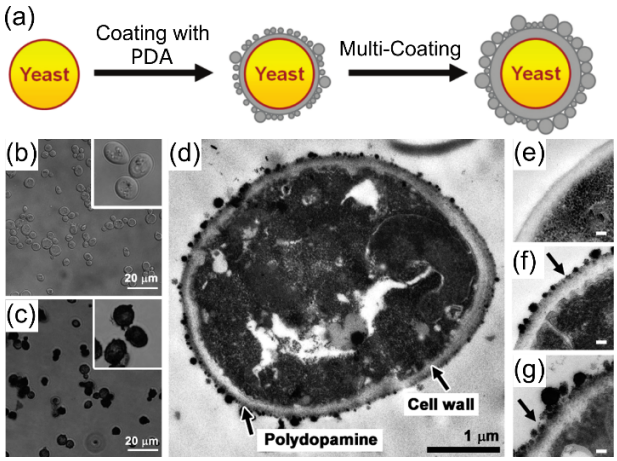

Fig. 17 PDA-enabled single cell encapsulation. (a) Illustration of PDA coating on yeast cells; the thickness of the PDA film can be increased by performing multiple coating steps. (b,c) Confocal microscopy images showing native yeasts (b) and PDA-coated yeasts (c). (d) TEM image showing a microtome-sliced PDA-coated yeast cell. (e–g) magnified TEM images of native yeast (e), PDA-coated yeast (f), and double PDA-coated yeast (g). Reproduced from Ref [287] with permission from American Chemical Society. Copyright 2011.

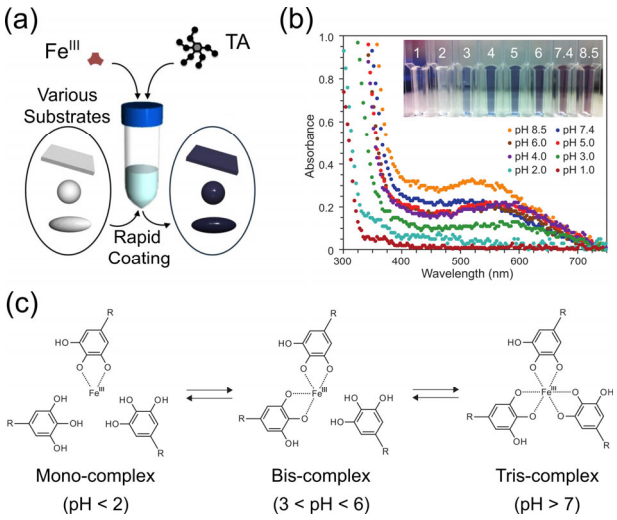

Fig. 18 (a) Illustration of MPN assembly by coating TA–Fe coordination complexes on various substrates. (b) UV absorbance spectra and photograph of MPN capsule dispersions at various pH. (c) pH-Dependent transition of TA–Fe coordination complexes. Reproduced from Ref [313] with permission from American Association for the Advancement of Science. Copyright 2013.

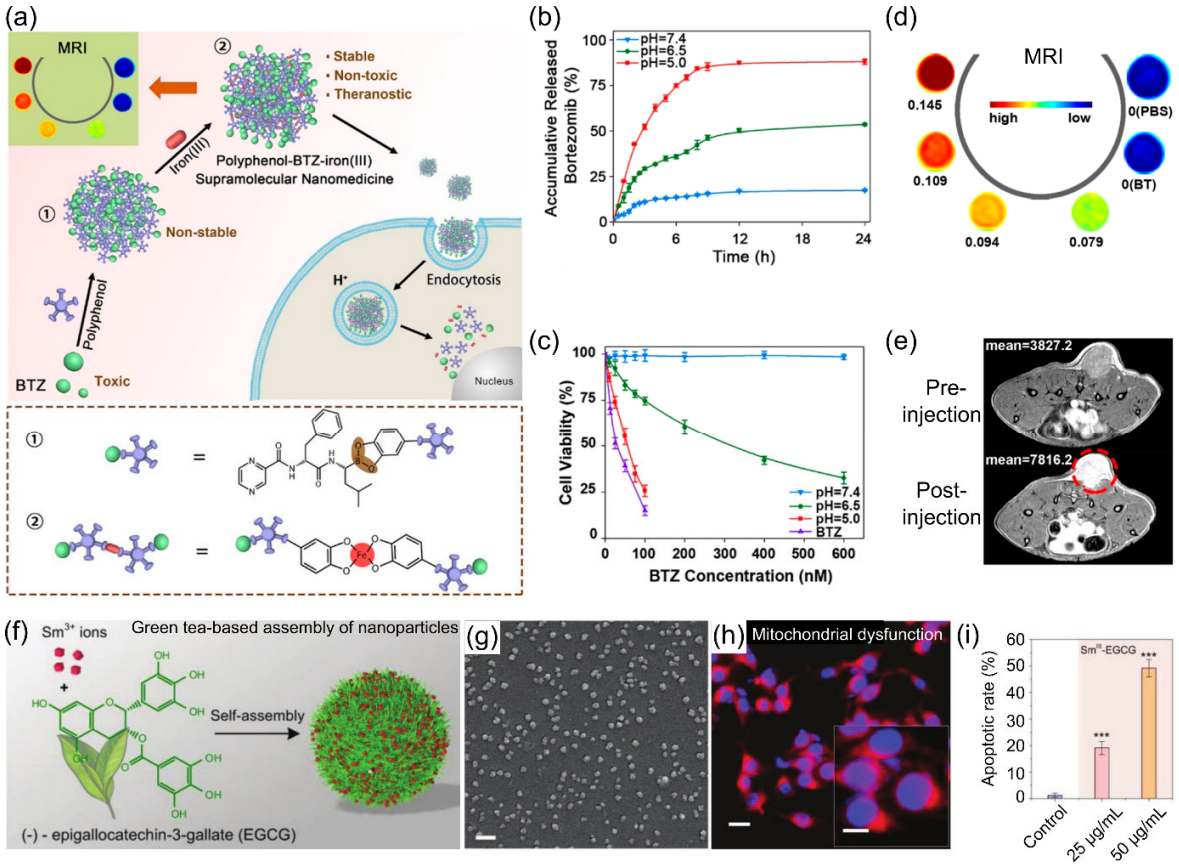

Fig. 19 Self-assembled MPN nanoparticles for medical imaging, controlled drug release, and synergistic chemotherapy. (a) Assembly of MPN nanoparticles using natural polyphenol, BTZ, and iron(III). (b) pH-Dependent BTZ release profile from MPN nanoparticles. (c) Viability of MDA-MB-231 cells after treatment with BTZ-loaded MPN nanoparticles at different pH for 48 h. (d) In vitro T_1-weighted MRI scan of MPN nanoparticle suspension as a function of iron(III) concentration (mM). (e) In vivo T_1-weighted MRI images showing tumor accumulation of MPN nanoparticles (indicated by the red circle) after intravenous injection in mice. (a–e) Reproduced from Ref [325] with permission from American Chemical Society. Copyright 2018. (f) Green tea polyphenol-based assembly of Sm^{III}–EGCG nanoparticles. (g) SEM imaging of Sm^{III}–EGCG nanoparticles. Scale bar is 100 nm. (h) Fluorescence microscopy image showing mitochondria membrane dysfunction of B16F10 cells after treatment with Sm^{III}–EGCG nanoparticles. The change of mitochondria membrane potential was detected by MitoTracker (red) probe. Scale bars are 20 and 10 μm in inset. (i) Apoptosis of B16F10 cells after 24 h incubation with Sm^{III}–EGCG nanoparticles at different particle concentrations. (f–i) Reproduced with permission from Ref [328]. Copyright 2019 Li et al. Published by Wiley-VCH Verlag GmbH & Co KGaA, Weinheim.

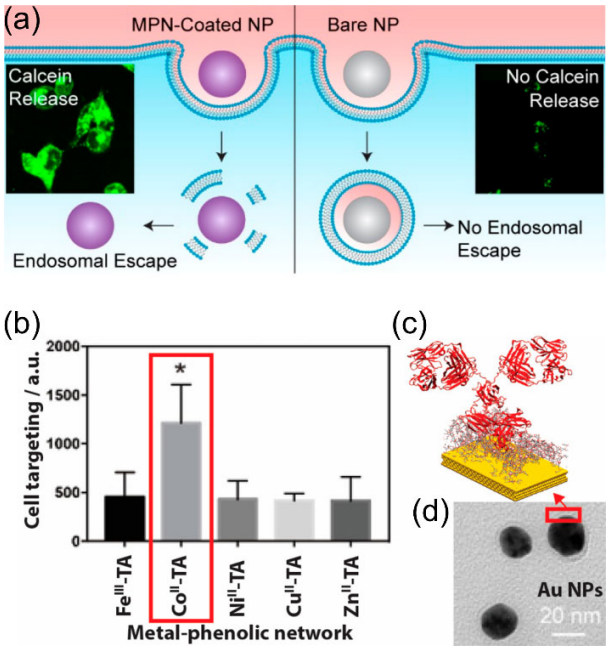

Fig. 20 Bio–nano interactions modulated by MPN coatings on nanoparticles. (a) Schematic illustration and fluorescence microscopy images (insets) of endosomal escape of bare and MPN-coated nanoparticles. Reproduced from Ref [334] with permission from American Chemical Society. Copyright 2019. (b) Cell targeting of MPN-coated gold nanoparticles with surface-adsorbed antibodies. (c) Illustration of the specific antibody orientation mediated by MPN coatings. (d) TEM image of antibody-immobilized MPN-coated gold nanoparticles. (b–d) Reproduced from Ref [336] with permission from American Chemical Society. Copyright 2020.

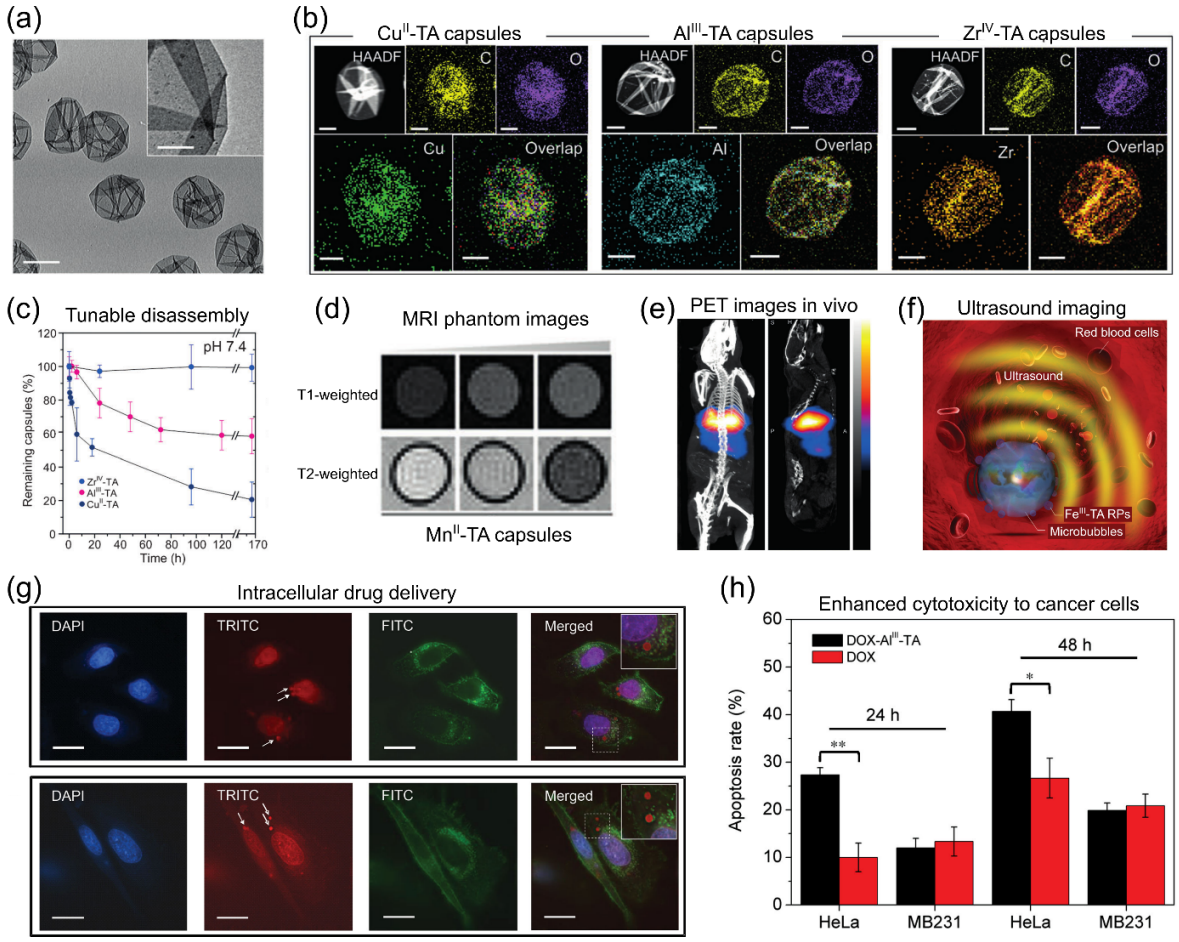

Fig. 21 Engineering multifunctional MPN capsules for medical imaging and controlled drug delivery. (a) TEM image of Cu^{II}–TA capsules. (b) Energy-dispersive X-ray spectroscopy elemental mapping of Cu^{II}–TA, Al^{III}–TA, Zr^{IV}–TA capsules. Scale bars are 2 μm and 200 nm (inset) in (a) and 1 μm in (b). (c) pH-Dependent disassembly profiles of Cu^{II}–TA, Al^{III}–TA, Zr^{IV}–TA capsules. (d) MRI phantom images of Mn^{II}–TA capsules immobilized in agarose gel. (e) PET/computed tomography scan of an in vivo mice model 30 min after intravenous injection of $^{64}Cu^{II}$–TA capsule suspension. (a–e) Reproduced from Ref [316] with permission from Wiley-VCH Verlag GmbH & Co. KGaA, Weinheim. Copyright 2014. (f) Schematic representation of microbubbles generated by Fe^{III}–TA replica particles (RPs) to probe H_2O_2 in vivo by ultrasound imaging. (f) Reproduced from Ref [341] with permission from Wiley-VCH Verlag GmbH & Co. KGaA, Weinheim. Copyright 2015. (g) Deconvolution microscopy images of intracellular delivery of DOX-loaded Al^{III}–TA capsules in MDA-MB-231 cells (top) and HeLa cells (bottom). Nucleus, DOX, and capsules are indicated in blue (4′,6-diamidino-2-phenylindole, DAPI), red (tetramethylrhodamine isothiocyanate, TRITC) and green (fluorescein isothiocyanate, FITC). (h) Apoptosis rate (%) of HeLa and MDA-MB-231 cells after treatment with free DOX or DOX-loaded Al^{III}–TA capsules for 24 or 48 h. (g,h) Reproduced from Ref [340] with permission from Wiley-VCH Verlag GmbH & Co. KGaA, Weinheim. Copyright 2015.

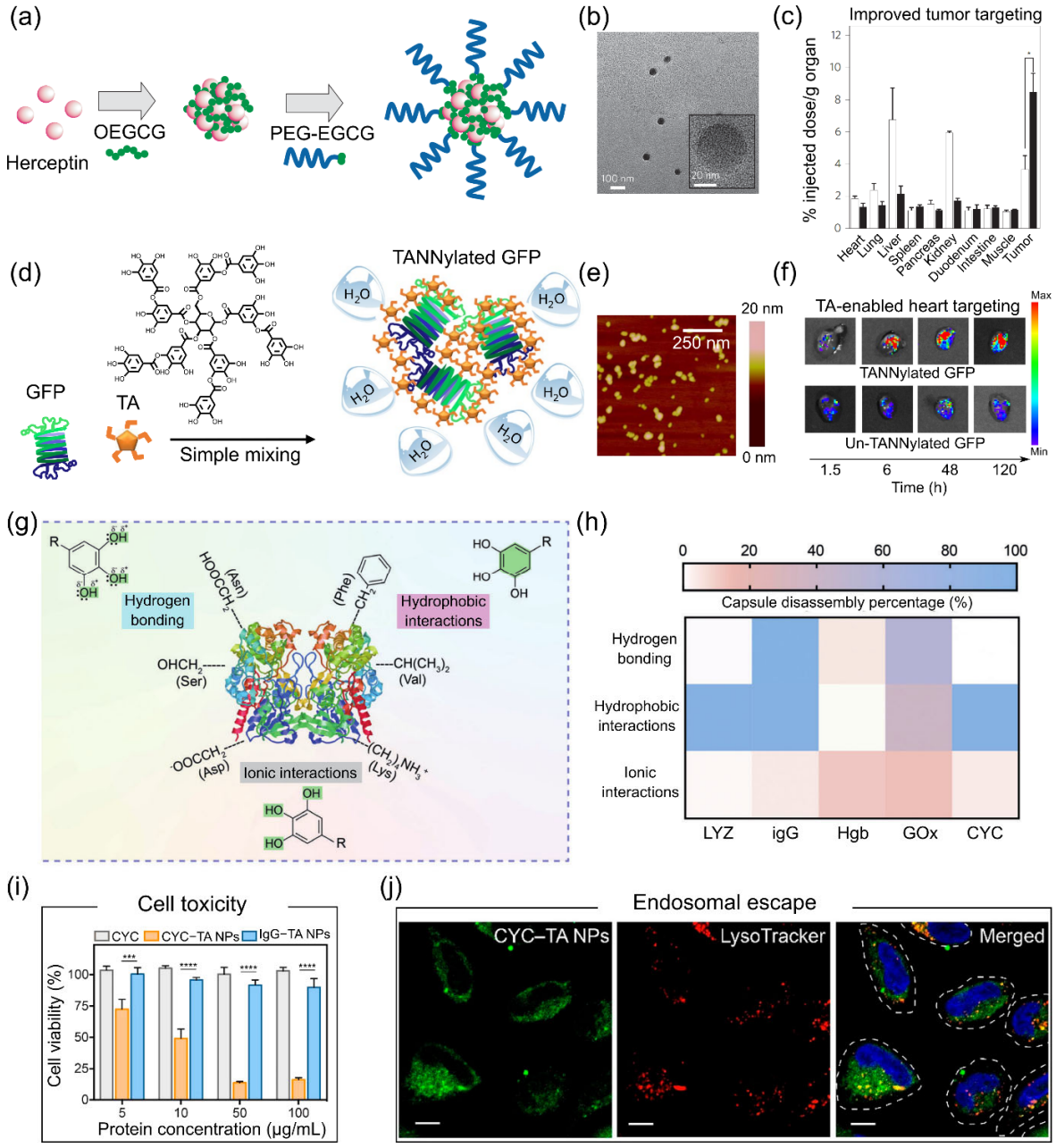

Fig. 22 Polyphenol–protein nanoparticles for targeted drug delivery. (a) Illustration of the self-assembly of Herceptin–EGCG nanoparticles. OEGCG, oligomerized EGCG. (b) TEM image of Herceptin–EGCG nanoparticles. (c) Biodistribution of free Herceptin (open bars) and Herceptin–EGCG nanoparticles (filled bars) in tumor and major organs at 24 h postinjection. (a–c) Adapted from Ref [25] with permission from Nature Publishing Group. Copyright 2014. (d) Schematic illustration of the assembly of TA-modified (TANNylated) green fluorescent protein (GFP). (e) AFM image of TANNylated GFP in nanoscale complexes. (f) Mapping of GFP fluorescence to show the accumulation of TANNylated GFP in heart as a function of time from

1.5 to 120 h. (d–f) Adapted from Ref [349] with permission from Nature Publishing Group. Copyright 2018. (g) Schematic illustration of the driving forces of protein–polyphenol interactions. (h) Disassembly percentage (%) of protein–polyphenol capsules (lysozyme (LYZ), immunoglobulin G (IgG), hemoglobin (Hgb), glucose oxidase (GOx), cytochrome C (CYC)) after 1 h incubation with 100 mM of urea, Tween 20, or NaCl, representing the dominant interactions between different proteins and TA. (g,h) Reproduced from Ref [350] with permission from Wiley-VCH Verlag GmbH & Co. KGaA, Weinheim. Copyright 2020. (i) Cell viability of MDA-MB-231 cells after 48 h incubation with free CYC, CYC–TA or IgG–TA nanoparticles at different protein concentrations. (j) Confocal laser scanning microscopy (CLSM) imaging of a LysoTracker colocalization assay showing the endosome escape of FITC-labeled CYC–TA nanoparticles after 24 h incubation with HeLa cells. Scale bares are 10 μm. (i,j) Reproduced from Ref [351] with permission from American Chemical Society. Copyright 2020.

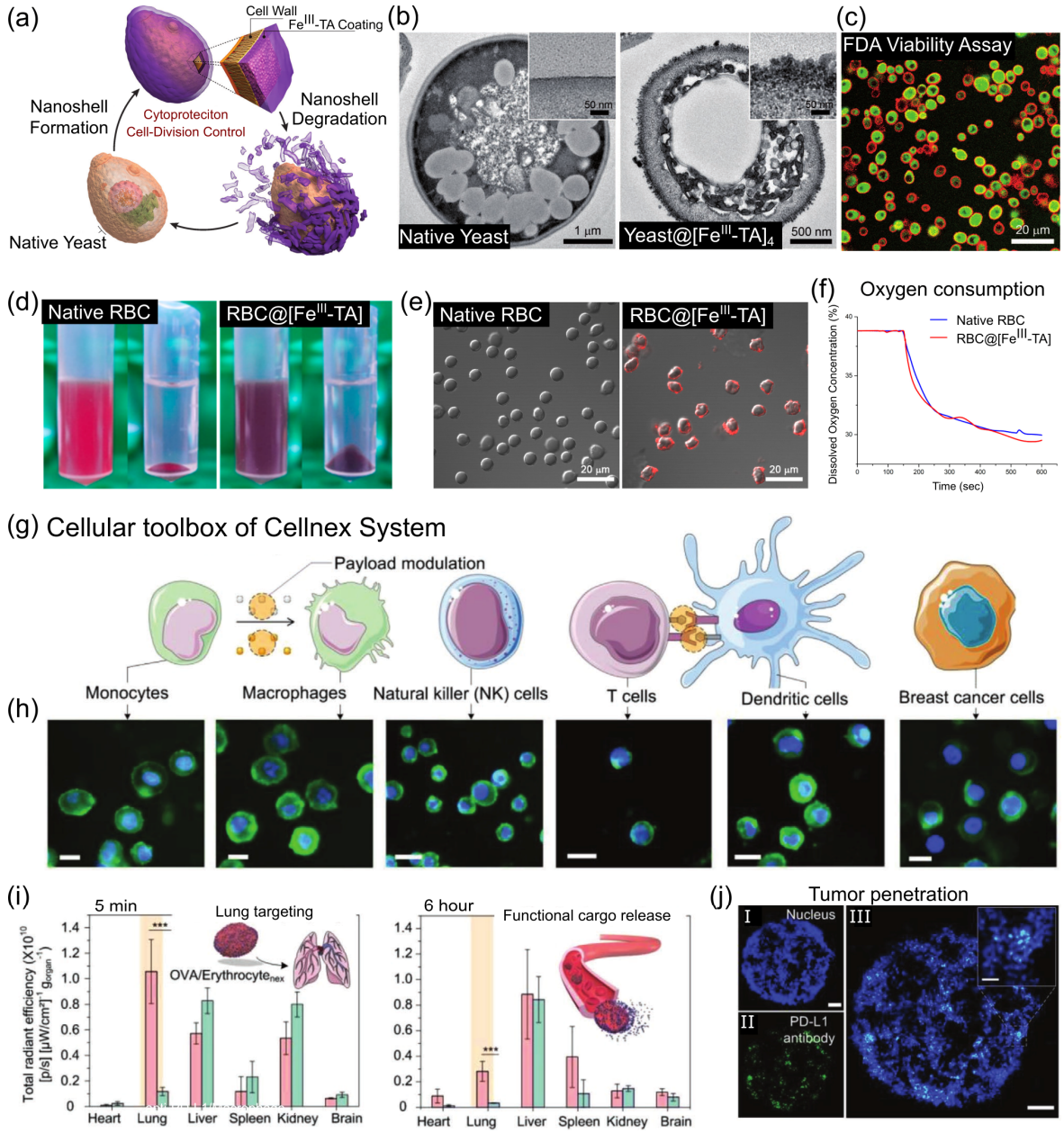

Fig. 23 Polyphenol-enabled cell engineering. (a) Schematic illustration of controlled MPN formation and disassembly on individual yeast cells. (b) TEM images of a native yeast and Fe^{III}–TA-coated yeast. (c) CLSM image of Fe^{III}–TA-coated yeast treated with bovine serum albumin-Alexa Fluor 647 and fluorescein diacetate for cell viability assay. (a–c) Reproduced from Ref [494] with permission from Wiley-VCH Verlag GmbH & Co. KGaA, Weinheim. Copyright 2014. (d) Photographs of native and Fe^{III}–TA-coated RBC suspension and pellets. (e) CLSM images of native and Fe^{III}–TA-coated RBCs treated with bovine serum albumin-Alexa Fluor 647. (f) Oxygen consumption of native and Fe^{III}–TA-coated RBCs as a function of time. (d–f) Reproduced from Ref [359] with permission from MDPI. Copyright 2017. (g) Schematic

illustration of the bio-functions and cross-interactions of immune cells that are used to prepare Cellnex systems through the assembly of polyphenol-functionalized nanocomplexes on cells. (h) Fluorescence microscopy images of six types of Cellnex systems prepared by coating polyphenol-functionalized bovine serum albumin-Alexa Fluor 488 on mammalian cells. Scale bars are 10 μm. (i) Biodistribution of free OVA (green) and OVA/Erythrocyte$_{nex}$ (pink) 5 min and 6 h after intravenous administration. (j) CLSM images of a representative 4T1 breast tumor spheroid treated with Macrophage$_{nex}$ conjugated with polyphenol-functionalized anti-PD-L1 antibody-Alexa Fluor 488. Blue and green colors represent nucleus stain and Alexa Fluor 488-labeled anti-PD-L1 antibody, respectively. Scale bars: 50 μm in (I) and (II); and 100 and 20 μm in (III) and inset, respectively. (g–j) Reproduced from Ref [361] with permission from Wiley-VCH Verlag GmbH & Co. KGaA, Weinheim. Copyright 2020.

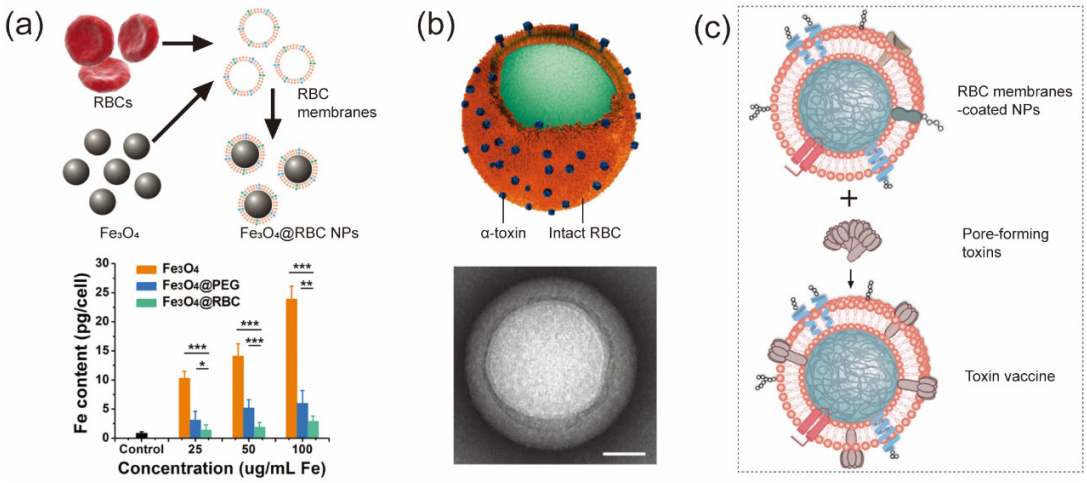

Fig. 24 Application of RBC membrane-based nanoparticles as biomimetic drug carriers. (a) (Top panel) Schematic of preparation of Fe_3O_4@RBC. (Lower panel) Quantitative analysis of the macrophage uptake of nanoparticles at different concentrations with an incubation time of 4 h. Adapted from Ref [366] with permission from Wiley-VCH Verlag GmbH & Co. KGaA, Weinheim. Copyright 2015. (b) (Top panel) Schematic structure of toxin-RBC nanosponges, which consist of substrate-supported RBC bilayer membranes into which PFTs can incorporate. (Lower panel) TEM visualization of nanosponges mixed with α-toxin (scale bar, 80 nm) and the magnified view of a single toxin-absorbed nanosponge (scale bar, 20 nm). Adapted from Ref [372] with permission from Nature Publishing Group. Copyright 2013. (c) Nanotoxoids are fabricated by inserting PFTs into RBC membrane-coated nanoparticles, a process that neutralizes their toxicity. Adapted from Ref [495] with permission from Wiley-VCH Verlag GmbH & Co. KGaA, Weinheim. Copyright 2018.

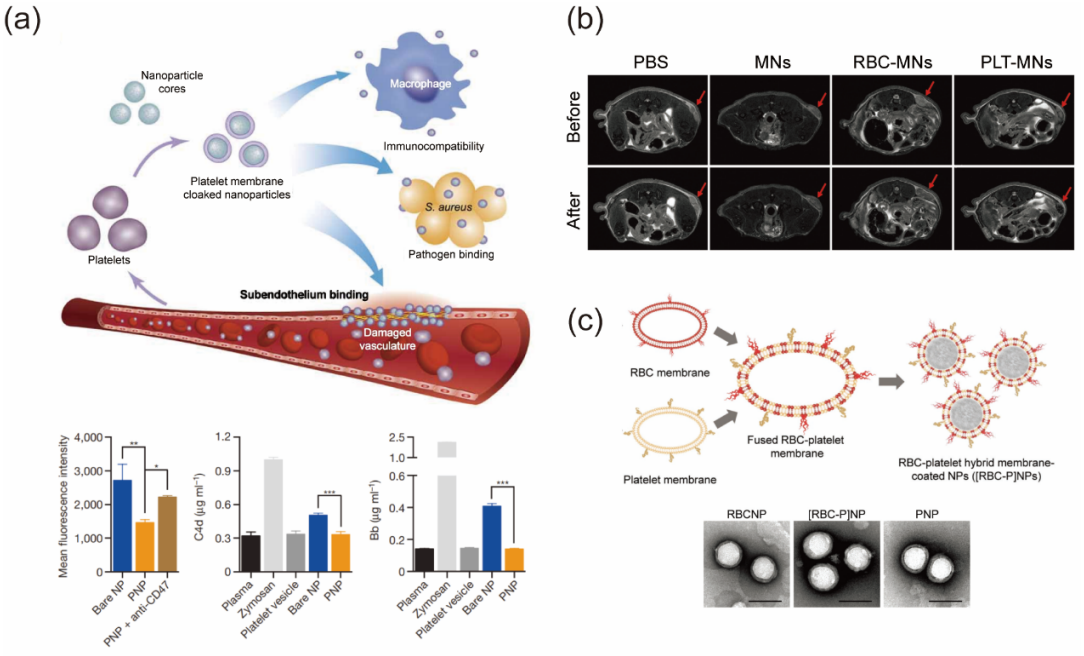

Fig. 25 Application of PLT membrane-based nanoparticles as biomimetic drug carriers. (a) (Top panel) PLGA nanoparticles are enclosed entirely within the plasma membrane derived from human PLTs. The resulting particles possess PLT-mimicking properties for immunocompatibility, subendothelium binding, and pathogen adhesion. (Lower panel) Low cytometric analysis of nanoparticle uptake by human THP-1 macrophage-like cells (n = 3). PNP, platelet membrane-cloaked nanoparticles. Reproduced from Ref [382] with permission from Nature Publishing Group. Copyright 2015. (b) Representative in vivo T2-weighted MRI images of MCF-7 tumor bearing mice before and after injection of PBS or PBS containing various nanoparticles. Red arrows indicate the sites of tumors. MN, magnetic nanoparticle. Reproduced from Ref [384] with permission from Wiley-VCH Verlag GmbH & Co. KGaA, Weinheim. Copyright 2017. (c) Schematic of membrane fusion using both RBCs and PLTs. The resulting fused membrane is used to coat PLGA polymeric cores to produce RBC–PLT nanoparticles. (c) Reproduced from Ref [385] with permission from Wiley-VCH Verlag GmbH & Co. KGaA, Weinheim. Copyright 2017.

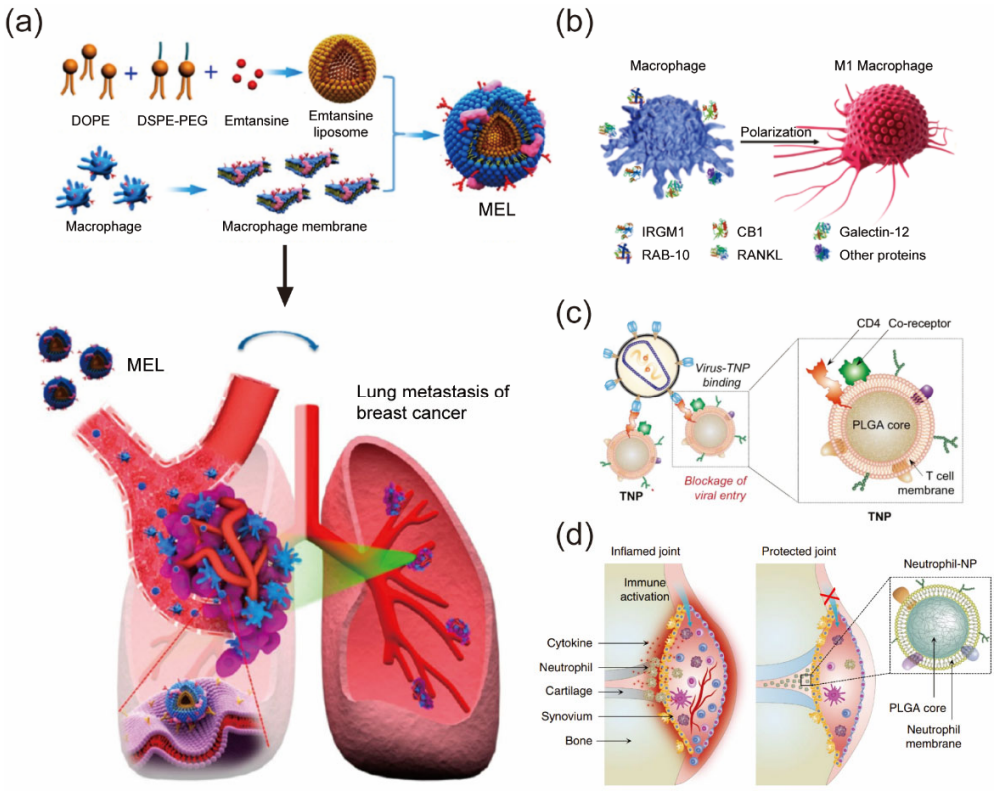

Fig. 26 Application of leukocyte membrane-based nanoparticles as biomimetic drug carriers. (a) Scheme of macrophage–membrane-coated emtansine liposomes with specific metastasis targeting for suppressing lung metastasis of breast cancer. MEL, macrophage–membrane-coated emtansine liposome. Reproduced from Ref [393] with permission from American Chemical Society. Copyright 2016. (b) Schematic illustration of human NK cell membrane proteins inducing M1-macrophage polarization. Reproduced from Ref [394] with permission from American Chemical Society. Copyright 2018. (c) Schematic representation of T-cell-membrane-coated nanoparticles (TNPs) designed for attenuating HIV infectivity. TNPs were constructed by wrapping polymeric cores with natural $CD4^+$ T cell membranes, which contain key antigens including CD4 receptor and CCR5 or CXCR4 coreceptors for viral targeting. Adapted from Ref [395] with permission from Wiley-VCH Verlag GmbH & Co. KGaA, Weinheim. Copyright 2018. (d) Schematic representation of neutrophil–nanoparticles designed for suppressing synovial inflammation and improving joint damage in inflammatory arthritis. Neutrophil–nanoparticles are constructed by wrapping polymeric cores in natural human neutrophil membranes, which mimic source cells to bind to immunoregulatory molecules without potentiating the immune cascades for disease progression. Reproduced from Ref [396] with permission from Nature Publishing Group. Copyright 2018.

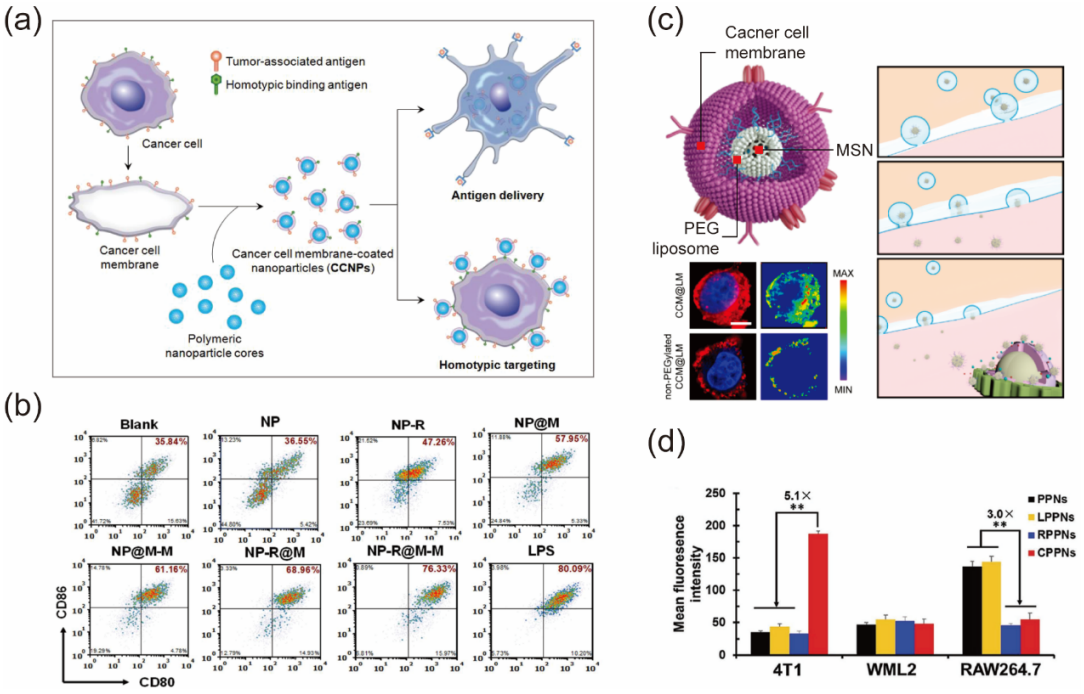

Fig. 27 Application of cancer cell membrane-based nanoparticles for targeted cancer therapies. (a) Schematic representation of cancer cell membrane-coated nanoparticle fabrication and potential applications. Reproduced from Ref [401] with permission from American Chemical Society. Copyright 2014. (b) Representative flow cytometry data to show DC maturation induced by different formulations of cell membrane-coated nanoparticles. NP-R, nanoparticles are loaded with R837; M, cancer cell membrane; M-M, cancer cell membrane modified with mannose moiety; LPS, lipopolysaccharides. Reproduced from Ref [398] with permission from American Chemical Society. Copyright 2018. (c) (Left, top panel) structure of a yolk–shell nanoparticle with a mesoporous silica nanoparticle (MSN)-supported PEGylated liposome yolk and cancer cell membrane coating (CCM@LM) for chemotherapy. (Left, lower panel) CLSM images and corresponding colorimetric maps of CCM@LM nanoparticle distributions in MCF-7 cells; red, nanoparticles. (Right) Schematic diagrams of the invasion pathway of CCM@LM: CCM@LM adheres to (top panel) and enters cells by membrane fusion (middle panel); and the released yolks gather around the nucleus after undergoing trafficking (bottom panel). Adapted from Ref [404] with permission from American Chemical Society. Copyright 2020. (d) Intracellular NIR fluorescence intensity showing the intracellular uptake of cancer-cell-biomimetic paclitaxel-loaded polymeric nanoparticles in 4T1 cells, WML2 cells, and RAW264.7 cells after 1 h incubation. PPNs, paclitaxel-loaded polymeric nanoparticles; LPPNs, liposome-coated PPNs; RPPNs, RBC-membrane-coated PPN; CPPNs, cancer-cell-membrane-coated PPNs. Reproduced from Ref [14] with permission from Wiley-VCH Verlag GmbH & Co. KGaA, Weinheim. Copyright 2016.

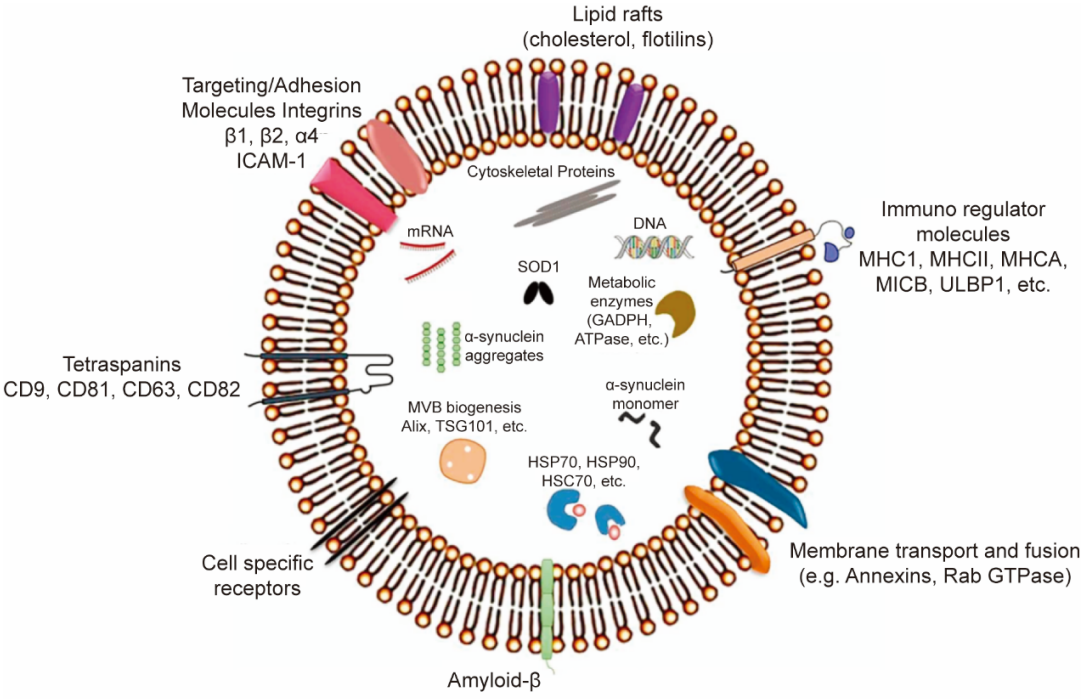

Fig. 28 Key components of a typical exosome. Reproduced from Ref [416] with permission from Elsevier Ltd. Copyright 2018.

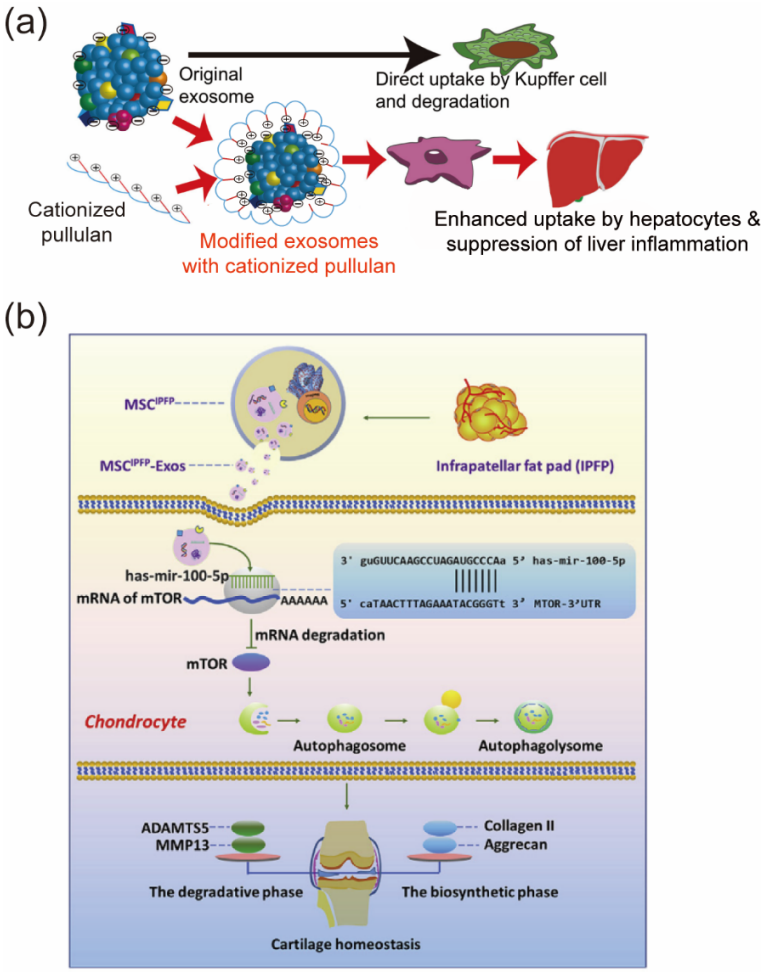

Fig. 29 Application of exosome nanoparticles derived from MSCs for immunotherapies. (a) Schematic representation of MSC-derived exosome nanoparticles modified with cationized pullulan for an enhanced anti-inflammatory effect on the targeted injured liver. Reproduced from Ref [430] with permission from Elsevier Ltd. Copyright 2017. (b) Proposed underlying mechanism of infrapatellar fat pad-derived MSC exosomes in cartilage protection. Reproduced from Ref [432] with permission from Elsevier Ltd. Copyright 2019.

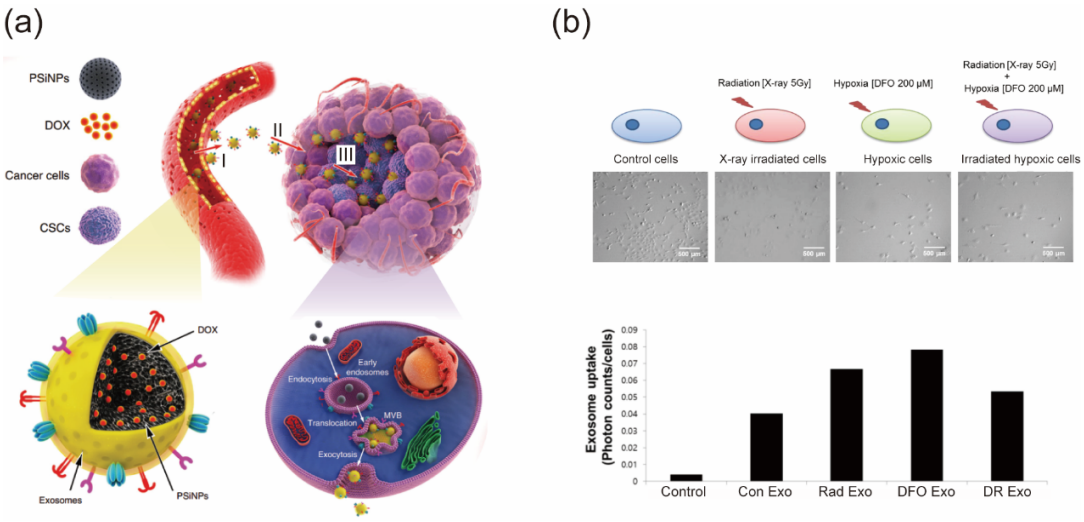

Fig. 30 Application of exosome nanoparticles derived from cancer cells for targeted cancer therapies. (a) (Left) Schematic illustration of the preparation of doxorubicin-loaded porous silicon exosome nanoparticles (DOX@E-PSiNPs). DOX@PSiNPs are endocytosed into cancer cells after incubation, then localized in multivesicular bodies (MVBs) and autophagosomes. After fusion of the MVBs or amphisomes with the cell membrane, DOX@E-PSiNPs are exocytosed into extracellular space. CSCs, cancer stem cells. (Right) Schematics showing how DOX@E-PSiNPs efficiently target tumor cells after intravenous injection into tumor-bearing mice: (I) DOX@E-PSiNPs efficiently accumulate in tumor tissues; (II) DOX@E-PSiNPs penetrate deeply into tumor parenchyma; and (III) DOX@E-PSiNPs are efficiently internalized into bulk cancer cells and cancer stem cells to achieve high anticancer efficacy. Adapted with permission from Ref [439]. Copyright 2019, Yong et al. Published by Nature Publishing Group. (b) (Top panel) Four different types of exosomes (generated under hypoxic or normoxic conditions, and with or without exposure to radiation) were isolated from human breast cancer MDA-MB-231 cells. (Lower panel) Uptake of fluorescence-labeled exosomes in hypoxic cancer cells was quantified by fluorescence, among which the highest uptake was for exosomes released by hypoxic cells. Con Exo, control exosome; Rad Exo, irradiated exosome; DFO Exo, hypoxic exosome; DR Exo, irradiated hypoxic exosome. Reproduced from Ref [436] with permission from Elsevier Ltd. Copyright 2018,

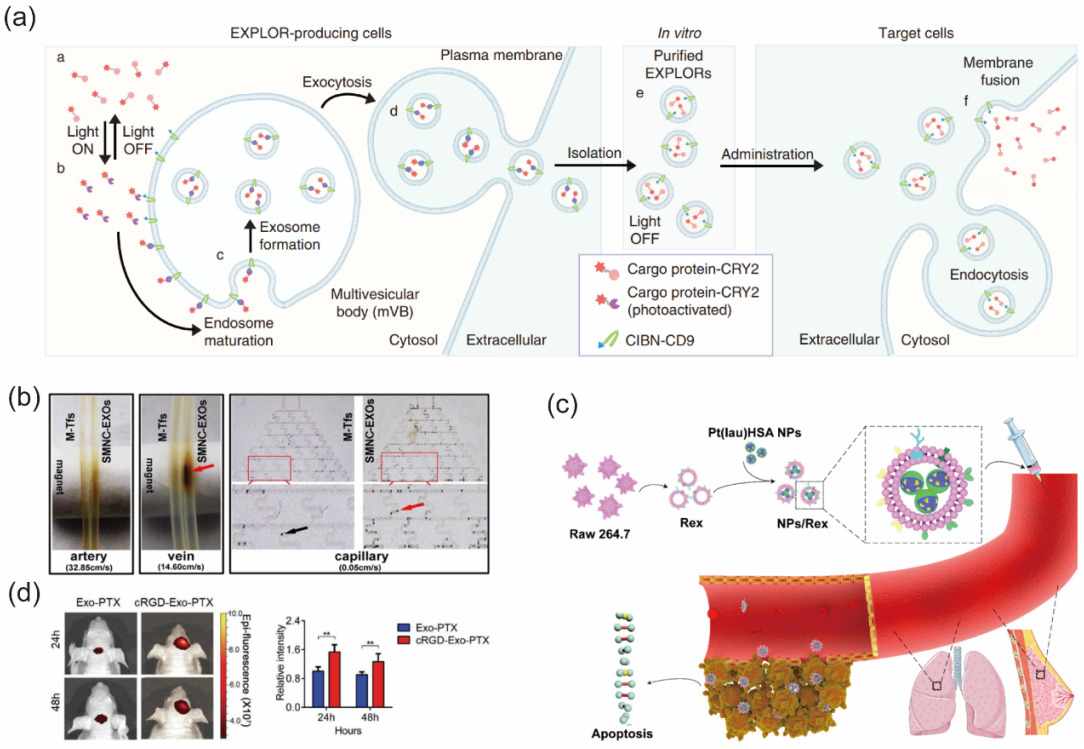

Fig. 31 Application of exosome nanoparticles derived from other sources for targeted therapies. (a) Schematic diagram of exosomes for protein loading via optically reversible protein–protein interactions (EXPLOR) technology. Reproduced with permission from Ref [440]. Copyright 2016, Yim et al. Published by Nature Publishing Group. (b) Magnetic retention of SPMN-Tf conjugations (M-Tfs) and SMNC-exosomes in simulated blood circulation system (flow velocities: artery, 32.85 cm s^{-1}; vein, 14.60 cm s^{-1}; and capillary, 0.05 cm s^{-1}); red arrows indicate SMNC-exosomes and the black arrow indicates M-Tfs. SPMN, superparamagnetic nanoparticles; SMNC, superparamagnetic nanoparticle cluster. M-Tfs, superparamagnetic nanoparticle–transferrin conjugations. Reproduced from Ref [426] with permission from American Chemical Society. Copyright 2016. (c) Schematic illustration of the Pt(lau)HSA nanoparticle-loaded macrophage exosome platform (NPs/Rex) for efficient chemotherapy of breast cancer. HSA, human serum albumin. Reproduced from Ref [443] with permission from American Chemical Society. Copyright 2019. (d) In vivo fluorescence images of embryonic stem cells-derived exosome-paclitaxel and the cRGD-exosome-paclitaxel at 24 and 48 h after intravenous injection, and quantitation of fluorescence intensity by the Spectrum/computed tomography software (n = 3). Reproduced with permission from Ref [446]. Copyright 2019, Zhu et al. Published by Wiley-VCH Verlag GmbH & Co KGaA, Weinheim.

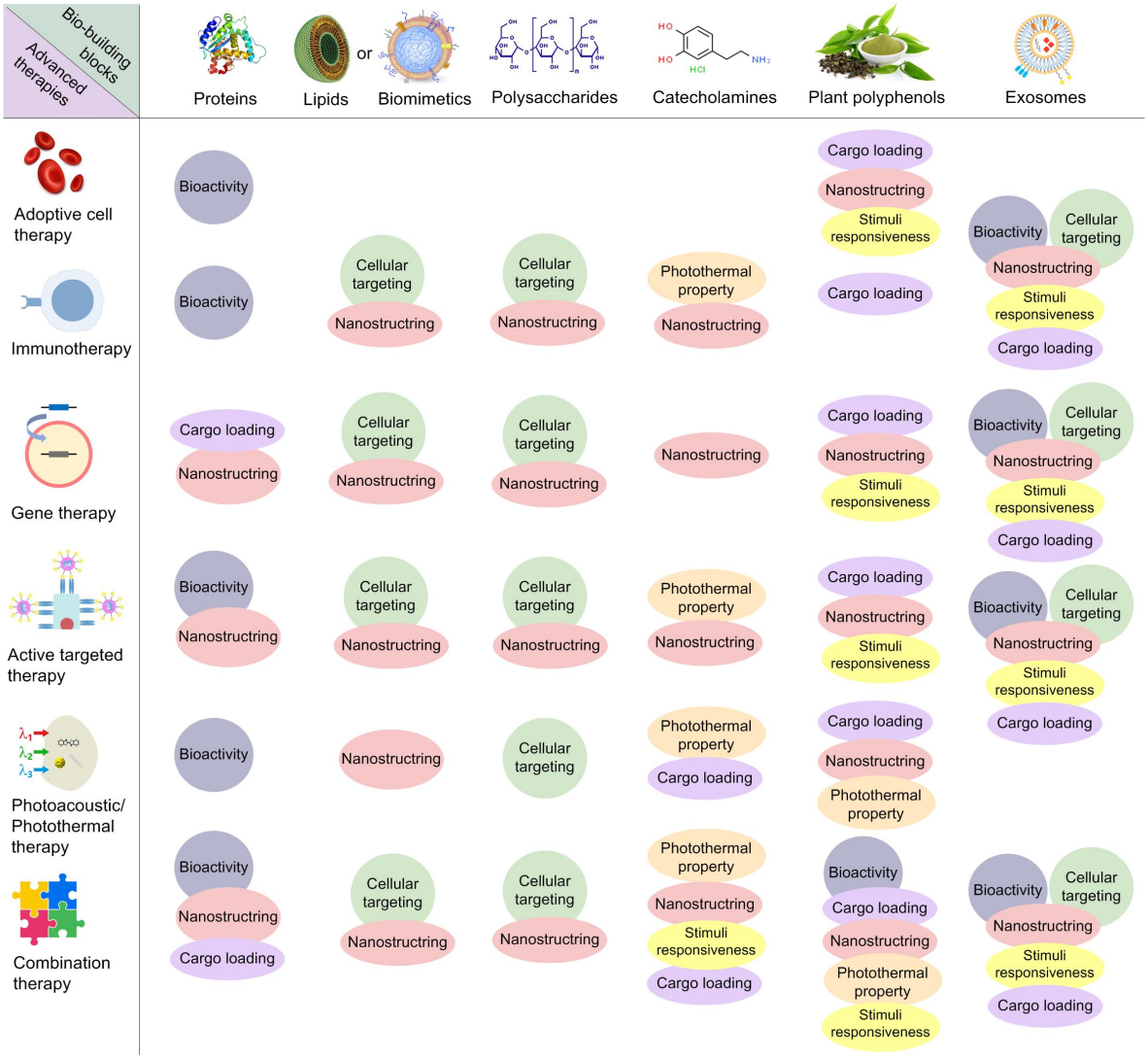

Fig. 32 Summary of the key functional properties of different natural building blocks and their use in the design of advanced therapies. (I) The ability to form nanoparticles through interactions with other therapeutic molecules or by themselves is the central property across the diagram. Lipid-based or biomimetic cell membrane-coated nanoparticles, and exosomes are studied extensively and widely used in nanoscale drug delivery systems. (II) Antibodies and polysaccharides are commonly used as bioactive compounds and cellular targeting components. (III) Mussel-inspired polydopamine, natural polyphenols, and other phenolics are versatile platforms for the engineering of particles meeting the requirements of emerging advanced therapies. (IV) Exosomes show great potential as next-generation therapies and as carriers owing to their high tailorability in structure and biological function.

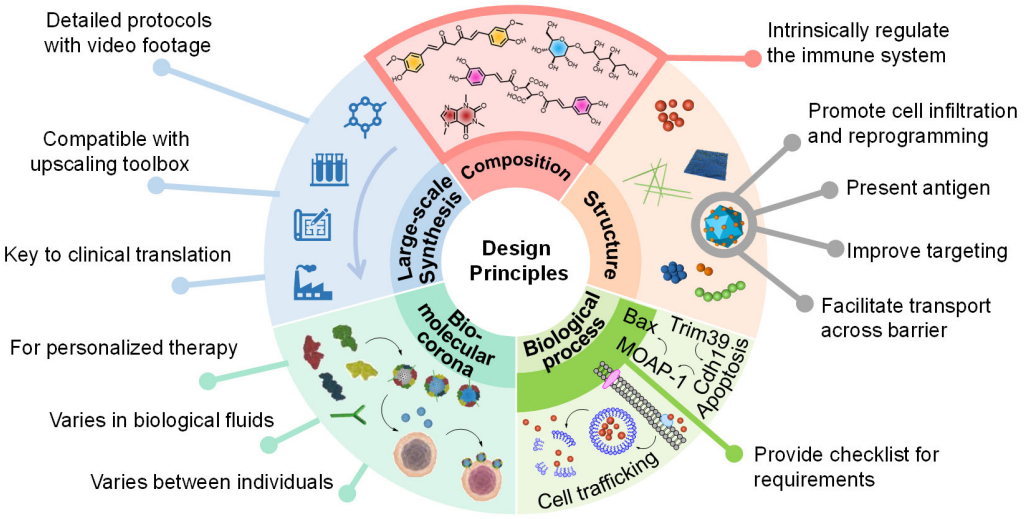

Fig. 33 Design principles for engineering natural building blocks into particles.

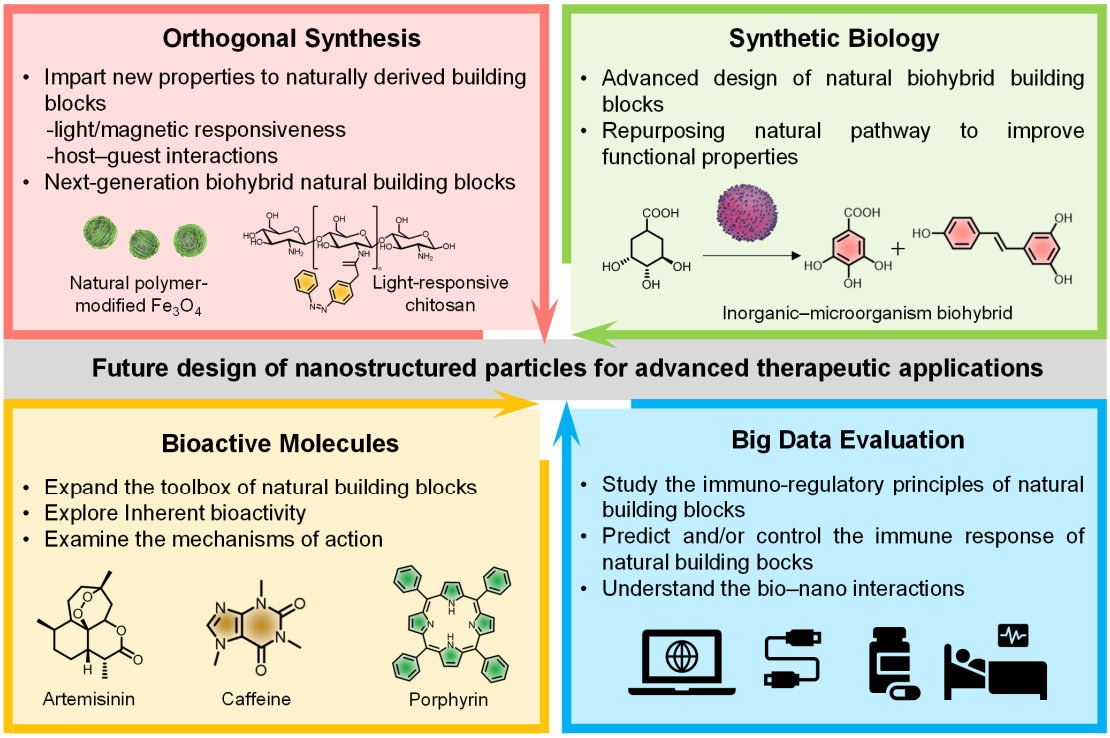

Fig. 34 Interdisciplinary approaches for the development of nanostructured particles from natural building blocks for emerging advanced therapeutic applications.

5. Reference

1. J. E. Cohen, S. Merims, S. Frank, R. Engelstein, T. Peretz and M. Lotem, *Immunotherapy*, 2017, **9**, 183-196.
2. K. Rezvani, *Bone Marrow Transplant.*, 2019, **54**, 785-788.
3. R. S. Riley, C. H. June, R. Langer and M. J. Mitchell, *Nat. Rev. Drug Discovery*, 2019, **18**, 175-196.
4. Y. Shi and T. Lammers, *Acc. Chem. Res.*, 2019, **52**, 1543-1554.
5. C. E. Dunbar, K. A. High, J. K. Joung, D. B. Kohn, K. Ozawa and M. Sadelain, *Science*, 2018, **359**, eaan4672.
6. C. Roma-Rodrigues, L. Rivas-García, P. V. Baptista and A. R. Fernandes, *Pharmaceutics*, 2020, **12**, 233.
7. M. J. Birrer, K. N. Moore, I. Betella and R. C. Bates, *J. Natl. Cancer Inst.*, 2019, **111**, 538-549.
8. H. Chen, W. Zhang, G. Zhu, J. Xie and X. Chen, *Nat. Rev. Mater.*, 2017, **2**, 17024.
9. A. Wicki, D. Witzigmann, V. Balasubramanian and J. Huwyler, *J. Controlled Release*, 2015, **200**, 138-157.
10. J. Cui, J. J. Richardson, M. Björnmalm, M. Faria and F. Caruso, *Acc. Chem. Res.*, 2016, **49**, 1139-1148.
11. V. F. Cardoso, A. Francesko, C. Ribeiro, M. Bañobre-López, P. Martins and S. Lanceros-Mendez, *Adv. Healthcare Mater.*, 2018, **7**, 1700845.
12. N. Kamaly, Z. Xiao, P. M. Valencia, A. F. Radovic-Moreno and O. C. Farokhzad, *Chem. Soc. Rev.*, 2012, **41**, 2971-3010.
13. M. Li, Z. Luo and Y. Zhao, *Chem. Mater.*, 2018, **30**, 25-53.
14. H. Sun, J. Su, Q. Meng, Q. Yin, L. Chen, W. Gu, P. Zhang, Z. Zhang, H. Yu, S. Wang and Y. Li, *Adv. Mater.*, 2016, **28**, 9581-9588.
15. J. Li, X. Chang, X. Chen, Z. Gu, F. Zhao, Z. Chai and Y. Zhao, *Biotechnol. Adv.*, 2014, **32**, 727-743.
16. C. J. Cheng, G. T. Tietjen, J. K. Saucier-Sawyer and W. M. Saltzman, *Nat. Rev. Drug Discovery*, 2015, **14**, 239-247.
17. Z. Cheng, A. Al Zaki, J. Z. Hui, V. R. Muzykantov and A. Tsourkas, *Science*, 2012, **338**, 903-910.
18. Q. Sun, Z. Zhou, N. Qiu and Y. Shen, *Adv. Mater.*, 2017, **29**, 1606628.
19. H. Ejima, J. J. Richardson and F. Caruso, *Nano Today*, 2017, **12**, 136-148.
20. N. Grimaldi, F. Andrade, N. Segovia, L. Ferrer-Tasies, S. Sala, J. Veciana and N. Ventosa, *Chem. Soc. Rev.*, 2016, **45**, 6520-6545.
21. A. Jain, S. K. Singh, S. K. Arya, S. C. Kundu and S. Kapoor, *ACS Biomater. Sci. Eng.*, 2018, **4**, 3939-3961.
22. M. Swierczewska, H. S. Han, K. Kim, J. H. Park and S. Lee, *Adv. Drug. Delivery Rev.*, 2016, **99**, 70-84.
23. J. Zhou, Z. Lin, Y. Ju, M. A. Rahim, J. J. Richardson and F. Caruso, *Acc. Chem. Res.*, 2020, **53**, 1269-1278.
24. K. Y. Choi, H. Chung, K. H. Min, H. Y. Yoon, K. Kim, J. H. Park, I. C. Kwon and S. Y. Jeong, *Biomaterials*, 2010, **31**, 106-114.
25. J. E. Chung, S. Tan, S. J. Gao, N. Yongvongsoontorn, S. H. Kim, J. H. Lee, H. S. Choi, H. Yano, L. Zhuo, M. Kurisawa and J. Y. Ying, *Nat. Nanotechnol.*, 2014, **9**, 907-912.
26. T. Kisby, A. Yilmazer and K. Kostarelos, *Nat. Nanotechnol.*, 2021, **16**, 843-850.
27. X. Hou, T. Zaks, R. Langer and Y. Dong, *Nat. Rev. Mater.*, 2021, **6**, 1078-1094.
28. J. C. Harris, M. A. Scully and E. S. Day, *Cancers*, 2019, **11**, 1836.
29. Q. Xia, Y. Zhang, Z. Li, X. Hou and N. Feng, *Acta Pharm. Sin. B*, 2019, **9**, 675-689.
30. H. M, E. Azzazy and R. H. Christenson, *Clin. Chem.*, 1997, **43**, 2014a-2015.
31. M. Garcovich, M. A. Zocco and A. Gasbarrini, *Blood Transfus.*, 2009, **7**, 268-277.

32. M. T. Larsen, M. Kuhlmann, M. L. Hvam and K. A. Howard, *Mol. Cell. Ther.*, 2016, **4**, 3.
33. W. Jurkowski, G. Porebski, K. Obtulowicz and I. Roterman, *Curr. Drug Metab.*, 2009, **10**, 448-458.
34. R. Li, K. Zheng, P. Hu, Z. Chen, S. Zhou, J. Chen, C. Yuan, S. Chen, W. Zheng, E. Ma, F. Zhang, J. Xue, X. Chen and M. Huang, *Theranostics*, 2014, **4**, 642-659.
35. I. Petitpas, C. E. Petersen, C. E. Ha, A. A. Bhattacharya, P. A. Zunszain, J. Ghuman, N. V. Bhagavan and S. Curry, *Proc. Natl. Acad. Sci. U.S.A*, 2003, **100**, 6440-6445.
36. S. Sugio, A. Kashima, S. Mochizuki, M. Noda and K. Kobayashi, *Protein. Eng.*, 1999, **12**, 439-446.
37. G. Fanali, A. di Masi, V. Trezza, M. Marino, M. Fasano and P. Ascenzi, *Mol. Aspects Med.*, 2012, **33**, 209-290.
38. Z. Liu and X. Chen, *Chem. Soc. Rev.*, 2016, **45**, 1432-1456.
39. Y. R. Zheng, K. Suntharalingam, T. C. Johnstone, H. Yoo, W. Lin, J. G. Brooks and S. J. Lippard, *J. Am. Chem. Soc.*, 2014, **136**, 8790-8798.
40. L. Guo, S. Luo, Z. Du, M. Zhou, P. Li, Y. Fu, X. Sun, Y. Huang and Z. Zhang, *Nat. Commun.*, 2017, **8**, 878.
41. Q. Sun, X. Sun, X. Ma, Z. Zhou, E. Jin, B. Zhang, Y. Shen, E. A. Van Kirk, W. J. Murdoch, J. R. Lott, T. P. Lodge, M. Radosz and Y. Zhao, *Adv. Mater.*, 2014, **26**, 7615-7621.
42. Q. Chen, L. Feng, J. Liu, W. Zhu, Z. Dong, Y. Wu and Z. Liu, *Adv. Mater.*, 2016, **28**, 7129-7136.
43. D. V. Peralta, Z. Heidari, S. Dash and M. A. Tarr, *ACS Appl. Mater. Interfaces*, 2015, **7**, 7101-7111.
44. Y. Wang, T. Yang, H. Ke, A. Zhu, Y. Wang, J. Wang, J. Shen, G. Liu, C. Chen, Y. Zhao and H. Chen, *Adv. Mater.*, 2015, **27**, 3874-3882.
45. T. Yang, Y. a. Tang, L. Liu, X. Lv, Q. Wang, H. Ke, Y. Deng, H. Yang, X. Yang, G. Liu, Y. Zhao and H. Chen, *ACS Nano*, 2017, **11**, 1848-1857.
46. W. Yang, W. Guo, W. Le, G. Lv, F. Zhang, L. Shi, X. Wang, J. Wang, S. Wang, J. Chang and B. Zhang, *ACS Nano*, 2016, **10**, 10245-10257.
47. Z. Yang, W. He, H. Zheng, J. Wei, P. Liu, W. Zhu, L. Lin, L. Zhang, C. Yi, Z. Xu and J. Ren, *Biomaterials*, 2018, **161**, 1-10.
48. L. Zhou, T. Yang, J. Wang, Q. Wang, X. Lv, H. Ke, Z. Guo, J. Shen, Y. Wang, C. Xing and H. Chen, *Theranostics*, 2017, **7**, 764-774.
49. V. Kushwah, S. S. Katiyar, C. P. Dora, A. Kumar Agrawal, D. A. Lamprou, R. C. Gupta and S. Jain, *Acta Biomater.*, 2018, **73**, 424-436.
50. L. Liu, Y. Bi, M. Zhou, X. Chen, X. He, Y. Zhang, T. Sun, C. Ruan, Q. Chen, H. Wang and C. Jiang, *ACS Appl. Mater. Interfaces*, 2017, **9**, 7424-7435.
51. X. Song, C. Liang, H. Gong, Q. Chen, C. Wang and Z. Liu, *Small*, 2015, **11**, 3932-3941.
52. H. Cao, L. Zou, B. He, L. Zeng, Y. Huang, H. Yu, P. Zhang, Q. Yin, Z. Zhang and Y. Li, *Adv. Funct. Mater.*, 2017, **27**, 1605679.
53. Z. Sheng, D. Hu, M. Zheng, P. Zhao, H. Liu, D. Gao, P. Gong, G. Gao, P. Zhang, Y. Ma and L. Cai, *ACS Nano*, 2014, **8**, 12310-12322.
54. P. Zhao, W. Yin, A. Wu, Y. Tang, J. Wang, Z. Pan, T. Lin, M. Zhang, B. Chen, Y. Duan and Y. Huang, *Adv. Funct. Mater.*, 2017, **27**, 1700403.
55. T. Lin, P. Zhao, Y. Jiang, Y. Tang, H. Jin, Z. Pan, H. He, V. C. Yang and Y. Huang, *ACS Nano*, 2016, **10**, 9999-10012.
56. G. Gao, Y. W. Jiang, W. Sun, Y. Guo, H. R. Jia, X. W. Yu, G. Y. Pan and F. G. Wu, *Small*, 2019, **15**,

e1900501.
57. M. J. Hawkins, P. Soon-Shiong and N. Desai, *Adv. Drug. Delivery Rev.*, 2008, **60**, 876-885.
58. T. Tanei, F. Leonard, X. Liu, J. F. Alexander, Y. Saito, M. Ferrari, B. Godin and K. Yokoi, *Cancer Res.*, 2016, **76**, 429-439.
59. N. Kurtul, E. A. Taşdemir, D. Ünal, M. İzmirli and C. Eroglu, *Cancer Biomarkers*, 2017, **18**, 459-466.
60. Y. Zhang, Y. Wan, Y. Chen, N. T. Blum, J. Lin and P. Huang, *ACS Nano*, 2020, **14**, 5560-5569.
61. Z. Zhou, B. Zhang, S. Wang, W. Zai, A. Yuan, Y. Hu and J. Wu, *Small*, 2018, **14**, e1801694.
62. B. Hoang, M. J. Ernsting, A. Roy, M. Murakami, E. Undzys and S. D. Li, *Biomaterials*, 2015, **59**, 66-76.
63. N. Desai, *AAPS J.*, 2012, **14**, 282-295.
64. N. Desai, V. Trieu, B. Damascelli and P. Soon-Shiong, *Transl. Oncol.*, 2009, **2**, 59-64.
65. N. Desai, V. Trieu, Z. Yao, L. Louie, S. Ci, A. Yang, C. Tao, T. De, B. Beals, D. Dykes, P. Noker, R. Yao, E. Labao, M. Hawkins and P. Soon-Shiong, *Clin. Cancer Res.*, 2006, **12**, 1317-1324.
66. Q. Chen, X. Wang, C. Wang, L. Feng, Y. Li and Z. Liu, *ACS Nano*, 2015, **9**, 5223-5233.
67. V. A. Myasoedova, D. A. Chistiakov, A. V. Grechko and A. N. Orekhov, *J. Mol. Cell Cardiol.*, 2018, **123**, 159-167.
68. L. Liu, F. Hu, H. Wang, X. Wu, A. S. Eltahan, S. Stanford, N. Bottini, H. Xiao, M. Bottini, W. Guo and X. J. Liang, *ACS Nano*, 2019, **13**, 5036-5048.
69. D. Chu, J. Gao and Z. Wang, *ACS Nano*, 2015, **9**, 11800-11811.
70. M. Li, S. Jiang, J. Simon, D. Paßlick, M.-L. Frey, M. Wagner, V. Mailänder, D. Crespy and K. Landfester, *Nano Lett.*, 2021, **21**, 1591-1598.
71. E. J. Lee, N. K. Lee and I. S. Kim, *Adv. Drug Delivery Rev.*, 2016, **106**, 157-171.
72. K. Fan, L. Gao and X. Yan, *Wiley Interdiscip. Rev. Nanomed. Nanobiotechnol.*, 2013, **5**, 287-298.
73. P. M. Harrison and P. Arosio, *Biochim. Biophys. Acta Bioenerg.*, 1996, **1275**, 161-203.
74. P. Huang, P. Rong, A. Jin, X. Yan, M. G. Zhang, J. Lin, H. Hu, Z. Wang, X. Yue, W. Li, G. Niu, W. Zeng, W. Wang, K. Zhou and X. Chen, *Adv. Mater.*, 2014, **26**, 6401-6408.
75. C. F. Bryce and R. R. Crichton, *Biochem. J.*, 1973, **133**, 301-309.
76. M. Kim, Y. Rho, K. S. Jin, B. Ahn, S. Jung, H. Kim and M. Ree, *Biomacromolecules*, 2011, **12**, 1629-1640.
77. S. Stefanini, S. Cavallo, C. Q. Wang, P. Tataseo, P. Vecchini, A. Giartosio and E. Chiancone, *Arch. Biochem. Biophys.*, 1996, **325**, 58-64.
78. E. Falvo, F. Malagrinò, A. Arcovito, F. Fazi, G. Colotti, E. Tremante, P. Di Micco, A. Braca, R. Opri, A. Giuffrè, G. Fracasso and P. Ceci, *J. Controlled Release*, 2018, **275**, 177-185.
79. E. Falvo, E. Tremante, A. Arcovito, M. Papi, N. Elad, A. Boffi, V. Morea, G. Conti, G. Toffoli, G. Fracasso, P. Giacomini and P. Ceci, *Biomacromolecules*, 2016, **17**, 514-522.
80. M. Bellini, B. Riva, V. Tinelli, M. A. Rizzuto, L. Salvioni, M. Colombo, F. Mingozzi, A. Visioli, L. Marongiu, G. Frascotti, M. S. Christodoulou, D. Passarella, D. Prosperi and L. Fiandra, *Small*, 2020, **16**, e2001450.
81. V. V. Shuvaev, M. Khoshnejad, K. W. Pulsipher, R. Y. Kiseleva, E. Arguiri, J. C. Cheung-Lau, K. M. LeFort, M. Christofidou-Solomidou, R. V. Stan, I. J. Dmochowski and V. R. Muzykantov, *Biomaterials*, 2018, **185**, 348-359.
82. M. Kanekiyo, C. J. Wei, H. M. Yassine, P. M. McTamney, J. C. Boyington, J. R. Whittle, S. S. Rao, W. P. Kong, L. Wang and G. J. Nabel, *Nature*, 2013, **499**, 102-106.

83. H. N. Munro and M. C. Linder, *Physiol. Rev.*, 1978, **58**, 317-396.
84. Z. Zhen, W. Tang, H. Chen, X. Lin, T. Todd, G. Wang, T. Cowger, X. Chen and J. Xie, *ACS Nano*, 2013, **7**, 4830-4837.
85. Z. Zhen, W. Tang, Y.-J. Chuang, T. Todd, W. Zhang, X. Lin, G. Niu, G. Liu, L. Wang, Z. Pan, X. Chen and J. Xie, *ACS Nano*, 2014, **8**, 6004-6013.
86. Z. Zhen, W. Tang, C. Guo, H. Chen, X. Lin, G. Liu, B. Fei, X. Chen, B. Xu and J. Xie, *ACS Nano*, 2013, **7**, 6988-6996.
87. Z. Wang, P. Huang, O. Jacobson, Z. Wang, Y. Liu, L. Lin, J. Lin, N. Lu, H. Zhang, R. Tian, G. Niu, G. Liu and X. Chen, *ACS Nano*, 2016, **10**, 3453-3460.
88. D. L. Schonberg, T. E. Miller, Q. Wu, W. A. Flavahan, N. K. Das, J. S. Hale, C. G. Hubert, S. C. Mack, A. M. Jarrar, R. T. Karl, A. M. Rosager, A. M. Nixon, P. J. Tesar, P. Hamerlik, B. W. Kristensen, C. Horbinski, J. R. Connor, P. L. Fox, J. D. Lathia and J. N. Rich, *Cancer Cell*, 2015, **28**, 441-455.
89. T. Tan, H. Wang, H. Cao, L. Zeng, Y. Wang, Z. Wang, J. Wang, J. Li, S. Wang, Z. Zhang and Y. Li, *Adv. Sci.*, 2018, **5**, 1801012.
90. S. Zhou, Z. Zhen, A. V. Paschall, L. Xue, X. Yang, A.-G. Bebin Blackwell, Z. Cao, W. Zhang, M. Wang, Y. Teng, G. Zhou, Z. Li, F. Y. Avci, W. Tang and J. Xie, *Adv. Funct. Mater.*, 2021, **31**, 2007017.
91. S. Tang, Z. Liu, W. Xu, Q. Li, T. Han, D. Pan, N. Yue, M. Wu, Q. Liu, W. Yuan, Z. Huang, D. Zhou, W. Zhou and Z. Qian, *Nano Lett.*, 2019, **19**, 5469-5475.
92. J. Cui, R. De Rose, J. P. Best, A. P. R. Johnston, S. Alcantara, K. Liang, G. K. Such, S. J. Kent and F. Caruso, *Adv. Mater.*, 2013, **25**, 3468-3472.
93. L. Gu, L. E. Ruff, Z. Qin, M. Corr, S. M. Hedrick and M. J. Sailor, *Adv. Mater.*, 2012, **24**, 3981-3987.
94. L. Xu, Y. Liu, Z. Chen, W. Li, Y. Liu, L. Wang, L. Ma, Y. Shao, Y. Zhao and C. Chen, *Adv. Mater.*, 2013, **25**, 5928-5936.
95. K. Fan, C. Cao, Y. Pan, D. Lu, D. Yang, J. Feng, L. Song, M. Liang and X. Yan, *Nat. Nanotechnol.*, 2012, **7**, 459-464.
96. M. Liang, K. Fan, M. Zhou, D. Duan, J. Zheng, D. Yang, J. Feng and X. Yan, *Proc. Natl. Acad. Sci. U.S.A*, 2014, **111**, 14900-14905.
97. R. Prior, G. Reifenberger and W. Wechsler, *Virchows Arch. A: Pathol. Anat. Histopathol.*, 1990, **416**, 491-496.
98. L. Recht, C. O. Torres, T. W. Smith, V. Raso and T. W. Griffin, *J. Neurosurg.*, 1990, **72**, 941-945.
99. Y. Lei, Y. Hamada, J. Li, L. Cong, N. Wang, Y. Li, W. Zheng and X. Jiang, *J. Controlled Release*, 2016, **232**, 131-142.
100. C. Wang, C. Zhang, Z. Li, S. Yin, Q. Wang, F. Guo, Y. Zhang, R. Yu, Y. Liu and Z. Su, *Biomacromolecules*, 2018, **19**, 773-781.
101. W. Liu, Q. Lin, Y. Fu, S. Huang, C. Guo, L. Li, L. Wang, Z. Zhang and L. Zhang, *J. Controlled Release*, 2019, **323**, 191-202.
102. K. Fan, X. Jia, M. Zhou, K. Wang, J. Conde, J. He, J. Tian and X. Yan, *ACS Nano*, 2018, **12**, 4105-4115.
103. M. G. Joyce, H. A. D. King, I. Elakhal-Naouar, A. Ahmed, K. K. Peachman, C. Macedo Cincotta, C. Subra, R. E. Chen, P. V. Thomas, W. H. Chen, R. S. Sankhala, A. Hajduczki, E. J. Martinez, C. E. Peterson, W. C. Chang, M. Choe, C. Smith, P. J. Lee, J. A. Headley, M. G. Taddese, H. A. Elyard, A. Cook, A. Anderson, K. McGuckin Wuertz, M. Dong, I. Swafford, J. B. Case, J. R. Currier, K. G. Lal, S. Molnar, M. S. Nair, V.

Dussupt, S. P. Daye, X. Zeng, E. K. Barkei, H. M. Staples, K. Alfson, R. Carrion, S. J. Krebs, D. Paquin-Proulx, N. Karasavva, V. R. Polonis, L. L. Jagodzinski, M. F. Amare, S. Vasan, P. T. Scott, Y. Huang, D. D. Ho, N. de Val, M. S. Diamond, M. G. Lewis, M. Rao, G. R. Matyas, G. D. Gromowski, S. A. Peel, N. L. Michael, D. L. Bolton and K. Modjarrad, *Sci. Transl. Med.*, 2022, **14**, eabi5735.

104. J. M. Carmen, S. Shrivastava, Z. Lu, A. Anderson, E. B. Morrison, R. S. Sankhala, W. H. Chen, W. C. Chang, J. S. Bolton, G. R. Matyas, N. L. Michael, M. G. Joyce, K. Modjarrad, J. R. Currier, E. Bergmann-Leitner, A. M. W. Malloy and M. Rao, *npj vaccines*, 2021, **6**, 151.
105. K. M. Wuertz, E. K. Barkei, W. H. Chen, E. J. Martinez, I. Lakhal-Naouar, L. L. Jagodzinski, D. Paquin-Proulx, G. D. Gromowski, I. Swafford, A. Ganesh, M. Dong, X. Zeng, P. V. Thomas, R. S. Sankhala, A. Hajduczki, C. E. Peterson, C. Kuklis, S. Soman, L. Wieczorek, M. Zemil, A. Anderson, J. Darden, H. Hernandez, H. Grove, V. Dussupt, H. Hack, R. de la Barrera, S. Zarling, J. F. Wood, J. W. Froude, M. Gagne, A. R. Henry, E. B. Mokhtari, P. Mudvari, S. J. Krebs, A. S. Pekosz, J. R. Currier, S. Kar, M. Porto, A. Winn, K. Radzyminski, M. G. Lewis, S. Vasan, M. Suthar, V. R. Polonis, G. R. Matyas, E. A. Boritz, D. C. Douek, R. A. Seder, S. P. Daye, M. Rao, S. A. Peel, M. G. Joyce, D. L. Bolton, N. L. Michael and K. Modjarrad, *npj vaccines*, 2021, **6**, 129.
106. M. Foox and M. Zilberman, *Expert Opin. Drug Delivery*, 2015, **12**, 1547-1563.
107. S. H. Nezhadi, P. F. Choong, F. Lotfipour and C. R. Dass, *J. Drug Targeting*, 2009, **17**, 731-738.
108. B. Balakrishnan and A. Jayakrishnan, *Biomaterials*, 2005, **26**, 3941-3951.
109. Y. Ikada and Y. Tabata, *Adv. Drug. Delivery Rev.*, 1998, **31**, 287-301.
110. K. Kawai, S. Suzuki, Y. Tabata, Y. Ikada and Y. Nishimura, *Biomaterials*, 2000, **21**, 489-499.
111. M. Yamamoto, Y. Ikada and Y. Tabata, *J. Biomater. Sci. Polym. Ed.*, 2001, **12**, 77-88.
112. S. Ruan, Q. He and H. Gao, *Nanoscale*, 2015, **7**, 9487-9496.
113. D. Xia, P. Xu, X. Luo, J. Zhu, H. Gu, D. Huo and Y. Hu, *Adv. Funct. Mater.*, 2019, **29**, 1807294.
114. W. M. Li, C. S. Chiang, W. C. Huang, C. W. Su, M. Y. Chiang, J. Y. Chen and S. Y. Chen, *J. Controlled Release*, 2015, **220**, 107-118.
115. W. M. Li, C. W. Su, Y. W. Chen and S. Y. Chen, *Acta Biomater.*, 2015, **15**, 191-199.
116. T. M. Allen and P. R. Cullis, *Adv. Drug. Delivery Rev.*, 2013, **65**, 36-48.
117. B. S. Pattni, V. V. Chupin and V. P. Torchilin, *Chem. Rev.*, 2015, **115**, 10938-10966.
118. W. Deng, W. Chen, S. Clement, A. Guller, Z. Zhao, A. Engel and E. M. Goldys, *Nat. Commun.*, 2018, **9**, 2713.
119. B. Kim, H. B. Pang, J. Kang, J. H. Park, E. Ruoslahti and M. J. Sailor, *Nat. Commun.*, 2018, **9**, 1969.
120. Z. Chen, F. Liu, Y. Chen, J. Liu, X. Wang, A. T. Chen, G. Deng, H. Zhang, J. Liu, Z. Hong and J. Zhou, *Adv. Funct. Mater.*, 2017, **27**, 1703036.
121. F. C. Lam, S. W. Morton, J. Wyckoff, T. L. Vu Han, M. K. Hwang, A. Maffa, E. Balkanska-Sinclair, M. B. Yaffe, S. R. Floyd and P. T. Hammond, *Nat. Commun.*, 2018, **9**, 1991.
122. R. Di Corato, G. Béalle, J. Kolosnjaj-Tabi, A. Espinosa, O. Clément, A. K. Silva, C. Ménager and C. Wilhelm, *ACS Nano*, 2015, **9**, 2904-2916.
123. Y. Yang, L. Wang, H. Cao, Q. Li, Y. Li, M. Han, H. Wang and J. Li, *Nano Lett.*, 2019, **19**, 1821-1826.
124. A. K. Rengan, A. B. Bukhari, A. Pradhan, R. Malhotra, R. Banerjee, R. Srivastava and A. De, *Nano Lett.*, 2015, **15**, 842-848.
125. T. Ji, J. Lang, J. Wang, R. Cai, Y. Zhang, F. Qi, L. Zhang, X. Zhao, W. Wu, J. Hao, Z. Qin, Y. Zhao and G.

Nie, *ACS Nano*, 2017, **11**, 8668-8678.

126. J. Viger-Gravel, A. Schantz, A. C. Pinon, A. J. Rossini, S. Schantz and L. Emsley, *J. Phys. Chem. B*, 2018, **122**, 2073-2081.
127. Y. Eygeris, S. Patel, A. Jozic and G. Sahay, *Nano Lett.*, 2020, **20**, 4543-4549.
128. S. Patel, N. Ashwanikumar, E. Robinson, Y. Xia, C. Mihai, J. P. Griffith, 3rd, S. Hou, A. A. Esposito, T. Ketova, K. Welsher, J. L. Joyal, Ö. Almarsson and G. Sahay, *Nat. Commun.*, 2020, **11**, 983.
129. K. T. Love, K. P. Mahon, C. G. Levins, K. A. Whitehead, W. Querbes, J. R. Dorkin, J. Qin, W. Cantley, L. L. Qin, T. Racie, M. Frank-Kamenetsky, K. N. Yip, R. Alvarez, D. W. Sah, A. de Fougerolles, K. Fitzgerald, V. Koteliansky, A. Akinc, R. Langer and D. G. Anderson, *Proc. Natl. Acad. Sci. U.S.A*, 2010, **107**, 1864-1869.
130. G. Sahay, W. Querbes, C. Alabi, A. Eltoukhy, S. Sarkar, C. Zurenko, E. Karagiannis, K. Love, D. Chen, R. Zoncu, Y. Buganim, A. Schroeder, R. Langer and D. G. Anderson, *Nat. Biotechnol.*, 2013, **31**, 653-658.
131. H. Yin, C. Q. Song, S. Suresh, Q. Wu, S. Walsh, L. H. Rhym, E. Mintzer, M. F. Bolukbasi, L. J. Zhu, K. Kauffman, H. Mou, A. Oberholzer, J. Ding, S. Y. Kwan, R. L. Bogorad, T. Zatsepin, V. Koteliansky, S. A. Wolfe, W. Xue, R. Langer and D. G. Anderson, *Nat. Biotechnol.*, 2017, **35**, 1179-1187.
132. C. Q. Song, T. Jiang, M. Richter, L. H. Rhym, L. W. Koblan, M. P. Zafra, E. M. Schatoff, J. L. Doman, Y. Cao, L. E. Dow, L. J. Zhu, D. G. Anderson, D. R. Liu, H. Yin and W. Xue, *Nat. Biomed. Eng.*, 2020, **4**, 125-130.
133. J. A. Kulkarni, M. M. Darjuan, J. E. Mercer, S. Chen, R. van der Meel, J. L. Thewalt, Y. Y. C. Tam and P. R. Cullis, *ACS Nano*, 2018, **12**, 4787-4795.
134. J. C. Kaczmarek, A. K. Patel, K. J. Kauffman, O. S. Fenton, M. J. Webber, M. W. Heartlein, F. DeRosa and D. G. Anderson, *Angew. Chem. Int. Ed. Engl.*, 2016, **55**, 13808-13812.
135. N. Pardi, M. J. Hogan, R. S. Pelc, H. Muramatsu, H. Andersen, C. R. DeMaso, K. A. Dowd, L. L. Sutherland, R. M. Scearce, R. Parks, W. Wagner, A. Granados, J. Greenhouse, M. Walker, E. Willis, J. S. Yu, C. E. McGee, G. D. Sempowski, B. L. Mui, Y. K. Tam, Y. J. Huang, D. Vanlandingham, V. M. Holmes, H. Balachandran, S. Sahu, M. Lifton, S. Higgs, S. E. Hensley, T. D. Madden, M. J. Hope, K. Karikó, S. Santra, B. S. Graham, M. G. Lewis, T. C. Pierson, B. F. Haynes and D. Weissman, *Nature*, 2017, **543**, 248-251.
136. C. Liang, B. Guo, H. Wu, N. Shao, D. Li, J. Liu, L. Dang, C. Wang, H. Li, S. Li, W. K. Lau, Y. Cao, Z. Yang, C. Lu, X. He, D. W. Au, X. Pan, B. T. Zhang, C. Lu, H. Zhang, K. Yue, A. Qian, P. Shang, J. Xu, L. Xiao, Z. Bian, W. Tan, Z. Liang, F. He, L. Zhang, A. Lu and G. Zhang, *Nat. Med.*, 2015, **21**, 288-294.
137. P. F. McKay, K. Hu, A. K. Blakney, K. Samnuan, J. C. Brown, R. Penn, J. Zhou, C. R. Bouton, P. Rogers, K. Polra, P. J. C. Lin, C. Barbosa, Y. K. Tam, W. S. Barclay and R. J. Shattock, *Nat. Commun.*, 2020, **11**, 3523.
138. E. H. Pilkington, E. J. A. Suys, N. L. Trevaskis, A. K. Wheatley, D. Zukancic, A. Algarni, H. Al-Wassiti, T. P. Davis, C. W. Pouton, S. J. Kent and N. P. Truong, *Acta Biomater.*, 2021, **131**, 16-40.
139. R. Ball, K. Hajj, J. Vizelman, P. Bajaj and K. Whitehead, *Nano Lett.*, 2018, **18**, 3814-3822.
140. M. Wang, J. A. Zuris, F. Meng, H. Rees, S. Sun, P. Deng, Y. Han, X. Gao, D. Pouli, Q. Wu, I. Georgakoudi, D. R. Liu and Q. Xu, *Proc. Natl. Acad. Sci. U.S.A*, 2016, **113**, 2868-2873.
141. J. D. Finn, A. R. Smith, M. C. Patel, L. Shaw, M. R. Youniss, J. van Heteren, T. Dirstine, C. Ciullo, R. Lescarbeau, J. Seitzer, R. R. Shah, A. Shah, D. Ling, J. Growe, M. Pink, E. Rohde, K. M. Wood, W. E.

Salomon, W. F. Harrington, C. Dombrowski, W. R. Strapps, Y. Chang and D. V. Morrissey, *Cell Rep.*, 2018, **22**, 2227-2235.
142. Y. L. Luo, C. F. Xu, H. J. Li, Z. T. Cao, J. Liu, J. L. Wang, X. J. Du, X. Z. Yang, Z. Gu and J. Wang, *ACS Nano*, 2018, **12**, 994-1005.
143. J. Liu, J. Chang, Y. Jiang, X. Meng, T. Sun, L. Mao, Q. Xu and M. Wang, *Adv. Mater.*, 2019, **31**, e1902575.
144. P. Wang, L. Zhang, W. Zheng, L. Cong, Z. Guo, Y. Xie, L. Wang, R. Tang, Q. Feng, Y. Hamada, K. Gonda, Z. Hu, X. Wu and X. Jiang, *Angew. Chem. Int. Ed. Engl.*, 2018, **57**, 1491-1496.
145. P. Wang, L. Zhang, Y. Xie, N. Wang, R. Tang, W. Zheng and X. Jiang, *Adv. Sci.*, 2017, **4**, 1700175.
146. D. Arcens, G. Le Fer, E. Grau, S. Grelier, H. Cramail and F. Peruch, *Polym. Chem.*, 2020, **11**, 3994-4004.
147. V. Faivre and V. Rosilio, *Expert Opin. Drug Delivery*, 2010, **7**, 1031-1048.
148. W. Li, X. Zhang, C. Zhang, J. Yan, X. Hou, S. Du, C. Zeng, W. Zhao, B. Deng, D. W. McComb, Y. Zhang, D. D. Kang, J. Li, W. E. Carson and Y. Dong, *Nat. Commun.*, 2021, **12**, 7264.
149. L. Wen, Y. Peng, K. Wang, Z. Huang, S. He, R. Xiong, L. Wu, F. Zhang and F. Hu, *Nano Res.*, 2022, **15**, 1455-1465.
150. L. Wen, K. Wang, F. Zhang, Y. Tan, X. Shang, Y. Zhu, X. Zhou, H. Yuan and F. Hu, *Biomaterials*, 2020, **237**, 119793.
151. K. Rajpoot, *Curr. Pharm. Des.*, 2019, **25**, 3943-3959.
152. S. D. Mandawgade and V. B. Patravale, *Int. J. Pharm.*, 2008, **363**, 132-138.
153. G. Erel-Akbaba, L. A. Carvalho, T. Tian, M. Zinter, H. Akbaba, P. J. Obeid, E. A. Chiocca, R. Weissleder, A. G. Kantarci and B. A. Tannous, *ACS Nano*, 2019, **13**, 4028-4040.
154. M. Geszke-Moritz and M. Moritz, *Mater. Sci. Eng., C*, 2016, **68**, 982-994.
155. P. Severino, M. Szymanski, M. Favaro, A. R. Azzoni, M. V. Chaud, M. H. Santana, A. M. Silva and E. B. Souto, *Eur. J. Pharm. Sci.*, 2015, **66**, 78-82.
156. W. H. Kong, K. Park, M. Y. Lee, H. Lee, D. K. Sung and S. K. Hahn, *Biomaterials*, 2013, **34**, 542-551.
157. T. Lobovkina, G. B. Jacobson, E. Gonzalez-Gonzalez, R. P. Hickerson, D. Leake, R. L. Kaspar, C. H. Contag and R. N. Zare, *ACS Nano*, 2011, **5**, 9977-9983.
158. S. Doktorovova, R. Shegokar, E. Rakovsky, E. Gonzalez-Mira, C. M. Lopes, A. M. Silva, P. Martins-Lopes, R. H. Muller and E. B. Souto, *Int. J. Pharm.*, 2011, **420**, 341-349.
159. X. Wu, H. Chen, C. Wu, J. Wang, S. Zhang, J. Gao, H. Wang, T. Sun and Y. G. Yang, *Biomaterials*, 2018, **156**, 77-87.
160. J.-H. Ryu, J. Drain, J. H. Kim, S. McGee, A. Gray-Weale, L. Waddington, G. J. Parker, M. Hargreaves, S.-H. Yoo and D. Stapleton, *Int. J. Biol. Macromol.*, 2009, **45**, 478-482.
161. Q. A. Besford, F. Cavalieri and F. Caruso, *Adv. Mater.*, 2020, **32**, 1904625.
162. D. K. Singh and A. R. Ray, *J. Macromol. Sci. C*, 2000, **40**, 69-83.
163. N. M. Alves and J. F. Mano, *Int. J. Biol. Macromol.*, 2008, **43**, 401-414.
164. C. A. Custodio, A. M. Frias, A. del Campo, R. L. Reis and J. F. Mano, *Biointerphases*, 2012, **7**, 65.
165. C. A. Custódio, V. E. Santo, M. B. Oliveira, M. E. Gomes, R. L. Reis and J. F. Mano, *Adv. Funct. Mater.*, 2014, **24**, 1391-1400.
166. C.-M. Lehr, J. A. Bouwstra, E. H. Schacht and H. E. Junginger, *Int. J. Pharm.*, 1992, **78**, 43-48.
167. Q. Lin, C. Bao, Y. Yang, Q. Liang, D. Zhang, S. Cheng and L. Zhu, *Adv. Mater.*, 2013, **25**, 1981-1986.
168. F. S. Majedi, M. M. Hasani-Sadrabadi, J. J. VanDersarl, N. Mokarram, S. Hojjati-Emami, E.

Dashtimoghadam, S. Bonakdar, M. A. Shokrgozar, A. Bertsch and P. Renaud, *Adv. Funct. Mater.*, 2014, **24**, 432-441.
169. Z. W. Jing, Y. Y. Jia, N. Wan, M. Luo, M. L. Huan, T. B. Kang, S. Y. Zhou and B. L. Zhang, *Biomaterials*, 2016, **84**, 276-285.
170. G. N. Shi, C. N. Zhang, R. Xu, J. F. Niu, H. J. Song, X. Y. Zhang, W. W. Wang, Y. M. Wang, C. Li, X. Q. Wei and D. L. Kong, *Biomaterials*, 2017, **113**, 191-202.
171. J. He, S. Duan, X. Yu, Z. Qian, S. Zhou, Z. Zhang, X. Huang, Y. Huang, J. Su, C. Lai, J. Meng, N. Zhou, X. Lu and Y. Zhao, *Theranostics*, 2016, **6**, 752-761.
172. Z. Hu, J. Chen, S. Zhou, N. Yang, S. Duan, Z. Zhang, J. Su, J. He, Z. Zhang, X. Lu and Y. Zhao, *Theranostics*, 2017, **7**, 1942-1952.
173. C. Corbet, H. Ragelle, V. Pourcelle, K. Vanvarenberg, J. Marchand-Brynaert, V. Preat and O. Feron, *J. Controlled Release*, 2016, **223**, 53-63.
174. M. Van Woensel, N. Wauthoz, R. Rosiere, V. Mathieu, R. Kiss, F. Lefranc, B. Steelant, E. Dilissen, S. W. Van Gool, T. Mathivet, H. Gerhardt, K. Amighi and S. De Vleeschouwer, *J. Controlled Release*, 2016, **227**, 71-81.
175. A. V. Nascimento, A. Singh, H. Bousbaa, D. Ferreira, B. Sarmento and M. M. Amiji, *Acta Biomater.*, 2017, **47**, 71-80.
176. J. Y. Yhee, S. Song, S. J. Lee, S. G. Park, K. S. Kim, M. G. Kim, S. Son, H. Koo, I. C. Kwon, J. H. Jeong, S. Y. Jeong, S. H. Kim and K. Kim, *J. Controlled Release*, 2015, **198**, 1-9.
177. F. Dosio, S. Arpicco, B. Stella and E. Fattal, *Adv. Drug. Delivery Rev.*, 2016, **97**, 204-236.
178. J. Fang, H. Nakamura and H. Maeda, *Adv. Drug. Delivery Rev.*, 2011, **63**, 136-151.
179. X. Han, Z. Li, J. Sun, C. Luo, L. Li, Y. Liu, Y. Du, S. Qiu, X. Ai, C. Wu, H. Lian and Z. He, *J. Controlled Release*, 2015, **197**, 29-40.
180. X. Wei, T. H. Senanayake, G. Warren and S. V. Vinogradov, *Bioconjugate Chem.*, 2013, **24**, 658-668.
181. S. Misra, P. Heldin, V. C. Hascall, N. K. Karamanos, S. S. Skandalis, R. R. Markwald and S. Ghatak, *FEBS J.*, 2011, **278**, 1429-1443.
182. C. Underhill, *J. Cell Sci.*, 1992, **103**, 293-298.
183. H. Duan, M. Donovan, F. Hernandez, C. Di Primo, E. Garanger, X. Schultze and S. Lecommandoux, *Angew. Chem. Int. Ed. Engl.*, 2020, **59**, 13591-13596.
184. X. Liang, L. Fang, X. Li, X. Zhang and F. Wang, *Biomaterials*, 2017, **132**, 72-84.
185. T. Lin, A. Yuan, X. Zhao, H. Lian, J. Zhuang, W. Chen, Q. Zhang, G. Liu, S. Zhang, W. Chen, W. Cao, C. Zhang, J. Wu, Y. Hu and H. Guo, *Acta Biomater.*, 2017, **53**, 427-438.
186. N. N. Parayath, A. Parikh and M. M. Amiji, *Nano Lett.*, 2018, **18**, 3571-3579.
187. J. Y. Lee, S. J. Chung, H. J. Cho and D. D. Kim, *Biomaterials*, 2016, **85**, 218-231.
188. G. Y. Lee, J. H. Kim, K. Y. Choi, H. Y. Yoon, K. Kim, I. C. Kwon, K. Choi, B. H. Lee, J. H. Park and I. S. Kim, *Biomaterials*, 2015, **53**, 341-348.
189. S. Gao, G. Wang, Z. Qin, X. Wang, G. Zhao, Q. Ma and L. Zhu, *Biomaterials*, 2017, **112**, 324-335.
190. L. Zhang, S. Gao, F. Zhang, K. Yang, Q. Ma and L. Zhu, *ACS Nano*, 2014, **8**, 12250-12258.
191. S. Z. F. Phua, G. Yang, W. Q. Lim, A. Verma, H. Chen, T. Thanabalu and Y. Zhao, *ACS Nano*, 2019, **13**, 4742-4751.
192. S. L. Kosaraju, *Crit. Rev. Food Sci. Nutr.*, 2005, **45**, 251-258.

193. C. Larsen, *Adv. Drug. Delivery Rev.*, 1989, **3**, 103-154.
194. J. Varshosaz, *Expert Opin. Drug Delivery*, 2012, **9**, 509-523.
195. K. Perica, A. Tu, A. Richter, J. G. Bieler, M. Edidin and J. P. Schneck, *ACS Nano*, 2014, **8**, 2252-2260.
196. R. Heo, D. G. You, W. Um, K. Y. Choi, S. Jeon, J. S. Park, Y. Choi, S. Kwon, K. Kim, I. C. Kwon, D. G. Jo, Y. M. Kang and J. H. Park, *Biomaterials*, 2017, **131**, 15-26.
197. T. Bauleth-Ramos, M.-A. Shahbazi, D. Liu, F. Fontana, A. Correia, P. Figueiredo, H. Zhang, J. P. Martins, J. T. Hirvonen, P. Granja, B. Sarmento and H. A. Santos, *Adv. Funct. Mater.*, 2017, **27**, 1703303.
198. M. P. A. Ferreira, V. Talman, G. Torrieri, D. Liu, G. Marques, K. Moslova, Z. Liu, J. F. Pinto, J. Hirvonen, H. Ruskoaho and H. A. Santos, *Adv. Funct. Mater.*, 2018, **28**, 1705134.
199. M. Alibolandi, F. Alabdollah, F. Sadeghi, M. Mohammadi, K. Abnous, M. Ramezani and F. Hadizadeh, *J. Controlled Release*, 2016, **227**, 58-70.
200. M. Lopes, N. Shrestha, A. Correia, M. A. Shahbazi, B. Sarmento, J. Hirvonen, F. Veiga, R. Seica, A. Ribeiro and H. A. Santos, *J. Controlled Release*, 2016, **232**, 29-41.
201. W. Lv, J. Xu, X. Wang, X. Li, Q. Xu and H. Xin, *ACS Nano*, 2018, **12**, 5417-5426.
202. F. Fontana, M.-A. Shahbazi, D. Liu, H. Zhang, E. Mäkilä, J. Salonen, J. T. Hirvonen and H. A. Santos, *Adv. Mater.*, 2017, **29**, 1603239.
203. F. Kong, H. Zhang, X. Zhang, D. Liu, D. Chen, W. Zhang, L. Zhang, H. A. Santos and M. Hai, *Adv. Funct. Mater.*, 2016, **26**, 6158-6169.
204. Z. Liu, Y. Li, W. Li, C. Xiao, D. Liu, C. Dong, M. Zhang, E. Mäkilä, M. Kemell, J. Salonen, J. T. Hirvonen, H. Zhang, D. Zhou, X. Deng and H. A. Santos, *Adv. Mater.*, 2018, **30**, 1703393.
205. A. Rhodes, L. E. Evans, W. Alhazzani, M. M. Levy, M. Antonelli, R. Ferrer, A. Kumar, J. E. Sevransky, C. L. Sprung and M. E. Nunnally, *Intensive Care Med.*, 2017, **43**, 304-377.
206. H. Lee, S. M. Dellatore, W. M. Miller and P. B. Messersmith, *Science*, 2007, **318**, 426-430.
207. S. M. Kang, J. Rho, I. S. Choi, P. B. Messersmith and H. Lee, *J. Am. Chem. Soc.*, 2009, **131**, 13224-13225.
208. S. Hong, J. Kim, Y. S. Na, J. Park, S. Kim, K. Singha, G.-I. Im, D.-K. Han, W. J. Kim and H. Lee, *Angew. Chem. Int. Ed. Engl.*, 2013, **52**, 9187-9191.
209. T. Ma, X.-Y. Ge, K.-Y. Hao, B.-R. Zhang, X. Jiang, Y. Lin and Y. Zhang, *Sci. Rep.*, 2017, **7**, 17849.
210. S. Hong, J. Yeom, I. T. Song, S. M. Kang, H. Lee and H. Lee, *Adv. Mater. Interfaces*, 2014, **1**, 1400113.
211. V. Ball, *Biointerphases*, 2014, **9**, 030801.
212. E. W. Danner, Y. Kan, M. U. Hammer, J. N. Israelachvili and J. H. Waite, *Biochemistry*, 2012, **51**, 6511-6518.
213. S. Hong, Y. Wang, S. Y. Park and H. Lee, *Sci. Adv.*, 2018, **4**.
214. S. Hong, Y. S. Na, S. Choi, I. T. Song, W. Y. Kim and H. Lee, *Adv. Funct. Mater.*, 2012, **22**, 4711-4717.
215. D. R. Dreyer, D. J. Miller, B. D. Freeman, D. R. Paul and C. W. Bielawski, *Langmuir*, 2012, **28**, 6428-6435.
216. J. r. Liebscher, R. Mrówczyński, H. A. Scheidt, C. Filip, N. D. Hădade, R. Turcu, A. Bende and S. Beck, *Langmuir*, 2013, **29**, 10539-10548.
217. S. Hong, K. Y. Kim, H. J. Wook, S. Y. Park, K. D. Lee, D. Y. Lee and H. Lee, *Nanomedicine*, 2011, **6**, 793-801.
218. X. Liu, J. Cao, H. Li, J. Li, Q. Jin, K. Ren and J. Ji, *ACS Nano*, 2013, **7**, 9384-9395.
219. Y. Liu, K. Ai, J. Liu, M. Deng, Y. He and L. Lu, *Adv. Mater.*, 2013, **25**, 1353-1359.

220. K.-Y. Ju, Y. Lee, S. Lee, S. B. Park and J.-K. Lee, *Biomacromolecules*, 2011, **12**, 625-632.
221. H. Peng, K. Rübsam, X. Huang, F. Jakob, M. Karperien, U. Schwaneberg and A. Pich, *Macromolecules*, 2016, **49**, 7141-7154.
222. Z. Wang, Y. Xie, Y. Li, Y. Huang, L. R. Parent, T. Ditri, N. Zang, J. D. Rinehart and N. C. Gianneschi, *Chem. Mater.*, 2017, **29**, 8195-8201.
223. J. Cui, Y. Ju, K. Liang, H. Ejima, S. Lörcher, K. T. Gause, J. J. Richardson and F. Caruso, *Soft Matter*, 2014, **10**, 2656-2663.
224. J. Cui, Y. Yan, G. K. Such, K. Liang, C. J. Ochs, A. Postma and F. Caruso, *Biomacromolecules*, 2012, **13**, 2225-2228.
225. R. Mrówczyński, *ACS Appl. Mater. Interfaces*, 2018, **10**, 7541-7561.
226. J. Park, H. Moon and S. Hong, *Biomater. Res.*, 2019, **23**, 24.
227. K. C. Black, J. Yi, J. G. Rivera, D. C. Zelasko-Leon and P. B. Messersmith, *Nanomedicine*, 2013, **8**, 17-28.
228. C.-C. Ho and S.-J. Ding, *J. Mater. Sci.: Mater. Med.*, 2013, **24**, 2381-2390.
229. L.-S. Lin, Z.-X. Cong, J.-B. Cao, K.-M. Ke, Q.-L. Peng, J. Gao, H.-H. Yang, G. Liu and X. Chen, *ACS Nano*, 2014, **8**, 3876-3883.
230. F. Liu, X. He, J. Zhang, H. Chen, H. Zhang and Z. Wang, *J. Mater. Chem. B*, 2015, **3**, 6731-6739.
231. Z.-H. Miao, H. Wang, H. Yang, Z.-L. Li, L. Zhen and C.-Y. Xu, *ACS Appl. Mater. Interfaces*, 2015, **7**, 16946-16952.
232. X. Zhong, K. Yang, Z. Dong, X. Yi, Y. Wang, C. Ge, Y. Zhao and Z. Liu, *Adv. Funct. Mater.*, 2015, **25**, 7327-7336.
233. Z. Dong, H. Gong, M. Gao, W. Zhu, X. Sun, L. Feng, T. Fu, Y. Li and Z. Liu, *Theranostics*, 2016, **6**, 1031.
234. R. Ge, X. Li, M. Lin, D. Wang, S. Li, S. Liu, Q. Tang, Y. Liu, J. Jiang, L. Liu, H. Sun, H. Zhang and B. Yang, *ACS Appl. Mater. Interfaces*, 2016, **8**, 22942-22952.
235. Z. Wang, L. Wang, N. Prabhakar, Y. Xing, J. M. Rosenholm, J. Zhang and K. Cai, *Acta Biomater.*, 2019, **86**, 416-428.
236. M. Tanaka, M. Yoshida, H. Emoto and H. Ishii, *Eur. J. Pharmacol.*, 2000, **405**, 397-406.
237. D. S. Goldstein, *Hypertension*, 1983, **5**, 86-99.
238. Z. Lu, A. M. Douek, A. M. Rozario, R. F. Tabor, J. Kaslin, B. Follink and B. M. Teo, *J. Mater. Chem. B*, 2020, **8**, 961-968.
239. N. F. Della Vecchia, A. Luchini, A. Napolitano, G. D'Errico, G. Vitiello, N. Szekely, M. d'Ischia and L. Paduano, *Langmuir*, 2014, **30**, 9811-9818.
240. X. Jiang, Y. Wang and M. Li, *Sci. Rep.*, 2014, **4**, 1-6.
241. D. J. Kim, K.-Y. Ju and J.-K. Lee, *Bull. Korean Chem. Soc.*, 2012, **33**, 3788-3792.
242. X. Wang, J. Zhang, Y. Wang, C. Wang, J. Xiao, Q. Zhang and Y. Cheng, *Biomaterials*, 2016, **81**, 114-124.
243. W. Cheng, J. Nie, L. Xu, C. Liang, Y. Peng, G. Liu, T. Wang, L. Mei, L. Huang and X. Zeng, *ACS Appl. Mater. Interfaces*, 2017, **9**, 18462-18473.
244. W.-Q. Li, Z. Wang, S. Hao, H. He, Y. Wan, C. Zhu, L.-P. Sun, G. Cheng and S.-Y. Zheng, *ACS Appl. Mater. Interfaces*, 2017, **9**, 16793-16802.
245. A. Priyam, P. Nagar, A. K. Sharma and P. Kumar, *Colloids Surf. B*, 2018, **161**, 403-412.
246. B. Poinard, S. Z. Y. Neo, E. L. L. Yeo, H. P. S. Heng, K. G. Neoh and J. C. Y. Kah, *ACS Appl. Mater. Interfaces*, 2018, **10**, 21125-21136.

247. Z. Dong, L. Feng, Y. Hao, M. Chen, M. Gao, Y. Chao, H. Zhao, W. Zhu, J. Liu, C. Liang, Q. Zhang and Z. Liu, *J. Am. Chem. Soc.*, 2018, **140**, 2165-2178.
248. R. Ge, M. Lin, X. Li, S. Liu, W. Wang, S. Li, X. Zhang, Y. Liu, L. Liu and F. Shi, *ACS Appl. Mater. Interfaces*, 2017, **9**, 19706-19716.
249. D. Hu, C. Liu, L. Song, H. Cui, G. Gao, P. Liu, Z. Sheng and L. Cai, *Nanoscale*, 2016, **8**, 17150-17158.
250. J. Lin, M. Wang, H. Hu, X. Yang, B. Wen, Z. Wang, O. Jacobson, J. Song, G. Zhang, G. Niu, P. Huang and X. Chen, *Adv. Mater.*, 2016, **28**, 3273-3279.
251. J.-S. Liu, S.-J. Peng, G.-F. Li, Y.-X. Zhao, X.-Y. Meng, X.-R. Yu, Z.-H. Li and J.-M. Chen, *ACS Biomater. Sci. Eng.*, 2020, **6**, 664-672.
252. M. Battaglini, A. Marino, A. Carmignani, C. Tapeinos, V. Cauda, A. Ancona, N. Garino, V. Vighetto, G. La Rosa, E. Sinibaldi and G. Ciofani, *ACS Appl. Mater. Interfaces*, 2020, **12**, 35782-35798.
253. X. Bao, J. Zhao, J. Sun, M. Hu and X. Yang, *ACS Nano*, 2018, **12**, 8882-8892.
254. A. K. Srivastava, S. Roy Choudhury and S. Karmakar, *Biomater. Sci.*, 2020, **8**, 1345-1363.
255. H. Zhao, Z. Zeng, L. Liu, J. Chen, H. Zhou, L. Huang, J. Huang, H. Xu, Y. Xu, Z. Chen, Y. Wu, W. Guo, J. H. Wang, J. Wang and Z. Liu, *Nanoscale*, 2018, **10**, 6981-6991.
256. X. Bao, J. Zhao, J. Sun, M. Hu and X. Yang, *ACS Nano*, 2018, **12**, 8882-8892.
257. W.-L. Liu, T. Liu, M.-Z. Zou, W.-Y. Yu, C.-X. Li, Z.-Y. He, M.-K. Zhang, M.-D. Liu, Z.-H. Li, J. Feng and X.-Z. Zhang, *Adv. Mater.*, 2018, **30**, 1802006.
258. N. Wang, Y. Yang, X. Wang, X. Tian, W. Qin, X. Wang, J. Liang, H. Zhang and X. Leng, *ACS Biomater. Sci. Eng.*, 2019, **5**, 2330-2342.
259. X. Wang, N. Wang, Y. Yang, X. Wang, J. Liang, X. Tian, H. Zhang and X. Leng, *Biomater. Sci.*, 2019, **7**, 3062-3075.
260. Q. V. Le, J. Suh, J. J. Choi, G. T. Park, J. W. Lee, G. Shim and Y. K. Oh, *ACS Nano*, 2019, **13**, 7442-7462.
261. L. Wang, Y. He, T. He, G. Liu, C. Lin, K. Li, L. Lu and K. Cai, *Biomaterials*, 2020, **255**, 120208.
262. R. Chen, C. Zhu, Y. Fan, W. Feng, J. Wang, E. Shang, Q. Zhou and Z. Chen, *ACS Appl. Bio Mater.*, 2019, **2**, 874-883.
263. Y. Cheng, S. Zhang, N. Kang, J. Huang, X. Lv, K. Wen, S. Ye, Z. Chen, X. Zhou and L. Ren, *ACS Appl. Mater. Interfaces*, 2017, **9**, 19296-19306.
264. S. Wang, X. Zhao, S. Wang, J. Qian and S. He, *ACS Appl. Mater. Interfaces*, 2016, **8**, 24368-24384.
265. L. Zhang, H. Su, J. Cai, D. Cheng, Y. Ma, J. Zhang, C. Zhou, S. Liu, H. Shi and Y. Zhang, *ACS Nano*, 2016, **10**, 10404-10417.
266. Z. Ouyang, T. Tan, C. Liu, J. Duan, W. Wang, X. Guo, Q. Zhang, Z. Li, Q. Huang and P. Dou, *Biomaterials*, 2019, **205**, 50-63.
267. D. Zhu, W. Tao, H. Zhang, G. Liu, T. Wang, L. Zhang, X. Zeng and L. Mei, *Acta Biomater.*, 2016, **30**, 144-154.
268. D. Chang, Y. Gao, L. Wang, G. Liu, Y. Chen, T. Wang, W. Tao, L. Mei, L. Huang and X. Zeng, *J. Colloid Interface Sci.*, 2016, **463**, 279-287.
269. R. Zhang, S. Su, K. Hu, L. Shao, X. Deng, W. Sheng and Y. Wu, *Nanoscale*, 2015, **7**, 19722-19731.
270. C. Wang, K. Kimura, J. Li, J. J. Richardson, M. Naito, K. Miyata, T. Ichiki and H. Ejima, *ChemNanoMat*, 2021, **7**, 592-595.
271. M. Li, X. Sun, N. Zhang, W. Wang, Y. Yang, H. Jia and W. Liu, *Adv. Sci.*, 2018, **5**, 1800155.

272. H. Li, Y. Jia, X. Feng and J. Li, *J. Colloid Interface Sci.*, 2017, **487**, 12-19.
273. F. Ding, X. Gao, X. Huang, H. Ge, M. Xie, J. Qian, J. Song, Y. Li, X. Zhu and C. Zhang, *Biomaterials*, 2020, **245**, 119976.
274. B. Poinard, S. A. E. Lam, K. G. Neoh and J. C. Y. Kah, *J. Controlled Release*, 2019, **300**, 161-173.
275. B. Poinard, S. Kamaluddin, A. Q. Q. Tan, K. G. Neoh and J. C. Y. Kah, *ACS Appl. Mater. Interfaces*, 2019, **11**, 4777-4789.
276. A. Postma, Y. Yan, Y. Wang, A. N. Zelikin, E. Tjipto and F. Caruso, *Chem. Mater.*, 2009, **21**, 3042-3044.
277. X. Chen, Y. Yan, M. Müllner, M. P. Van Koeverden, K. F. Noi, W. Zhu and F. Caruso, *Langmuir*, 2014, **30**, 2921-2925.
278. L. Zhang, J. Shi, Z. Jiang, Y. Jiang, R. Meng, Y. Zhu, Y. Liang and Y. Zheng, *ACS Appl. Mater. Interfaces*, 2011, **3**, 597-605.
279. Z. Ye, S. Wu, C. Zheng, L. Yang, P. Zhang and Z. Zhang, *Langmuir*, 2017, **33**, 12952-12959.
280. B. Yu, D. A. Wang, Q. Ye, F. Zhou and W. Liu, *Chem. Commun.*, 2009, 6789-6791.
281. L. Yang, C. Wang, Z. Ye, P. Zhang, S. Wu, S. Jia, Z. Li and Z. Zhang, *RSC Adv.*, 2017, **7**, 21686-21696.
282. J. Cui, Y. Wang, A. Postma, J. Hao, L. Hosta-Rigau and F. Caruso, *Adv. Funct. Mater.*, 2010, **20**, 1625-1631.
283. Y.-Z. Ni, W.-F. Jiang, G.-S. Tong, J.-X. Chen, J. Wang, H.-M. Li, C.-Y. Yu, X.-h. Huang and Y.-F. Zhou, *Org. Biomol. Chem.*, 2015, **13**, 686-690.
284. L. Tan, W. Tang, T. Liu, X. Ren, C. Fu, B. Liu, J. Ren and X. Meng, *ACS Appl. Mater. Interfaces*, 2016, **8**, 11237-11245.
285. W. Tang, B. Liu, S. Wang, T. Liu, C. Fu, X. Ren, L. Tan, W. Duan and X. Meng, *RSC Adv.*, 2016, **6**, 32434-32440.
286. H. Zhuang, H. Su, X. Bi, Y. Bai, L. Chen, D. Ge, W. Shi and Y. Sun, *ACS Biomater. Sci. Eng.*, 2017, **3**, 1799-1808.
287. S. H. Yang, S. M. Kang, K.-B. Lee, T. D. Chung, H. Lee and I. S. Choi, *J. Am. Chem. Soc.*, 2011, **133**, 2795-2797.
288. L. Wang, Z.-Y. Hu, X.-Y. Yang, B.-B. Zhang, W. Geng, G. Van Tendeloo and B.-L. Su, *Chem. Commun.*, 2017, **53**, 6617-6620.
289. B. Wang, G. Wang, B. Zhao, J. Chen, X. Zhang and R. Tang, *Chem. Sci.*, 2014, **5**, 3463-3468.
290. T. T. Nguyen, T. T. Pham, H. T. Nguyen, M. R. Nepal, C. D. Phung, Z. You, N. Katila, N. T. Pun, T. C. Jeong, D.-Y. Choi, P.-H. Park, C. S. Yong, J. O. Kim, S. Yook and J.-H. Jeong, *Biomaterials*, 2019, **221**, 119415.
291. Q. Dai, H. Geng, Q. Yu, J. Hao and J. Cui, *Theranostics*, 2019, **9**, 3170-3190.
292. M. A. Rahim, S. L. Kristufek, S. Pan, J. J. Richardson and F. Caruso, *Angew. Chem. Int. Ed. Engl.*, 2018, **58**, 1904-1927.
293. Z. Zhang, L. Xie, Y. Ju and Y. Dai, *Small*, 2021, **17**, 2100314.
294. D. Wu, J. Zhou, M. N. Creyer, W. Yim, Z. Chen, P. B. Messersmith and J. V. Jokerst, *Chem. Soc. Rev.*, 2021, **50**, 4432-4483.
295. A. Escarpa and M. Gonzalez, *Crit. Rev. Anal. Chem.*, 2001, **31**, 57-139.
296. S. Quideau, D. Deffieux, C. Douat-Casassus and L. Pouysegu, *Angew. Chem. Int. Ed.*, 2011, **50**, 586-621.
297. K. Robards and M. Antolovich, *Analyst*, 1997, **122**, 11R-34R.

298. J. Macheix, A. Fleuriet and J. Billot, in *Fruit Phenolics*, ed. J. Macheix, A. Fleuriet and J. Billot, CRC Press, Boca Raton, FL, 1st edn., 1990, pp. 295-358.
299. F. He, Q.-H. Pan, Y. Shi and C.-Q. Duan, *Molecules*, 2008, **13**, 3007-3032.
300. N.-E. Es-Safi, S. Ghidouche and P. H. Ducrot, *Molecules*, 2007, **12**, 2228-2258.
301. Y. Zhang, S.-Z. Li, J. Li, X. Pan, R. E. Cahoon, J. G. Jaworski, X. Wang, J. M. Jez, F. Chen and O. Yu, *J. Am. Chem. Soc.*, 2006, **128**, 13030-13031.
302. Z. L. Fowler and M. A. Koffas, *Appl. Microbiol. Biotechnol.*, 2009, **83**, 799-808.
303. F. Daayf and V. Lattanzio, *Recent Advances in Polyphenol Research*, John Wiley & Sons, 2009.
304. L. Mira, M. Tereza Fernandez, M. Santos, R. Rocha, M. Helena Florêncio and K. R. Jennings, *Free Radical Res.*, 2002, **36**, 1199-1208.
305. N. Sugihara, M. Ohnishi, M. Imamura and K. Furuno, *J. Health Sci.*, 2001, **47**, 99-106.
306. H. Sasaki, M. Matsumoto, T. Tanaka, M. Maeda, M. Nakai, S. Hamada and T. Ooshima, *Caries Res.*, 2003, **38**, 2-8.
307. S. Sakanaka, L. R. Juneja and M. Taniguchi, *J. Biosci. Bioeng.*, 2000, **90**, 81-85.
308. D. E. Ehrnhoefer, J. Bieschke, A. Boeddrich, M. Herbst, L. Masino, R. Lurz, S. Engemann, A. Pastore and E. E. Wanker, *Nat. Struct. Mol. Biol.*, 2008, **15**, 558-566.
309. I. A. Siddiqui, V. M. Adhami, F. Afaq, N. Ahmad and H. Mukhtar, *J. Cell. Biochem.*, 2004, **91**, 232-242.
310. S. Quideau, D. Deffieux, C. Douat-Casassus and L. Pouységu, *Angew. Chem. Int. Ed. Engl.*, 2011, **50**, 586-621.
311. E. Haslam, *Practical Polyphenolics: From Structure to Molecular Recognition and Physiological Action*, Cambridge University Press, 1998.
312. T. S. Sileika, D. G. Barrett, R. Zhang, K. H. A. Lau and P. B. Messersmith, *Angew. Chem. Int. Ed. Engl.*, 2013, **52**, 10766-10770.
313. H. Ejima, J. J. Richardson, K. Liang, J. P. Best, M. P. van Koeverden, G. K. Such, J. Cui and F. Caruso, *Science*, 2013, **341**, 154-157.
314. L. Jakobek, *Food Chem.*, 2015, **175**, 556-567.
315. J. Guo, T. Suma, J. J. Richardson and H. Ejima, *ACS Biomater. Sci. Eng.*, 2019, **5**, 5578-5596.
316. J. Guo, Y. Ping, H. Ejima, K. Alt, M. Meissner, J. J. Richardson, Y. Yan, K. Peter, D. von Elverfeldt and C. E. Hagemeyer, *Angew. Chem. Int. Ed. Engl.*, 2014, **53**, 5546-5551.
317. M. A. Rahim, K. Kempe, M. Müllner, H. Ejima, Y. Ju, M. P. van Koeverden, T. Suma, J. A. Braunger, M. G. Leeming and B. F. Abrahams, *Chem. Mater.*, 2015, **27**, 5825-5832.
318. Y. Ju, C. Cortez-Jugo, J. Chen, T.-Y. Wang, A. J. Mitchell, E. Tsantikos, N. Bertleff-Zieschang, Y.-W. Lin, J. Song, Y. Cheng, S. Mettu, M. A. Rahim, S. Pan, G. Yun, M. L. Hibbs, L. Y. Yeo, C. E. Hagemeyer and F. Caruso, *Adv. Sci.*, 2020, **7**, 1902650.
319. S. Spoljaric, Y. Ju and F. Caruso, *Chem. Mater.*, 2021, **33**, 1099-1115.
320. K. Saowalak, T. Titipun, T. Somchai and P. Chalermchai, *Sci. Rep.*, 2018, **8**, 6647-6647.
321. C. Xu, Y. Wang, H. Yu, H. Tian and X. Chen, *ACS Nano*, 2018, **12**, 8255-8265.
322. F. Liu, X. He, H. Chen, J. Zhang, H. Zhang and Z. Wang, *Nat. Commun.*, 2015, **6**, 8003.
323. X. Wang, J. Yan, D. Pan, R. Yang, L. Wang, Y. Xu, J. Sheng, Y. Yue, Q. Huang, Y. Wang, R. Wang and M. Yang, *Adv. Healthcare Mater.*, 2018, **7**, 1701505.
324. W. Zhu, S. Liang, J. Wang, Z. Yang, L. Zhang, T. Yuan, Z. Xu, H. Xu and P. Li, *J. Mater. Sci. Mater. Med.*,

2017, **28**, 74.
325. C. Wang, H. Sang, Y. Wang, F. Zhu, X. Hu, X. Wang, X. Wang, Y. Li and Y. Cheng, *Nano Lett.*, 2018, **18**, 7045-7051.
326. Z. Ren, S. Sun, R. Sun, G. Cui, L. Hong, B. Rao, A. Li, Z. Yu, Q. Kan and Z. Mao, *Adv. Mater.*, 2020, **32**, 1906024.
327. D.-W. Zheng, Q. Lei, J.-Y. Zhu, J.-X. Fan, C.-X. Li, C. Li, Z. Xu, S.-X. Cheng and X.-Z. Zhang, *Nano Lett.*, 2017, **17**, 284-291.
328. K. Li, G. Xiao, J. J. Richardson, B. L. Tardy, H. Ejima, W. Huang, J. Guo, X. Liao and B. Shi, *Adv. Sci.*, 2019, **6**, 1801688.
329. K. Li, Y. Dai, W. Chen, K. Yu, G. Xiao, J. J. Richardson, W. Huang, J. Guo, X. Liao and B. Shi, *Adv. Biosyst.*, 2019, **3**, 1800241.
330. H. Xiong, Z. Wang, C. Wang and J. Yao, *Nano Lett.*, 2020, **20**, 1781-1790.
331. G. Shen, R. Xing, N. Zhang, C. Chen, G. Ma and X. Yan, *ACS Nano*, 2016, **10**, 5720-5729.
332. H. Huang, P. Li, C. Liu, H. Ma, H. Huang, Y. Lin, C. Wang and Y. Yang, *RSC Adv.*, 2017, **7**, 2829-2835.
333. T. Liu, W. Liu, M. Zhang, W. Yu, F. Gao, C. Li, S.-B. Wang, J. Feng and X.-Z. Zhang, *ACS Nano*, 2018, **12**, 12181-12192.
334. J. Chen, J. Li, J. Zhou, Z. Lin, F. Cavalieri, E. Czuba-Wojnilowicz, Y. Hu, A. Glab, Y. Ju, J. J. Richardson and F. Caruso, *ACS Nano*, 2019, **13**, 11653-11664.
335. W. Zhang, A. J. Christofferson, Q. A. Besford, J. J. Richardson, J. Guo, Y. Ju, K. Kempe, I. Yarovsky and F. Caruso, *Nanoscale*, 2019, **11**, 1921-1928.
336. W. Zhang, Q. A. Besford, A. J. Christofferson, P. Charchar, J. J. Richardson, A. Elbourne, K. Kempe, C. E. Hagemeyer, M. R. Field, C. F. McConville, I. Yarovsky and F. Caruso, *Nano Lett.*, 2020, **20**, 2660-2666.
337. J.-X. Fan, D.-W. Zheng, W.-W. Mei, S. Chen, S.-Y. Chen, S.-X. Cheng and X.-Z. Zhang, *Small*, 2017, **13**, 1702714.
338. T. Liu, M. Zhang, W. Liu, X. Zeng, X. Song, X. Yang, X. Zhang and J. Feng, *ACS Nano*, 2018, **12**, 3917-3927.
339. M. Björnmalm, J. Cui, N. Bertleff-Zieschang, D. Song, M. Faria, M. A. Rahim and F. Caruso, *Chem. Mater.*, 2017, **29**, 289-306.
340. Y. Ping, J. Guo, H. Ejima, X. Chen, J. J. Richardson, H. Sun and F. Caruso, *Small*, 2015, **11**, 2032-2036.
341. J. Guo, X. Wang, D. C. Henstridge, J. J. Richardson, J. Cui, A. Sharma, M. A. Febbraio, K. Peter, J. B. de Haan and C. E. Hagemeyer, *Adv. Healthcare Mater.*, 2015, **4**, 2170-2175.
342. Y. Ju, J. Cui, M. Müllner, T. Suma, M. Hu and F. Caruso, *Biomacromolecules*, 2015, **16**, 807-814.
343. Y. Ju, J. Cui, H. Sun, M. Müllner, Y. Dai, J. Guo, N. Bertleff-Zieschang, T. Suma, J. J. Richardson and F. Caruso, *Biomacromolecules*, 2016, **17**, 2268-2276.
344. Q. A. Besford, Y. Ju, T.-Y. Wang, G. Yun, P. Cherepanov, C. E. Hagemeyer, F. Cavalieri and F. Caruso, *Small*, 2018, **14**, 1802342.
345. Y. Ju, Q. Dai, J. Cui, Y. Dai, T. Suma, J. J. Richardson and F. Caruso, *ACS Appl. Mater. Interfaces*, 2016, **8**, 22914-22922.
346. S. Li, Y. Ju, J. Zhou, K. F. Noi, A. J. Mitchell, T. Zheng, S. J. Kent, C. J. H. Porter and F. Caruso, *ACS Appl. Mater. Interfaces*, 2021, **13**, 35494-35505.
347. D. Gan, W. Xing, L. Jiang, J. Fang, C. Zhao, F. Ren, L. Fang, K. Wang and X. Lu, *Nat. Commun.*, 2019, **10**,

1487.
348. E. Haslam, *Plant Polyphenols: Vegetable Tannins Revisited*, Cambridge University Press, 1989.
349. M. Shin, H.-A. Lee, M. Lee, Y. Shin, J.-J. Song, S.-W. Kang, D.-H. Nam, E. J. Jeon, M. Cho, M. Do, S. Park, M. S. Lee, J.-H. Jang, S.-W. Cho, K.-S. Kim and H. Lee, *Nat. Biomed. Eng.*, 2018, **2**, 304-317.
350. Y. Han, Z. Lin, J. Zhou, G. Yun, R. Guo, J. J. Richardson and F. Caruso, *Angew. Chem. Int. Ed. Engl.*, 2020, **59**, 15618-15625.
351. Y. Han, J. Zhou, Y. Hu, Z. Lin, Y. Ma, J. J. Richardson and F. Caruso, *ACS Nano*, 2020, **14**, 12972–12981.
352. H. Lee, D. T. Nguyen, N. Kim, S. Y. Han, Y. J. Hong, G. Yun, B. J. Kim and I. S. Choi, *ACS Appl. Mater. Interfaces*, 2021, **13**, 52385-52394.
353. Q.-Z. Zhong, J. J. Richardson, S. Li, W. Zhang, Y. Ju, J. Li, S. Pan, J. Chen and F. Caruso, *Angew. Chem. Int. Ed. Engl.*, 2020, **59**, 1711-1717.
354. Y. Honda, T. Nomoto, M. Matsui, H. Takemoto, Y. Miura and N. Nishiyama, *ACS Appl. Mater. Interfaces*, 2021, **13**, 54850-54859.
355. J. H. Park, K. Kim, J. Lee, J. Y. Choi, D. Hong, S. H. Yang, F. Caruso, Y. Lee and I. S. Choi, *Angew. Chem. Int. Ed.*, 2014, **53**, 12420-12425.
356. J. Lee, H. Cho, J. Choi, D. Kim, D. Hong, J. H. Park, S. H. Yang and I. S. Choi, *Nanoscale*, 2015, **7**, 18918-18922.
357. W. Li, W. Bing, S. Huang, J. Ren and X. Qu, *Adv. Funct. Mater.*, 2015, **25**, 3775-3784.
358. J. Y. Kim, H. Lee, T. Park, J. Park, M. H. Kim, H. Cho, W. Youn, S. M. Kang and I. S. Choi, *Chem. Asian J.*, 2016, **11**, 3183-3187.
359. T. Park, J. Y. Kim, H. Cho, H. C. Moon, B. J. Kim, J. H. Park, D. Hong, J. Park and I. S. Choi, *Polymers*, 2017, **9**, 140.
360. X. Wang, Z. Chen, C. Zhang, C. Zhang, G. Ma, J. Yang, X. Wei and H. Sun, *Adv. Healthcare Mater.*, 2019, **8**, 1900474.
361. Z. Zhao, D. C. Pan, Q. M. Qi, J. Kim, N. Kapate, T. Sun, C. W. Shields IV, L. L. W. Wang, D. Wu and C. J. Kwon, *Adv. Mater.*, 2020, **32**, 2003492.
362. W. Zhu, J. Guo, S. Amini, Y. Ju, J. O. Agola, A. Zimpel, J. Shang, A. Noureddine, F. Caruso, S. Wuttke, J. G. Croissant and C. J. Brinker, *Adv. Mater.*, 2019, **31**, 1900545.
363. C. M. Hu, L. Zhang, S. Aryal, C. Cheung, R. H. Fang and L. Zhang, *Proc. Natl. Acad. Sci. U.S.A*, 2011, **108**, 10980-10985.
364. M. Föller, S. M. Huber and F. Lang, *IUBMB life*, 2008, **60**, 661-668.
365. P. A. Oldenborg, A. Zheleznyak, Y. F. Fang, C. F. Lagenaur, H. D. Gresham and F. P. Lindberg, *Science*, 2000, **288**, 2051-2054.
366. L. Rao, L. L. Bu, J. H. Xu, B. Cai, G. T. Yu, X. Yu, Z. He, Q. Huang, A. Li, S. S. Guo, W. F. Zhang, W. Liu, Z. J. Sun, H. Wang, T. H. Wang and X. Z. Zhao, *Small*, 2015, **11**, 6225-6236.
367. W. Chen, K. Zeng, H. Liu, J. Ouyang, L. Wang, Y. Liu, H. Wang, L. Deng and Y.-N. Liu, *Adv. Funct. Mater.*, 2017, **27**, 1605795.
368. L. Zhang, Z. Wang, Y. Zhang, F. Cao, K. Dong, J. Ren and X. Qu, *ACS Nano*, 2018, **12**, 10201-10211.
369. Y. Zhai, W. Ran, J. Su, T. Lang, J. Meng, G. Wang, P. Zhang and Y. Li, *Adv. Mater.*, 2018, e1802378.
370. M. Xuan, J. Shao, J. Zhao, Q. Li, L. Dai and J. Li, *Angew. Chem. Int. Ed. Engl.*, 2018, **57**, 6049-6053.
371. C.-M. J. Hu, R. H. Fang, J. Copp, B. T. Luk and L. Zhang, *Nat. Nanotechnol.*, 2013, **8**, 336-340.

372. C. M. Hu, R. H. Fang, B. T. Luk and L. Zhang, *Nat. Nanotechnol.*, 2013, **8**, 933-938.
373. Y. Guo, D. Wang, Q. Song, T. Wu, X. Zhuang, Y. Bao, M. Kong, Y. Qi, S. Tan and Z. Zhang, *ACS Nano*, 2015, **9**, 6918-6933.
374. Y. Godfrin, F. Horand and M. Cremel, *Immunotherapy*, 2012, **4**, 871-873.
375. M. Cremel, N. Guérin, F. Horand, A. Banz and Y. Godfrin, *Int. J. Pharm.*, 2013, **443**, 39-49.
376. L. Rao, B. Cai, L. L. Bu, Q. Q. Liao, S. S. Guo, X. Z. Zhao, W. F. Dong and W. Liu, *ACS Nano*, 2017, **11**, 3496-3505.
377. M. Olsson, P. Bruhns, W. A. Frazier, J. V. Ravetch and P. A. Oldenborg, *Blood*, 2005, **105**, 3577-3582.
378. P. J. Sims, S. A. Rollins and T. Wiedmer, *J. Biol. Chem.*, 1989, **264**, 19228-19235.
379. J. R. Fitzgerald, T. J. Foster and D. Cox, *Nat. Rev. Microbiol.*, 2006, **4**, 445-457.
380. B. Nieswandt and S. P. Watson, *Blood*, 2003, **102**, 449-461.
381. M. R. Yeaman, *Cell Mol. Life Sci.*, 2010, **67**, 525-544.
382. C.-M. J. Hu, R. H. Fang, K.-C. Wang, B. T. Luk, S. Thamphiwatana, D. Dehaini, P. Nguyen, P. Angsantikul, C. H. Wen, A. V. Kroll, C. Carpenter, M. Ramesh, V. Qu, S. H. Patel, J. Zhu, W. Shi, F. M. Hofman, T. C. Chen, W. Gao, K. Zhang, S. Chien and L. Zhang, *Nature*, 2015, **526**, 118-121.
383. M. Labelle, S. Begum and R. O. Hynes, *Proc. Natl. Acad. Sci. U.S.A*, 2014, **111**, E3053-3061.
384. L. Rao, L.-L. Bu, Q.-F. Meng, B. Cai, W.-W. Deng, A. Li, K. Li, S.-S. Guo, W.-F. Zhang, W. Liu, Z.-J. Sun and X.-Z. Zhao, *Adv. Funct. Mater.*, 2017, **27**, 1604774.
385. D. Dehaini, X. Wei, R. H. Fang, S. Masson, P. Angsantikul, B. T. Luk, Y. Zhang, M. Ying, Y. Jiang, A. V. Kroll, W. Gao and L. Zhang, *Adv. Mater.*, 2017, **29**, 1606209.
386. Y. Zhang, K. Cai, C. Li, Q. Guo, Q. Chen, X. He, L. Liu, Y. Zhang, Y. Lu, X. Chen, T. Sun, Y. Huang, J. Cheng and C. Jiang, *Nano Lett.*, 2018, **18**, 1908-1915.
387. R. Noy and J. W. Pollard, *Immunity*, 2014, **41**, 49-61.
388. D. F. Quail and J. A. Joyce, *Nat. Med.*, 2013, **19**, 1423-1437.
389. B. Z. Qian and J. W. Pollard, *Cell*, 2010, **141**, 39-51.
390. L. Wan, K. Pantel and Y. Kang, *Nat. Med.*, 2013, **19**, 1450-1464.
391. Q. Chen, X. H. Zhang and J. Massagué, *Cancer Cell*, 2011, **20**, 538-549.
392. B. Z. Qian, J. Li, H. Zhang, T. Kitamura, J. Zhang, L. R. Campion, E. A. Kaiser, L. A. Snyder and J. W. Pollard, *Nature*, 2011, **475**, 222-225.
393. H. Cao, Z. Dan, X. He, Z. Zhang, H. Yu, Q. Yin and Y. Li, *ACS Nano*, 2016, **10**, 7738-7748.
394. G. Deng, Z. Sun, S. Li, X. Peng, W. Li, L. Zhou, Y. Ma, P. Gong and L. Cai, *ACS Nano*, 2018, **12**, 12096-12108.
395. X. Wei, G. Zhang, D. Ran, N. Krishnan, R. H. Fang, W. Gao, S. A. Spector and L. Zhang, *Adv. Mater.*, 2018, **30**, e1802233.
396. Q. Zhang, D. Dehaini, Y. Zhang, J. Zhou, X. Chen, L. Zhang, R. H. Fang, W. Gao and L. Zhang, *Nat. Nanotechnol.*, 2018, **13**, 1182-1190.
397. J. Y. Zhu, D. W. Zheng, M. K. Zhang, W. Y. Yu, W. X. Qiu, J. J. Hu, J. Feng and X. Z. Zhang, *Nano Lett.*, 2016, **16**, 5895-5901.
398. R. Yang, J. Xu, L. Xu, X. Sun, Q. Chen, Y. Zhao, R. Peng and Z. Liu, *ACS Nano*, 2018, **12**, 5121-5129.
399. A. V. Kroll, R. H. Fang, Y. Jiang, J. Zhou, X. Wei, C. L. Yu, J. Gao, B. T. Luk, D. Dehaini, W. Gao and L. Zhang, *Adv. Mater.*, 2017, **29**.

400. F. Fontana, M. A. Shahbazi, D. Liu, H. Zhang, E. Mäkilä, J. Salonen, J. T. Hirvonen and H. A. Santos, *Adv. Mater.*, 2017, **29**, 1703969.
401. R. H. Fang, C. M. Hu, B. T. Luk, W. Gao, J. A. Copp, Y. Tai, D. E. O'Connor and L. Zhang, *Nano Lett.*, 2014, **14**, 2181-2188.
402. D. Shao, M. Li, Z. Wang, X. Zheng, Y. H. Lao, Z. Chang, F. Zhang, M. Lu, J. Yue, H. Hu, H. Yan, L. Chen, W. F. Dong and K. W. Leong, *Adv. Mater.*, 2018, **30**, e1801198.
403. H. Sun, J. Su, Q. Meng, Q. Yin, L. Chen, W. Gu, Z. Zhang, H. Yu, P. Zhang, S. Wang and Y. Li, *Adv. Funct. Mater.*, 2017, **27**, 1604300.
404. D. Nie, Z. Dai, J. Li, Y. Yang, Z. Xi, J. Wang, W. Zhang, K. Qian, S. Guo, C. Zhu, R. Wang, Y. Li, M. Yu, X. Zhang, X. Shi and Y. Gan, *Nano Lett.*, 2020, **20**, 936-946.
405. S. Y. Li, H. Cheng, B. R. Xie, W. X. Qiu, J. Y. Zeng, C. X. Li, S. S. Wan, L. Zhang, W. L. Liu and X. Z. Zhang, *ACS Nano*, 2017, **11**, 7006-7018.
406. W. Xie, W. W. Deng, M. Zan, L. Rao, G. T. Yu, D. M. Zhu, W. T. Wu, B. Chen, L. W. Ji, L. Chen, K. Liu, S. S. Guo, H. M. Huang, W. F. Zhang, X. Zhao, Y. Yuan, W. Dong, Z. J. Sun and W. Liu, *ACS Nano*, 2019, **13**, 2849-2857.
407. H. Tian, Z. Luo, L. Liu, M. Zheng, Z. Chen, A. Ma, R. Liang, Z. Han, C. Lu and L. Cai, *Adv. Funct. Mater.*, 2017, **27**, 1703197.
408. M. Simons and G. Raposo, *Curr. Opin. Cell Biol.*, 2009, **21**, 575-581.
409. J. J. Richardson and H. Ejima, *Chem. Mater.*, 2019, **31**, 2191-2201.
410. G. Raposo and W. Stoorvogel, *J. Cell. Biol.*, 2013, **200**, 373-383.
411. R. van der Meel, M. H. Fens, P. Vader, W. W. van Solinge, O. Eniola-Adefeso and R. M. Schiffelers, *J. Controlled Release*, 2014, **195**, 72-85.
412. S. M. van Dommelen, P. Vader, S. Lakhal, S. A. Kooijmans, W. W. van Solinge, M. J. Wood and R. M. Schiffelers, *J. Controlled Release*, 2012, **161**, 635-644.
413. S. Kamerkar, V. S. LeBleu, H. Sugimoto, S. Yang, C. F. Ruivo, S. A. Melo, J. J. Lee and R. Kalluri, *Nature*, 2017, **546**, 498-503.
414. T. R. Lunavat, S. C. Jang, L. Nilsson, H. T. Park, G. Repiska, C. Lasser, J. A. Nilsson, Y. S. Gho and J. Lotvall, *Biomaterials*, 2016, **102**, 231-238.
415. J. S. Choi, H. I. Yoon, K. S. Lee, Y. C. Choi, S. H. Yang, I. S. Kim and Y. W. Cho, *J. Controlled Release*, 2016, **222**, 107-115.
416. S. G. Darband, M. Mirza-Aghazadeh-Attari, M. Kaviani, A. Mihanfar, S. Sadighparvar, B. Yousefi and M. Majidinia, *J. Controlled Release*, 2018, **289**, 158-170.
417. Z. G. Zhang, B. Buller and M. Chopp, *Nat. Rev. Neurol.*, 2019, **15**, 193-203.
418. A. Safdar, A. Saleem and M. A. Tarnopolsky, *Nat. Rev. Endocrinol.*, 2016, **12**, 504-517.
419. S. Sahoo and D. W. Losordo, *Circ. Res.*, 2014, **114**, 333-344.
420. S. W. Ferguson and J. Nguyen, *J. Controlled Release*, 2016, **228**, 179-190.
421. S. Rani and T. Ritter, *Adv. Mater.*, 2016, **28**, 5542-5552.
422. J. M. Pitt, F. Andre, S. Amigorena, J. C. Soria, A. Eggermont, G. Kroemer and L. Zitvogel, *J. Clin. Invest.*, 2016, **126**, 1224-1232.
423. T. Ochiya and J. Lotvall, *Adv. Drug. Delivery Rev.*, 2013, **65**, v.
424. A. Tan, J. Rajadas and A. M. Seifalian, *Adv. Drug. Delivery Rev.*, 2013, **65**, 357-367.

425. J. G. van den Boorn, M. Schlee, C. Coch and G. Hartmann, *Nat. Biotechnol.*, 2011, **29**, 325-326.
426. H. Qi, C. Liu, L. Long, Y. Ren, S. Zhang, X. Chang, X. Qian, H. Jia, J. Zhao, J. Sun, X. Hou, X. Yuan and C. Kang, *ACS Nano*, 2016, **10**, 3323-3333.
427. H. Cheng, J. H. Fan, L. P. Zhao, G. L. Fan, R. R. Zheng, X. Z. Qiu, X. Y. Yu, S. Y. Li and X. Z. Zhang, *Biomaterials*, 2019, **211**, 14-24.
428. C. Théry, L. Zitvogel and S. Amigorena, *Nat. Rev. Immunol.*, 2002, **2**, 569-579.
429. W. Du, K. Zhang, S. Zhang, R. Wang, Y. Nie, H. Tao, Z. Han, L. Liang, D. Wang, J. Liu, N. Liu, Z. Han, D. Kong, Q. Zhao and Z. Li, *Biomaterials*, 2017, **133**, 70-81.
430. R. Tamura, S. Uemoto and Y. Tabata, *Acta Biomater.*, 2017, **57**, 274-284.
431. T. Tian, H. X. Zhang, C. P. He, S. Fan, Y. L. Zhu, C. Qi, N. P. Huang, Z. D. Xiao, Z. H. Lu, B. A. Tannous and J. Gao, *Biomaterials*, 2018, **150**, 137-149.
432. J. Wu, L. Kuang, C. Chen, J. Yang, W. N. Zeng, T. Li, H. Chen, S. Huang, Z. Fu, J. Li, R. Liu, Z. Ni, L. Chen and L. Yang, *Biomaterials*, 2019, **206**, 87-100.
433. R. C. Lai, R. W. Y. Yeo and S. K. Lim, *Semin. Cell Dev. Biol.*, 2015, **40**, 82-88.
434. R. Kalluri, *J. Clin. Invest.*, 2016, **126**, 1208-1215.
435. X. Zhang, X. Yuan, H. Shi, L. Wu, H. Qian and W. Xu, *J. Hematol. Oncol.*, 2015, **8**, 83.
436. K. O. Jung, H. Jo, J. H. Yu, S. S. Gambhir and G. Pratx, *Biomaterials*, 2018, **177**, 139-148.
437. H. Saari, E. Lázaro-Ibáñez, T. Viitala, E. Vuorimaa-Laukkanen, P. Siljander and M. Yliperttula, *J. Controlled Release*, 2015, **220**, 727-737.
438. Z. Yang, J. Xie, J. Zhu, C. Kang, C. Chiang, X. Wang, X. Wang, T. Kuang, F. Chen, Z. Chen, A. Zhang, B. Yu, R. J. Lee, L. Teng and L. J. Lee, *J. Controlled Release*, 2016, **243**, 160-171.
439. T. Yong, X. Zhang, N. Bie, H. Zhang, X. Zhang, F. Li, A. Hakeem, J. Hu, L. Gan, H. A. Santos and X. Yang, *Nat. Commun.*, 2019, **10**, 3838.
440. N. Yim, S. W. Ryu, K. Choi, K. R. Lee, S. Lee, H. Choi, J. Kim, M. R. Shaker, W. Sun, J. H. Park, D. Kim, W. D. Heo and C. Choi, *Nat. Commun.*, 2016, **7**, 12277.
441. M. Qu, Q. Lin, L. Huang, Y. Fu, L. Wang, S. He, Y. Fu, S. Yang, Z. Zhang, L. Zhang and X. Sun, *J. Controlled Release*, 2018, **287**, 156-166.
442. S. C. Jang, O. Y. Kim, C. M. Yoon, D. S. Choi, T. Y. Roh, J. Park, J. Nilsson, J. Lotvall, Y. K. Kim and Y. S. Gho, *ACS Nano*, 2013, **7**, 7698-7710.
443. F. Xiong, X. Ling, X. Chen, J. Chen, J. Tan, W. Cao, L. Ge, M. Ma and J. Wu, *Nano Lett.*, 2019, **19**, 3256-3266.
444. M. J. Haney, N. L. Klyachko, Y. Zhao, R. Gupta, E. G. Plotnikova, Z. He, T. Patel, A. Piroyan, M. Sokolsky, A. V. Kabanov and E. V. Batrakova, *J. Controlled Release*, 2015, **207**, 18-30.
445. G. Jia, Y. Han, Y. An, Y. Ding, C. He, X. Wang and Q. Tang, *Biomaterials*, 2018, **178**, 302-316.
446. Q. Zhu, X. Ling, Y. Yang, J. Zhang, Q. Li, X. Niu, G. Hu, B. Chen, H. Li, Y. Wang and Z. Deng, *Adv. Sci.*, 2019, **6**, 1801899.
447. S. Samanta, S. Rajasingh, N. Drosos, Z. Zhou, B. Dawn and J. Rajasingh, *Acta Pharmacol. Sin.*, 2018, **39**, 501-513.
448. C. Raffin, L. T. Vo and J. A. Bluestone, *Nat. Rev. Immunol.*, 2020, **20**, 158-172.
449. N. L. Klyachko, R. Polak, M. J. Haney, Y. Zhao, R. J. G. Neto, M. C. Hill, A. V. Kabanov, R. E. Cohen, M. F. Rubner and E. V. Batrakova, *Biomaterials*, 2017, **140**, 79-87.

450. X. Li, M. Wenes, P. Romero, S. C.-C. Huang, S.-M. Fendt and P.-C. Ho, *Nat. Rev. Clin. Oncol.*, 2019, **16**, 425-441.
451. L. Tang, Y. Zheng, M. B. Melo, L. Mabardi, A. P. Castaño, Y.-Q. Xie, N. Li, S. B. Kudchodkar, H. C. Wong and E. K. Jeng, *Nat. Biotechnol.*, 2018, **36**, 707-716.
452. A. C. Anselmo, V. Gupta, B. J. Zern, D. Pan, M. Zakrewsky, V. Muzykantov and S. Mitragotri, *ACS Nano*, 2013, **7**, 11129-11137.
453. M. Shin, H.-A. Lee, M. Lee, Y. Shin, J.-J. Song, S.-W. Kang, D.-H. Nam, E. J. Jeon, M. Cho and M. Do, *Nat. Biomed. Eng.*, 2018, **2**, 304-317.
454. S. Lim, J. Park, M. K. Shim, W. Um, H. Y. Yoon, J. H. Ryu, D.-K. Lim and K. Kim, *Theranostics*, 2019, **9**, 7906.
455. H. Y. Yoon, S. T. Selvan, Y. Yang, M. J. Kim, D. K. Yi, I. C. Kwon and K. Kim, *Biomaterials*, 2018, **178**, 597-607.
456. J. M. Caster, C. Callaghan, S. N. Seyedin, K. Henderson, B. Sun and A. Z. Wang, *Adv. Drug. Delivery Rev.*, 2019, **144**, 3-15.
457. X. Zhou, Q. Su, H. Zhao, X. Cao, Y. Yang and W. Xue, *Mol. Pharm.*, 2020, **17**, 4603-4615.
458. C. Huang, L. Zhang, Q. Guo, Y. Zuo, N. Wang, H. Wang, D. Kong, D. Zhu and L. Zhang, *Adv. Funct. Mater.*, 2021, **31**, 2010637.
459. J. Buck, P. Grossen, P. R. Cullis, J. r. Huwyler and D. Witzigmann, *ACS Nano*, 2019, **13**, 3754-3782.
460. C. Sabu, C. Rejo, S. Kotta and K. Pramod, *J. Controlled Release*, 2018, **287**, 142-155.
461. I. M. Degors, C. Wang, Z. U. Rehman and I. S. Zuhorn, *Acc. Chem. Res.*, 2019, **52**, 1750-1760.
462. W. Wang, R. A. Azizyan, A. Garro, A. V. Kajava and S. Ventura, *Biomacromolecules*, 2020, **21**, 4302-4312.
463. M.-A. Shahbazi, M. Sedighi, T. s. Bauleth-Ramos, K. Kant, A. Correia, N. Poursina, B. Sarmento, J. Hirvonen and H. l. A. Santos, *ACS Omega*, 2018, **3**, 18444-18455.
464. T. Tian, H.-X. Zhang, C.-P. He, S. Fan, Y.-L. Zhu, C. Qi, N.-P. Huang, Z.-D. Xiao, Z.-H. Lu and B. A. Tannous, *Biomaterials*, 2018, **150**, 137-149.
465. J. K. Wong, R. Mohseni, A. A. Hamidieh, R. E. MacLaren, N. Habib and A. M. Seifalian, *Trends Biotechnol.*, 2017, **35**, 434-451.
466. Y. Liu, P. Bhattarai, Z. Dai and X. Chen, *Chem. Soc. Rev.*, 2019, **48**, 2053-2108.
467. C. Moore and J. V. Jokerst, *Theranostics*, 2019, **9**, 1550.
468. B. Yang, S. Zhou, J. Zeng, L. Zhang, R. Zhang, K. Liang, L. Xie, B. Shao, S. Song and G. Huang, *Nano Res.*, 2020, **13**, 1013-1019.
469. X. Meng, L. Chen, R. Lv, M. Liu, N. He and Z. Wang, *J. Mater. Chem. B*, 2020, **8**, 2177-2188.
470. T. Chen, R. Huang, J. Liang, B. Zhou, X. L. Guo, X. C. Shen and B. P. Jiang, *Chem. Eur. J.*, 2020, **26**, 15159-15169.
471. X. Zhang, L. Chen, C. Zhang and L. Liao, *ACS Appl. Mater. Interfaces*, 2021, **13**, 18175-18183.
472. X. Zeng, M. Luo, G. Liu, X. Wang, W. Tao, Y. Lin, X. Ji, L. Nie and L. Mei, *Adv. Sci.*, 2018, **5**, 1800510.
473. J. Liang, H. Wang, W. Ding, J. Huang, X. Zhou, H. Wang, X. Dong, G. Li, E. Chen and F. Zhou, *Sci. Adv.*, 2020, **6**, eabc3646.
474. J. Guo, T. Suma, J. J. Richardson and H. Ejima, *ACS Biomater. Sci. Eng.*, 2019, **5**, 5578-5596.
475. A. Rejhová, A. Opattová, A. Čumová, D. Slíva and P. Vodička, *Eur. J. Med. Chem.*, 2018, **144**, 582-594.
476. J. Sun, Z. Wan, J. Xu, Z. Luo, P. Ren, B. Zhang, D. Diao, Y. Huang and S. Li, *Biomaterials*, 2021, **269**,

120629.
477. F. Yu, M. Zhu, N. Li, M. Ao, Y. Li, M. Zhong, Q. Yuan, H. Chen, Z. Fan and Y. Wang, *Chem. Eng. J.*, 2020, **380**, 122426.
478. W. Sang, L. Xie, G. Wang, J. Li, Z. Zhang, B. Li, S. Guo, C. X. Deng and Y. Dai, *Adv. Sci.*, 2021, **8**, 2003338.
479. Y. Zhu, J. Xue, W. Chen, S. Bai, T. Zheng, C. He, Z. Guo, M. Jiang, G. Du and X. Sun, *J. Controlled Release*, 2020, **322**, 300-311.
480. C. W. Shields IV, L. L. W. Wang, M. A. Evans and S. Mitragotri, *Adv. Mater.*, 2020, **32**, 1901633.
481. Z. Zhao, A. Ukidve, V. Krishnan, A. Fehnel, D. C. Pan, Y. Gao, J. Kim, M. A. Evans, A. Mandal, J. Guo, V. R. Muzykantov and S. Mitragotri, *Nat. Biomed. Eng.*, 2021, **5**, 441-454.
482. Z. Zhang, W. Sang, L. Xie, W. Li, B. Li, J. Li, H. Tian, Z. Yuan, Q. Zhao and Y. Dai, *Angew. Chem. Int. Ed. Engl.*, 2021, **60**, 1967-1975.
483. F. X. Wang, J. W. Liu, X. Q. Hong, C. P. Tan and Z. W. Mao, *CCS Chem.*, 2021, **3**, 2527–2537.
484. J. J. Rennick, A. P. R. Johnston and R. G. Parton, *Nat. Nanotechnol.*, 2021, **16**, 266-276.
485. C. Yao, P. Wang, L. Zhou, R. Wang, X. Li, D. Zhao and F. Zhang, *Anal. Chem.*, 2014, **86**, 9749-9757.
486. Y. Ju, H. G. Kelly, L. F. Dagley, A. Reynaldi, T. E. Schlub, S. K. Spall, C. A. Bell, J. Cui, A. J. Mitchell, Z. Lin, A. K. Wheatley, K. J. Thurecht, M. P. Davenport, A. I. Webb, F. Caruso and S. J. Kent, *ACS Nano*, 2020, **14**, 15723-15737.
487. M. Cao, R. Cai, L. Zhao, M. Guo, L. Wang, Y. Wang, L. Zhang, X. Wang, H. Yao, C. Xie, Y. Cong, Y. Guan, X. Tao, Y. Wang, S. Xu, Y. Liu, Y. Zhao and C. Chen, *Nat. Nanotechnol.*, 2021, **16**, 708-716.
488. S. A. Dilliard, Q. Cheng and D. J. Siegwart, *Proc. Natl. Acad. Sci. U.S.A*, 2021, **118**, e2109256118.
489. L. Ma, L. Diao, Z. Peng, Y. Jia, H. Xie, B. Li, J. Ma, M. Zhang, L. Cheng, D. Ding, X. Zhang, H. Chen, F. Mo, H. Jiang, G. Xu, F. Meng, Z. Zhong and M. Liu, *Adv. Mater.*, 2021, **33**, 2104849.
490. N. Hoshyar, S. Gray, H. Han and G. Bao, *Nanomedicine*, 2016, **11**, 673-692.
491. R. Tenchov, R. Bird, A. E. Curtze and Q. Zhou, *ACS Nano*, 2021, **15**, 16982-17015.
492. N. F. Santos-Sánchez, R. Salas-Coronado, B. Hernández-Carlos and C. Villanueva-Cañongo, in *Plant Physiological Aspects of Phenolic Compounds*, ed. M. Soto-Hernández, IntechOpen, 2019, Chapter 3, pp. 35-50.
493. R. W. van der Pluijm, R. Tripura, R. M. Hoglund, A. P. Phyo, D. Lek, A. Ul Islam, A. R. Anvikar, P. Satpathi, S. Satpathi and P. K. Behera, *Lancet*, 2020, **395**, 1345-1360.
494. J. H. Park, K. Kim, J. Lee, J. Y. Choi, D. Hong, S. H. Yang, F. Caruso, Y. Lee and I. S. Choi, *Angew. Chem. Int. Ed. Engl.*, 2014, **53**, 12420-12425.
495. R. H. Fang, A. V. Kroll, W. Gao and L. Zhang, *Adv. Mater.*, 2018, **30**, 1706759.

Biographies

Yi Ju received his PhD degree in 2017 at The University of Melbourne under the supervision of Prof. Frank Caruso. Following his PhD completion, he undertook a Research Fellow position in the same group exploring various low-fouling nanomaterials for controlled bio–nano interactions and served as a Co-Leader (2017–2021) of the Signature Project ‘Mediating Protein Interactions’ within the ARC Centre of Excellence in Convergent Bio–Nano Science and Technology. From 2021, he moved to RMIT University as a Vice-Chancellor’s Postdoctoral Fellow in Prof. Magdalena Plebanski’s group where he investigates how nanomaterials interact with immune system.

Haotian Liao received his PhD degree from the Department of Liver Surgery, West China Hospital of Sichuan University under the supervision of Prof. Yong Zeng in 2021. He is currently a Resident Physician of West China Hospital and is conducting research as a Postdoctoral Fellow in Prof. Junling Guo's group in College of Biomass Science and Engineering, Sichuan University. His research interests focus on the development of multifunctional materials and cellular engineering for cancer therapy.

Joseph J. (JJ) Richardson was born in the sunshine state of the USA, Florida. He pursued his BA in Philosophy and MS in Industrial and Systems Engineering at the University of Florida and moved to Australia to complete his PhD in Chemical and Biomolecular Engineering at The University of Melbourne. JJ has lived and worked in seven countries and his research lies at the interface of nanomaterials and biological systems. His current focus as a Research Fellow at the University of Tokyo is on the translation of antimicrobial nanocoatings into consumer products and the development of new nanobiohybrid systems.

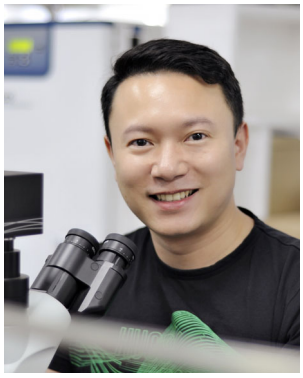

Junling Guo is a Full Professor and National Excellent Young Professor at Sichuan University, where he is currently the Founding Director of BMI Center for Biomass Materials and Nanointerfaces. He received his PhD in Chemical and Biomolecular Engineering at The University of Melbourne and moved to Harvard University to conduct his research as a Wyss Fellow. He has made numerous contributions to the field of polyphenol-based materials science, leading to the fundamental understanding of polyphenol chemistry and development of new technologies for biomedical engineering, cellular engineering, carbon-neutral materials, and environmental protection, among others.

Frank Caruso is a Melbourne Laureate Professor and an NHMRC Senior Principal Research Fellow at The University of Melbourne. He received his PhD in 1994 from The University of Melbourne and thereafter conducted postdoctoral research at CSIRO Division of Chemicals and Polymers. In 1997–2002, he was a Humboldt Research Fellow and Group Leader at the Max Planck Institute of Colloids and Interfaces (Germany). Since 2003, he has been a professor at The University of Melbourne and has held ARC Federation and ARC Australian Laureate Fellowships. His research interests focus on developing advanced nano- and biomaterials for biotechnology and medicine.